Biosensors and Bioelectronics 231 (2023) 115271

Contents lists available at ScienceDirect

Biosensors and Bioelectronics

journal homepage: www.elsevier.com/locate/bios

Organs-on-chips technologies – A guide from disease models to opportunities for drug development

Anna Grazia Monteduro [a,1], Silvia Rizzato [a,1], Giusi Caragnano [a], Adriana Trapani [b], Gianluigi Giannelli [c], Giuseppe Maruccio [a,*]

[a] Omnics Research Group, Department of Mathematics and Physics "Ennio De Giorgi", University of Salento and Institute of Nanotechnology, CNR-Nanotec and INFN Sezione di Lecce, Via per Monteroni, 73100, Lecce, Italy
[b] Department of Pharmacy-Drug Sciences, University of Bari "Aldo Moro", Bari, Italy
[c] National Institute of Gastroenterology IRCCS "Saverio de Bellis", Research Hospital, Castellana Grotte, Bari, Italy

ARTICLE INFO

Keywords:
Organ on chip
Microphysiological systems
Multiorgan models
Lab on chip
Drug screening
Drug research
Disease models
Cancer
Microfluidics
Biosensors

ABSTRACT

Current in-vitro 2D cultures and animal models present severe limitations in recapitulating human physiopathology with striking discrepancies in estimating drug efficacy and side effects when compared to human trials. For these reasons, microphysiological systems, organ-on-chip and multiorgans microdevices attracted considerable attention as novel tools for high-throughput and high-content research to achieve an improved understanding of diseases and to accelerate the drug development process towards more precise and eventually personalized standards. This review takes the form of a guide on this fast-growing field, providing useful introduction to major themes and indications for further readings.

We start analyzing Organs-on-chips (OOC) technologies for testing the major drug administration routes: (1) oral/rectal route by intestine-on-a-chip, (2) inhalation by lung-on-a-chip, (3) transdermal by skin-on-a-chip and (4) intravenous through vascularization models, considering how drugs penetrate in the bloodstream and are conveyed to their targets. Then, we focus on OOC models for (other) specific organs and diseases: (1) neurodegenerative diseases with brain models and blood brain barriers, (2) tumor models including their vascularization, organoids/spheroids, engineering and screening of antitumor drugs, (3) liver/kidney on chips and multiorgan models for gastrointestinal diseases and metabolic assessment of drugs and (4) biomechanical systems recapitulating heart, muscles and bones structures and related diseases. Successively, we discuss technologies and materials for organ on chips, analyzing (1) microfluidic tools for organs-on-chips, (2) sensor integration for real-time monitoring, (3) materials and (4) cell lines for organs on chips. (Nano)delivery approaches for therapeutics and their on chip assessment are also described. Finally, we conclude with a critical discussion on current significance/relevance, trends, limitations, challenges and future prospects in terms of revolutionary impact on biomedical research, preclinical models and drug development.

1. Introduction

Fighting human diseases and improving life expectations are key challenges for the modern society. In these efforts, two major routes can be identified: on one side, a better understanding of disease mechanisms and the involved pathological processes; on the other, the development of effective therapeutic strategies for disease treatment with limited side effects and impact on life conditions. Organs-on-chips (OOC) technologies have the ambition to provide a resource-efficient response to this demand in the form of miniaturized microphysiological systems for biomedical research.

In this review, we provide an overview on the current status and latest trends in on-chip disease models with special attention to opportunities for drug development. As sketched in the graphical summary in Fig. 1, we will start with **(1)** an analysis of OOC technologies with applications for testing the major drug administration routes: **(1.1)** intestine-on-a-chip (oral/rectal route), **(1.2)** lung-on-a-chip (inhalation), **(1.3)** skin-on-a-chip (transdermal) and **(1.4)** vascularization

* Corresponding author.
E-mail address: giuseppe.maruccio@unisalento.it (G. Maruccio).
[1] These authors equally contributed to the work.

https://doi.org/10.1016/j.bios.2023.115271
Received 13 December 2021; Received in revised form 24 November 2022; Accepted 26 March 2023
Available online 31 March 2023

models (intravenous). Here, we will consider how drugs can penetrate in the bloodstream, directly or across relevant blood organ barriers and be conveyed to their targets, including analysis of inflammatory processes.

Then, we will focus on **(2)** microphysiological systems for (other) specific organs, processes and diseases studies: **(2.1)** neurodegenerative diseases (with brain models and blood brain barriers), **(2.2)** tumor models (including their vascularization, spheroids/organoids, engineering and screening of antitumor drugs), **(2.3)** biomechanical systems recapitulating heart, muscles and bones structures and related diseases, **(2.4)** liver/kidney on chips and **(2.5)** multiorgan models for gastrointestinal diseases and metabolic assessment of drugs.

In section 3, we will discuss **(3)** technologies and materials for organ on chips, analyzing **(3.1)** microfluidic tools for organs-on-chips, **(3.2)** sensor integration for real-time monitoring, **(3.3)** materials and **(3.4)** cell lines for organs on chips. Finally, we conclude with a critical discussion on current significance/relevance, trends, limitations, challenges and future prospects in terms of revolutionary impact on biomedical research, preclinical models and drug development.

This review is not intended to provide exhaustive information on the OOC research (an impossible task for this fast-growing field) but takes

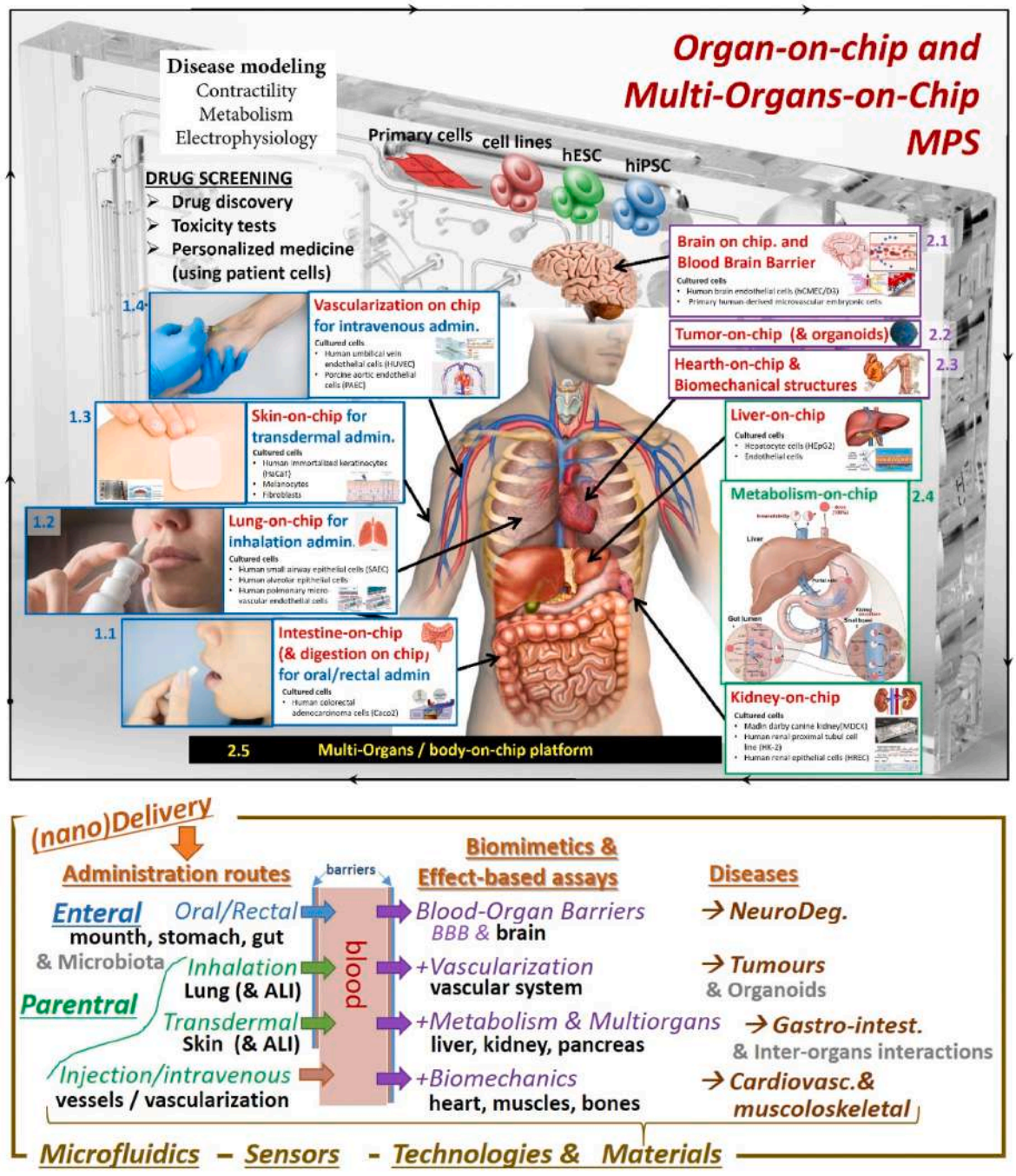

Fig. 1. Graphical summary and main topics covered by the present review, from enteral (oral/rectal) and parenteral (inhalation, transdermal, injection/intravenous) administration routes with relevant organ models (see Section 2) to biomimetics and effect-based assays with relevant organs and related diseases (see Section 3). These sections include discussion also on aspects related to relevant blood organ barriers to cross, vascularization, organoids, metabolisms, multiorgans models. In the external frame are then reported the microfluidics and sensor technologies and materials available for the development of organs-on-chips and automated platforms for high-throughput screening (see Section 4).

the form of an atlas for both researchers approaching the topic and advanced users, providing useful introduction to major themes and indications for further readings.

2. Microphysiological systems for testing drug administration routes

The development of new drugs from discovery within proper candidate libraries to preclinical and clinical phases is a quite inefficient, long and costly process (Fig. 2 A). Indeed, establishing one new drug typically requires several years of research and hundreds of millions of dollars/euros, with the involvement of specialized personnel and a validation procedure characterized by strictly regulated clinical phases and high risk in front of such huge investments. The success rate of new compounds is as low as 5% resulting in significant resources' loss every year. In addition, in the search for novel drugs, another crucial issue to improve therapeutic efficacy concerns the availability of effective routes for pharmaceuticals delivery in patients, e.g. by oral/rectal, inhalation, transdermal or intravenous administration (Fig. 2 B). Organ-on-chip devices can provide useful support in both these directions, since they allow to recapitulate intrinsic and extrinsic features of an organ/tissue/construct, its microenvironment and biological barriers and enable testing drug efficacy, solubility, permeability, targeted delivery and toxicity in a more appropriate and reliable way (Low et al., 2021; Bhatia and Ingber, 2014; Huh et al., 2010a, 2011; Skardal et al., 2016; Caplin et al., 2015a; Benam et al., 2015).

Today, drug research relies on the use of conventional in-vitro 2D cell cultures and animal experiments which are not able to properly predict clinical efficacy, toxicity and side effects of therapeutics in humans since they are inadequate to reproduce human physiology. For these reasons, organs-on-chips technologies recently attracted considerable attention as alternative platforms for drug development with research grown tremendously worldwide. The interest is motivated by their potential use for high-throughput, high-content and resource-efficient screening (Fig. 3). This represents a paradigm change and is important to review recent innovations and advances in the field in order to catch the opportunities provided by most appropriate disease models which are becoming more and more accepted by pharmaceutical companies as novel tools able to accelerate the drug development process towards more precise and eventually personalized standards (Dhiman et al., 2019).

Before starting to review cases relevant for various organ and diseases, it is worth noticing that a general classification of OOC architecture can be done in terms of ECM dimensionality distinguishing among 2D, 2.5D and 3D models (Bennet et al., 2021). In 2D models, a synthetic membrane separates two vertically-stacked compartments and ECM provides coating, favors cell adhesion/growth and participates in defining the barrier and transport properties with respect to nutrients and drugs. 2.5D models are realized either using multiple ECM coated membranes or replacing the membrane with a thin hydrogel film. Instead, in 3D models, thick 3D hydrogel layers are used so that stromal cells can be incorporated to better recapitulate the interstitial matrix (Bennet et al., 2021).

2.1. Intestine-on-a-chip for testing oral/rectal administration

A major route for drug administration relies on oral/rectal delivery. Thus, in this section, we focus on intestine-on-a-chip models. Key challenges in this case are represented by gastro-intestinal drug solubility and permeability since drugs must enter the blood circulation upon intestinal absorption in order to become effective. Moreover, potential side effects must be evaluated, in particular on the involved organs (see Section 2.4 and **2.5** for metabolism-on-chip, digestion-on-chip and toxicity studies involving liver, kidney and multiorgans microphysiological systems).

The intestine plays a fundamental role mediating nutrient, water and drug uptake, performing a critical immunological function and hosting a complex pattern of commensal and mutualistic microorganisms (gut microbiota). Thus it is a relevant model to reproduce in terms of barrier function (from 2D cell cultures to 3D villi microstructures) and physiological conditions including oxygen gradient, shear stress and mechanical deformations (Ashammakhi et al., 2020a; Fois et al., 2019; Hewes et al., 2020; Marrero et al., 2021a).

Various intestine-on-a-chip/gut-on-a-chip designs were reported in literature integrating 3D compartmentalized systems, perfusable chambers, 3D hydrogel scaffolds and stretchable materials for mimicking peristaltic movements (Fois et al., 2019; Hewes et al., 2020; Bein et al., 2018; Maurer et al., 2019; Marrero et al., 2021b). 3D compartmentalized systems with upper and bottom chambers separated by a porous membrane provide a simple, popular strategy for organ-on-a-chip layout and the implementation of biological barrier models. Ingber group employed this approach modifying their previously reported breathing lung-on-a-chip (Huh et al., 2010a) (see Section 1.2) in the form of gut-on-a-chip (Kim et al., 2012). In particular, Kim et al. (2012) integrated an ECM-coated polydimethylsiloxane (PDMS) membrane among two PDMS microfluidic channels to obtain two vertically stacked chambers (Fig. 4 A1-A3). Caco-2 cells were used as human intestinal epithelial cells. The addition of two vacuum chambers on the channel sides permitted to mimic the peristaltic motions, while a strain of Lactobacillys rhamnosus was added to simulate intestinal native microbes. Polarized Caco-2 cells were instead seeded by Kimura et al. to better mimic human intestine (Kimura et al., 2008) since they express morphological and functional characteristics of mature small intestinal enterocytes with better barrier functions.

Focusing on drug delivery, the oral uptake of the chemotherapeutic agent SN-38 (7-ethyl-10-hydroxycamptothecin) was investigated by Pocock and coworkers using an intestine-on-chip model (Pocock et al., 2017) which improves conventional Caco-2 Transwell approach by better mimicking the biological barrier function (Fig. 4 B1–B3). In more detail, they differentiated an epithelial cell monolayer using external mechanical stimuli and obtained a 3D rippling morphology mimicking microvilli expression. Then, they investigated the structure permeability for SN38 modified with fatty acid esters of different lengths and at different positions, demonstrating that lipophilic prodrugs can contribute to tackle low oral bioavailability issues. These models are also applicable to nanoformulations and biological entities.

The transport of both high- and low-permeability drug compounds across the intestinal barrier was studied by Kultong et al. (Kulthong et al., 2020) with a dynamic gut-on-chip model (Fig. 4 C1–C3). Specifically, the investigated compounds were antipyrine, ketoprofen, digoxin, and amoxicillin with concentrations up to 500 μM, 300 μM, 250 μM, and 500 μM, respectively, for 24 h on a differentiated monolayer of human colorectal adenocarcinoma cells (Caco-2). The authors compared the apparent permeability (P_{app}) values of the four compounds and observed that for antipyrine and ketoprofen, P_{app} values were lower in Caco-2 cells under dynamic flow conditions than under static conditions in transwell systems. These differences may be due to the effect of the chip design, the material composing the diffusion membrane, and the presence of laminar flow. For amoxicillin which is a low permeability compound, the P_{app} values are instead similar under both dynamic and static flow conditions. Based on a comparison of OOC approach with the static transwell model, Kultong et al. concluded that their gut-on-chip model was adequate to study drug transport (Kulthong et al., 2020).

Notably, gut-on-a-chip models were likewise employed to study (with improved efficacy) the response to nutrients and to emulate gut inflammation, host-microbiota interplay as well as interactions with environmental factors where the imbalance between pro-inflammatory and anti-inflammatory cytokines and alterations of the composition and function of the gut microbiota (dysbiosis) play a pivotal role (Maurer et al., 2019; Beaurivage et al., 2019; Kim et al., 2016; Neurath, 2014). As a result, OOC can provide valuable insights on intestinal

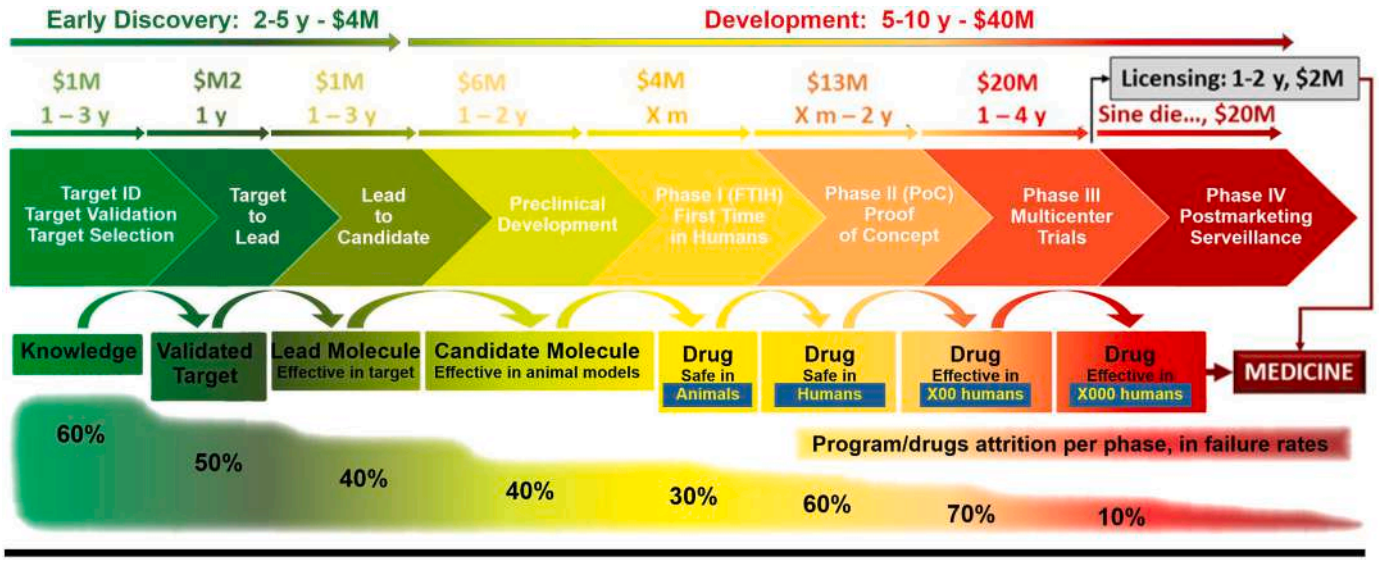

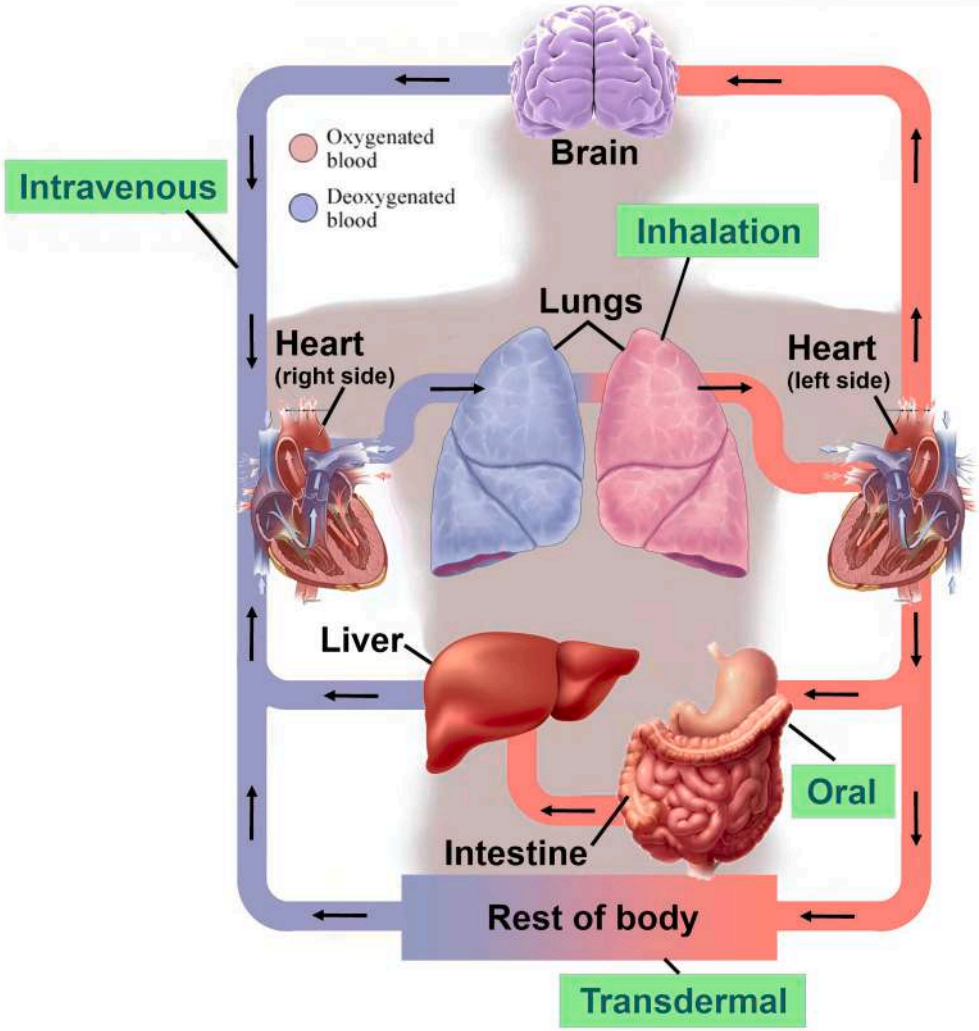

Fig. 2. A. The drug discovery process [https://doctortarget.com/machine-learning-applied-drug-discovery/] and major drug administration routes (beyond the involved organs/barriers, also the time until effect changes with the administration routes from short to long (30–60 s for intravenous administration; 2–3 min for inhalation; 5–30 min for rectal; minutes to hours for transdermal). **B** Routes of drug administration.

Model properties/ applications	Animals	2D cell cultures	3D cell cultures	Spheroids/ Organoids	Single OOC	Multiple OOC
Biomimetics / Recapitulation	−	✗	−	✓	✓	+
Complexity	✓	✗	−	✓	✓	+
Disease models	−	−	−	✓	✓	✓
Drug research	−	−	−	✓	✓	+
Cell-cell interactions	✓	✗	✓	✓	✓	✓
Organ-organ interactions	✓	✗	✗	✗	✗	✓
Vascularization	✓	✗	✗	−	−	✓
Integration of biosensors for real time	−	✓	✓	✓	✓	✓
Throughput	✗	✓	✓	✓	✓	✓
Costs	✗	✓	✓	−	−	−
Ethics	✗	✓	✓	✓	✓	✓

Fig. 3. Advantages of single and multiple OOC platforms in comparison to other methodologies.

dysfunction and physiopathology, the involved pathways and their relation to severe and chronic gut diseases with complex etiology from early stage to full manifestation and eventual worsening (Hewes et al., 2020; Marrero et al., 2021a; Bein et al., 2018; Maurer et al., 2019). In this respect, OOC are expected to overcome animal models which often fail when extrapolated to humans due to the differences in microbiota composition and immune system. Furthermore, OOC models are expected to overcome limitations of 2D and 3D cultures, such as the lack of cell-matrix interaction and mechanical stimuli respectively (Wang et al., 2021; Ashammakhi et al., 2020b).

2.2. *Lung-on-a-chip for testing inhalation administration*

Administration by inhalation provides another important route which is particularly relevant for respiratory and pulmonary diseases including viral and bacterial lung infections, chronic obstructive pulmonary disease (COPD), pulmonary edemas, tuberculosis and lung cancer which are among the top 10 causes of death according to World Health Organisation (World Health Organisation [WHO]). Against these diseases, inhaled drugs can be advantageous for rapid delivery/action and in terms of targeted instead than systemic exposure with drugs directly deposited within the airways. In this case, the absence of interaction with liver or kidney can result in reduced toxicity and side effects and thereby improve therapeutic efficacy, patient outcomes and patient quality of life (Cidem et al., 2020; Borghardt et al., 2018). By reproducing human in vivo pulmonary microenvironment, the air-liquid interface and the lung-blood barrier for inhaled agents, lung-on-chip platforms facilitate research (Huh et al., 2010a; Bennet et al., 2021; Ainslie et al., 2019; Khedoe et al., 2020; Barros et al., 2021; Campillo et al., 2021).

Major difficulties in recapitulating lungs airways lies in their morphological and histological complexities with the presence of different types of cells and epithelium in addition to mucus and the relevance of branching and breathing movements. Remarkably, in their seminal work, Huh et al. (2010a) demonstrated a breathing lung-on-a-chip (Fig. 5 A1-A2) having the form of a compartmentalized system with vertically-stacked chambers separated by a porous membrane. Specifically, the upper and bottom chambers were seeded with human alveolar epithelial cells and lung capillary endothelial cells respectively. An air-liquid interface (ALI) mimicking the alveolar-capillary barrier was then reproduced by depleting the cellular media in the upper compartment. Two side vacuum chambers were also realized to reproduce the cyclic strain and mechanical forces on the culture membrane associated to breathing (Fig. 5 A1). This architecture then became very popular and extensively used in OOC models, beyond the lung-on-a-chip case (Frost et al., 2019; Ishahak et al., 2020).

Known biomarkers (e.g. fluorescent albumin, transferrin and dextrans) are habitually employed to evaluate the barrier permeability and the influence of shear stress on paracellular and transcellular transport, i.e. between epithelial/endothelial cell junctions or through cell lacking

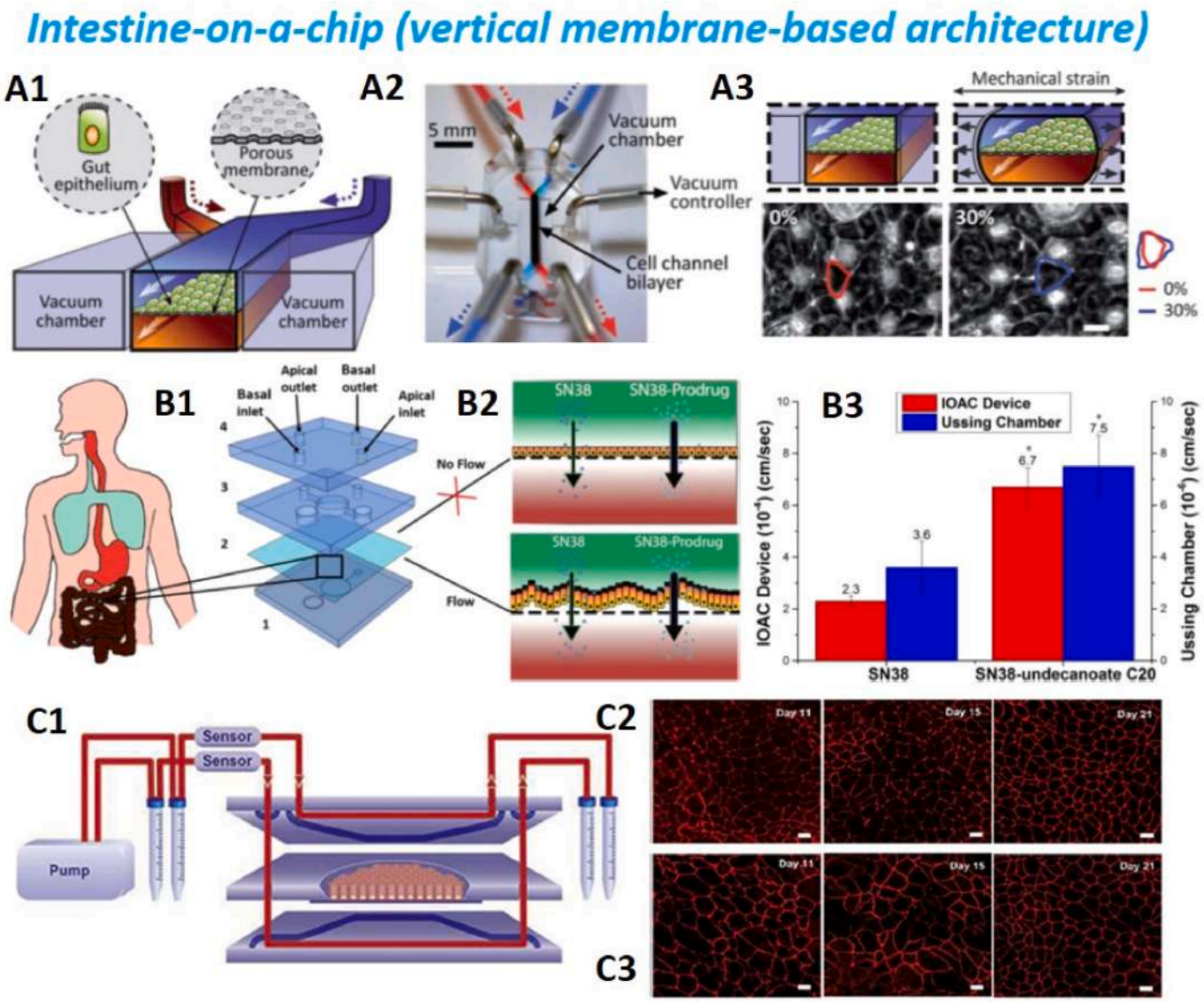

Fig. 4. ***(A1)*** *Schematic representation of the gut-on-a-chip device in which the ECM membrane is covered by gut epithelial cells and cross the central microchannel between two vacuum chambers.* ***(A2)*** *A photo of the gut-on-a-chip device. Blue and red dyes flow through tubing to the upper and lower microchannels, respectively, to visualize these channels.* ***(A3)*** *Schematic (top) and phase contrast images (bottom) of intestinal monolayers cultured within the gut-on-a-chip in the absence (left) or presence (right) of mechanical strain. Reproduced from Ref.* (Kim et al., 2012). ***(B1)*** *Structure of the intestine-on-a-chip reported by Pocock* et al. *with apical and basal chambers separated by a PC membrane.* ***(B2)*** *Scheme of the performed permeability assay for chemotherapeutic agent SN38 through Caco-2 cell monolayers.* ***(B3)*** *Comparison among results from the OOC platform and rat intestinal mucosal membrane mounted in an Ussing Chamber. Reproduced from Ref.* (Pocock et al., 2017). ***(C1)*** *Microfluidic gut-on-chip realized by Kulthong* et al. *and consisting of three re-sealable glass slides resulting in two microfluidic chambers separated by a polyester (PET) membrane where Caco-2 cells were cultured. The flow was injected by use of a multichannel air pressure pump. Confocal microscope images of top view of the Caco-2 cells layer, evidencing tight junction patterns (ZO-1/TJP1) in red, cultured for 21 days in a static Transwell system* ***(C2)*** *or a gut-on-chip system* ***(C3)*** *under a continuous flow of* 100 μL/h. *Reproduced from Ref.* (Kulthong et al., 2020).

the required active transporters (Huh et al., 2010a; Frost et al., 2019). In this respect, confocal microscopy is a valuable technique since it permits localization of the biomarkers in the different compartments to investigate transport across the barrier. In general, the alveolar barrier permeability was found to be significantly smaller than in the case of liquid cultures (Huh et al., 2010a). Trans-epithelial electrical resistance (TEER) measurements provide an useful alternative to confocal microscopy for evaluating the barrier characteristics since the resistance correlates to the tightness of the cell junctions (Huh et al., 2010a; Henry et al., 2017; Stucki et al., 2018) (Fig. 5 A3).

A model of drug toxicity–induced pulmonary edema was also implemented by Ingber group using a similar alveolar-capillary interface with human pulmonary epithelial and endothelial cells that experience both air and fluid flow. In this study, the applied cyclic mechanical forces (Huh et al., 2012) mimicking the breath were found to play a relevant role in the edema formation and the authors had the possibility to test some therapeutic approaches.

This membrane-based architecture, however, does not exhaust all the proposed approaches. Various models and interfaces have been reported using different architectures and types of cell culture. They span from simple monocultures for the epithelium (Felder et al., 2019; Huang et al., 2021) to co-cultures for epithelial-endothelial (in alveolar-capillary (Huh et al., 2010a; Douville et al., 2010; Jain et al., 2018a; Stucki et al., 2015; Zamprogno et al., 2021) and small-airway models (Benam et al., 2016)) and epithelial-mesenchymal (Humayun et al., 2018) interfaces. Tri-cultures with epithelial, fibroblast and

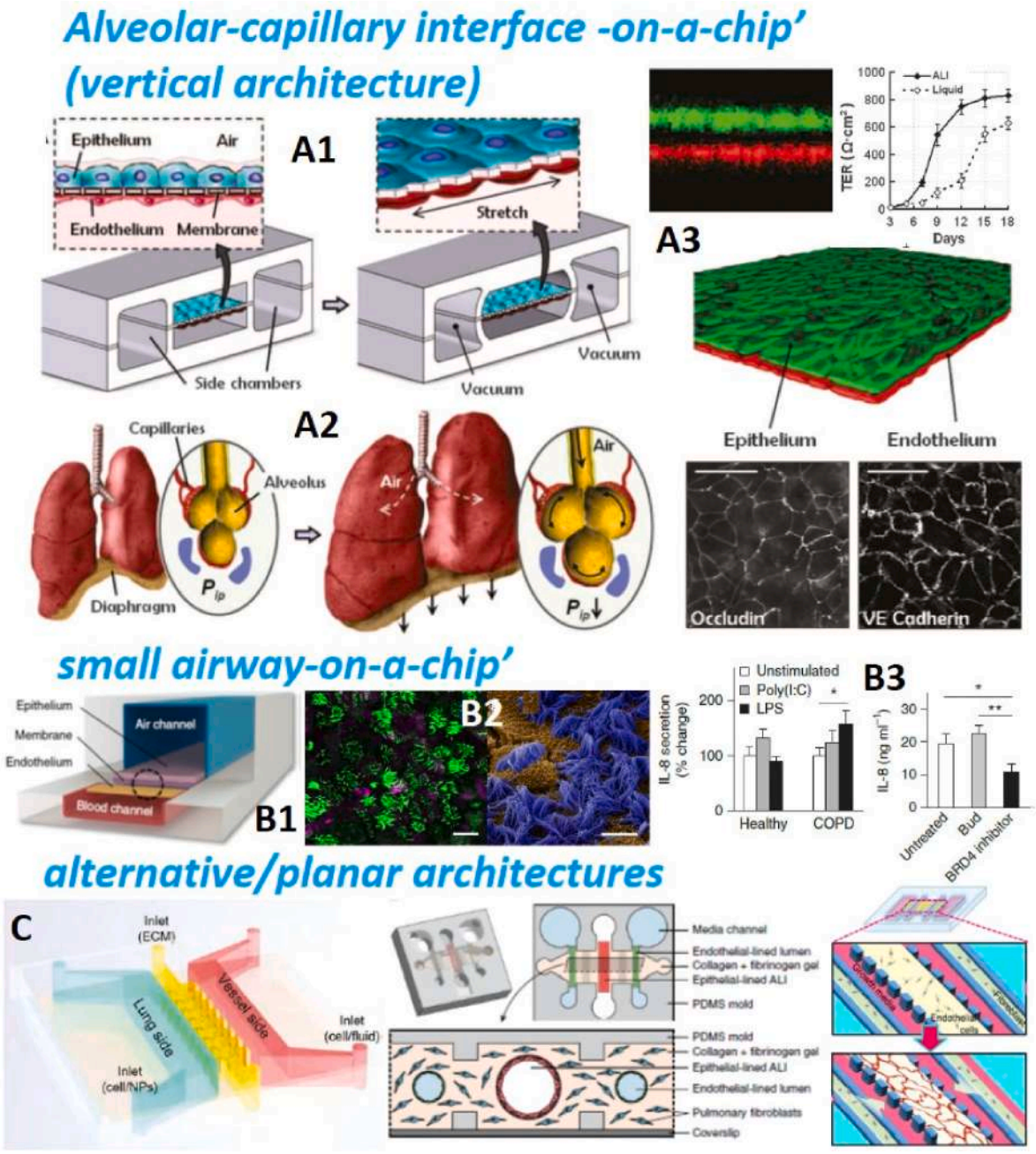

Fig. 5. **(A1-A2)** Alveolar air-liquid interface model which uses a cyclic pressure to mimic breathing. **(A3)** Assessment of the interface by TEER measurements and fluorescent staining. Reproduced from Ref. Huh et al. (2010a). **(B1)** Air-liquid interface model workflow with seeding of endothelial cells (LMECs) and then alveolar epithelial cells (AECs) on a transwell system. **(B2)** Human airway epithelium grown on chip (scale bar, 20 μm) and cilia (blue) on the apical surface of the airway epithelium (scale bar, 10 μm). **(B3)** Effects on production of the cytokines IL-8 on small airway chips lined by either normal or chronic obstructive pulmonary disease epithelial cells (left) and upon therapeutic modulation of cytokine inflammation (right). Reproduced from Ref. (Benam et al., 2016). **(C)** Schematic of structures of lung-on-a-chip with alternative/planar architecture. Reproduced from Ref. (Barkal et al., 2017; Park et al., 2018; Zhang et al., 2018a).

endothelial cells were instead employed for recapitulating epithelial-stromal/vascular tissue interfaces (Sellgren et al., 2014; Barkal et al., 2017; Park et al., 2018). In this way, through an appropriate cell selection, lung barrier function, inflammation, immune response and injury were modeled in lung-on-a-chip format providing unprecedented tools for physiopathological investigations, drug development, inhalation assays, exposure studies and airborne toxicological assessment (Huh et al., 2010a; Bennet et al., 2021; Khedoe et al., 2020; Lin et al., 2022; Zhang et al., 2018a).

In particular, microphysiological models of human asthmatic and COPD airways are relevant for better understanding and contrasting diseases which have a high personal, societal and economic impact and are associated to inflammatory processes affecting the whole respiratory tract, from central to peripheral (small) airways (van den Berge et al., 2011) which have sizes <2 mm in internal diameter and include bronchioles and alveoli. Remarkably, an organotypic small-airway-on-chip was reported by Ingber group using membrane-separated chambers and microvascular endothelium and mucociliary bronchiolar epithelium from patients (Fig. 5 B1–B3) (Benam et al., 2016). Interestingly, the authors analyzed the exposure to interleukin-13 (IL-13, which has a key role in asthma), viral mimic poly(I:C) (an analogue of dsRNA produced by cells infected by respiratory viruses) and lipopolysaccharide

endotoxin (LPS, a bacterial wall derived component) in terms of effect on inflammatory cytokine/chemokine secretion, decreased ciliary function, globet cell hyperplasia and neutrophil recruitment. Then, they used the same platform for drug discovery applications and in particular testing therapeutic agents capable to contrast the inflammation. Viral-induced exacerbation of asthma was investigated by Nawroth et al. too (Nawroth et al., 2020). Stucki et al. instead employed micro-diaphragms and an electro-pneumatic setup to stretch the alveolar barrier and showed the effect of these mechanical cues on metabolic activities and cytokine secretion (Stucki et al., 2015). A layout with three vertically stacked chambers with arrayable suspended gels was realized by Humayun et al. to examine the interactions among airway epithelial cells and smooth muscle cells which are relevant in chronic lung diseases (Humayun et al., 2018).

Injuries, alveolar epithelial wound healing under mechanical strain and intravascular thrombosis were another subject of study for the development of new anti-inflammatory therapeutic agents (Felder et al., 2019; Jain et al., 2018b). The inclusion of fibroblasts in these models is important to contemplate their interactions with epithelial and immune cells and their role in airway repair through ECM deposition and degradation, once triggered by epithelial cells after an injury (Bennet et al., 2021). In this respect, Sellgren et al. employed an architecture with three vertically stacked chambers to produce an airways model with epithelial cells, lung fibroblasts and polarized microvascular endothelial cells (Sellgren et al., 2014); while Bovard et al. combined lung/liver-on-a-chip for toxicity studies (Bovard et al., 2018) (for multi-organ on chips models see Section 2.5). Other recent reports focused on modeling fibrotic diseases (Mejias et al., 2020), investigated endotheliitis and vascular damage during SARS-CoV-2 infection (Thacker et al., 2021), and intriguingly the spontaneous evolution of influenza viruses (Si et al., 2021).

Beyond the membrane-based approach, different architectures with adjacent chambers were recently reported with the target to provide improved 3D models able to better mimic in vivo structures (Barros et al., 2021; Barkal et al., 2017; Park et al., 2018; Zhang et al., 2018a). In particular, Zhang et al. realized three parallel channels (Fig. 5 C) with a lung and a vessel side respectively lined with human pulmonary alveolar epithelial cells and vascular endothelial cells. The middle ECM channel was then filled with Matrigel to recapitulate the alveolar capillary barrier. This platform was employed for nanotoxicity tests (Zhang et al., 2018a). The bronchiole model by Barkal and colleagues has some similarities and differences. This approach offers more physiologically relevant microarchitectures in terms of sizes, geometries and 3D interactions as compared to flat conformations with porous membranes. Furthermore, the various compartments can be addressed separately and the cell types are exposed to different conditions thanks to gel polymerization in a stable 3D structure and the presence of appropriate ports for injection/removal/sampling. The counterpart is the inherent difficulty in collecting gel-embedded cells since device disassembly for gel extraction and subsequent digestion is required. This process became even harder in multicellular hydrogel-based models (Park et al., 2018), when cell collection is necessary before digestion or requires cell sorting method.

3D cell printing was employed by Park et al. to fabricate an airways model comprising a blood vessel network made of human dermal microvascular endothelial cells and human lung fibroblasts in decellularized ECM. Primary human tracheal epithelial cells were instead seeded on a Transwell insert containing an ECM membrane (Park et al., 2018). The presence of a vascular network improves the physiological relevance of this model, although the co-culture of endothelial cells and fibroblasts complicate the analysis (Bennet et al., 2021). Recently, in the search for more physiologically relevant models and materials, alternative architectures were proposed using nanofiber membranes (Yang et al., 2018), reverse engineered hydrogels with inverse opal structure (Huang et al., 2021) and stretchable collagen-elastin biomembranes.

2.3. Skin-on-a-chip for testing transdermal administration

Skin implements several functions for the body: (i) thermoregulation through sweat glands, (ii) heat, pressure and strain sensing through several sensory receptors, (iii) vitamin D synthesis. As a physical barrier, it preserves from dehydration, maintains gas concentration gradients (for O_2, CO_2, N_2) and protects the body against exposure to external agents and threats (including microorganisms, ultraviolet radiation, toxic and mechanical agents). Within the therapeutic field, transdermal drug administration provides a mean for administration of systemically acting drugs through vessels or adipose tissue after overcoming the skin barrier.

Human skin-on-a-chip (SOC) models (van den Broek et al., 2017; Cui et al., 2022; Nitsche et al., 2022; Zoio and Oliva, 2022; Risueno et al., 2021; Mathes et al., 2014) attracted significant attention for dermatological studies, wound healing, risk assessment for external agents/chemicals, evaluation of cosmetic products and their ingredients and transdermal drug administration research. In this case, differences with animal skin are considerable in terms of structural and biochemical properties, lipid profile, hair density and stratum corneum thickness (Cui et al., 2022). As the more external layer consisting of protein-rich dead cells in a lipid matrix, the stratum corneum influences drug permeation with its thickness and lipid composition contributing in establishing the barrier penetration characteristics. 2D cell cultures suffer in appropriately recapitulating attachments and growth kinetics and the lipid profile and, for example, can exhibit limitations in evaluating permeability of hydrophilic compounds depending on the use of non-lipid or lipid-based membrane models. 3D skin-on-a-chip models can better mimic in vivo physiological conditions.

Human skin consists of three structural compartments. The external, avascular epidermis layer is mainly composed of keratinocytes producing keratin as a protective protein. The intermediate dermis compartment is a connective tissue with fibroblasts as the primary cell component in a collagen microenvironment, elastin fibers providing elastic properties and hyaluronic acid involved in skin hydration. It is pervaded by blood and lymph vessels and contains nerves, sensory receptors, sweat and sebaceous glands, hair follicles and shafts. The inner subcutaneous tissue is predominantly made of adipocytes (fat cells) in addition to fibroblast and macrophages and is characterized by larger nerves and blood vessels. For widening the range of functions and possible investigations, it can be relevant to include additional cell types (e.g. melanocytes and Langerhans cells in the epidermis) (Zoio and Oliva, 2022). Both skin biopsies or models generated off-chip were integrated in chip models.

Progress in the field came through the development of more and more appropriate and complete models. We can distinguish different categories of in vitro skin models (Fig. 6 A) with increasing physiological relevance and complexity and skin-on-a-chip followed a similar development (van den Broek et al., 2017; Cui et al., 2022; Nitsche et al., 2022; Risueno et al., 2021; Mathes et al., 2014):

- reconstructed human epidermis (RHE) models typically uses only one cell type (keratinocytes): they provide a well-established and reproducible platform for risk assessment and were employed in skin irritation, corrosion and sensitization studies in toxicological and cosmetic research as well as transdermal drug delivery, phototoxicity, metabolization assays (Gibbs et al., 2013). With the incorporation of melanocytes, RHE models allow skin lightning and pigmentation assays (Jain et al., 2012). However, more advanced models are needed for drug efficacy tests, recapitulating cross talk with other cell types;
- dermo-epidermal human skin equivalents (HSE) (Mathes et al., 2014; Asbill et al., 2000) are cultivated in serum and include the dermis compartment with collagen I and fibroblast cells in proximity to the keratinocytes which are seeded in a second phase and cultivated at the air-liquid interface to form the adjacent epidermal

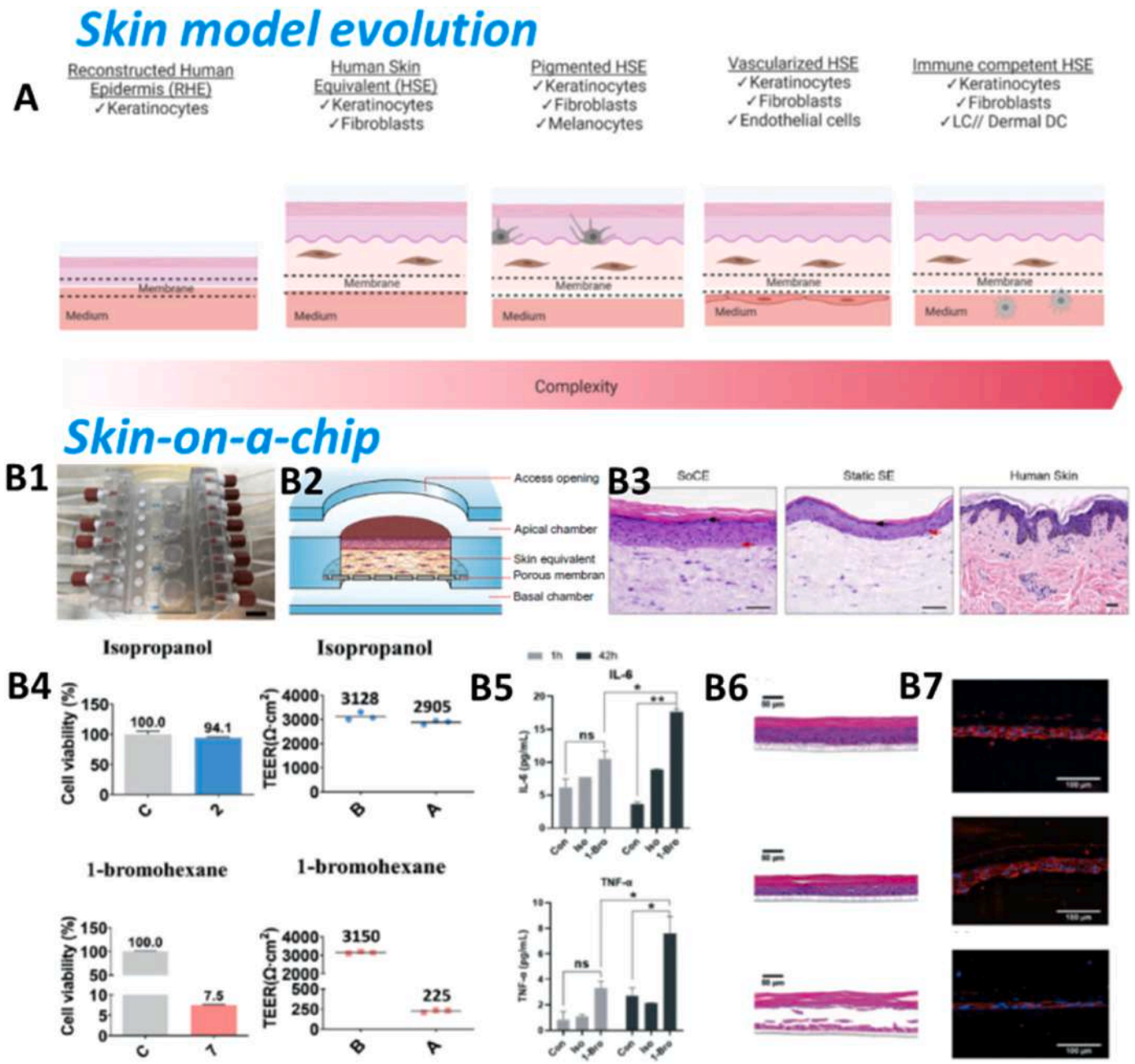

Fig. 6. (A) *Summary of selected 3D* in vitro *skin tissue models, depicted with increasing biological complexity from left to right and their research applicability and predictability for NGRA using an open access OOC device for air–liquid culturing. Reproduced from Ref.* (Nitsche et al., 2022). ***(B1–B2)*** *Photographs and scheme of skin-on-chip equivalent (SoCE);* ***(B3)*** *Histological images representing epidermal morphogenesis in skin-on-a-chip equivalent compared to static human skin equivalents. Reproduced from Ref.* (Sriram et al., 2018) ***(B4)*** *MTT Cell viability (C = negative control) and TEER values of the skin-on-chips before and after 42h exposure to isopropanol and 1-bromohexane irritation (label B means before, A means after).* ***(B5)*** *Inflammatory cytokine release following isopropanol and 1-bromohexane irritation.* ***(B6)*** *Hematoxylin–eosin staining of integrated epidermis-on-chip (iEOC) system:(from top to bottom) control, isopropanol irritation and 1-bromohexane irritation.* ***(B7)*** *Tight junction maker ZO-1 staining of integrated epidermis-on-a-chip: control, isopropanol irritation and 1-bromohexane irritation. Scale bars:* 100 μm. *Reproduced from Ref.* (Zhang et al., 2021)

compartment. These models allow to investigate cell-cell crosstalk and provide more biomimetic barrier properties. In vitro, they exhibit high reproducibility and standardization and enable evaluation of wound healing and bacterial adhesion. Major drawbacks concern the limited lifespan and the limited cell types employed.

- human skin equivalents integrating other cell types to perform investigation of basic melanogenesis and vitiligo pathogenesis (incorporating melanocytes), innate immune response, irritant exposure and allergen assessment (incorporating immune or Langerhans cells); epidermal development, wound healing, pigmentation disorders and autologous transportation (incorporating stem cells) (Mathes et al., 2014; Duval et al., 2012; Ouwehand et al., 2011; Nissan et al., 2011). Dorsal root ganglion neurons were also incorporated to reconstruct a peripheral skin nerve system (Risueno et al., 2021). Models with trans-appendageal moieties were furthermore developed, e.g. hair follicles for substance penetration studies (Michel et al., 1999). Limitations include lower standardization and limited tissue survival.
- vascularized human skin equivalents are the next technological step which allows nutrients and oxygen supply and waste removal

resulting in extended tissue survival. This approach enables the assessment of transdermal penetration of drugs in the bloodstream, angiostatic therapies and adipose metabolism, impact of drugs on adipose tissue and angiogenesis. While long term cultivation becomes feasible, this technology is less standardized than the previous ones.

- skin-on-a-chip models promise to provide the ultimate step of technological innovation in the form of miniaturized microfluidic platforms which allow high throughput physiologically relevant studies at reduced costs by applying different physical and biochemical stimuli (including shear stress, mechanical forces and chemical gradients). Skin fragments have been either transferred to the chip from a biopsy or a HSE (Abaci et al., 2015; Kim et al., 2019a) or directly generated in situ (in an open structure or in channels as tissue-holding compartments) (Lee et al., 2017; Song et al., 2017, 2018a; Jeon et al., 2020; Kim et al., 2020; Sriram et al., 2018; Ramadan and Ting, 2016; Wufuer et al., 2016; Au - Risueño et al., 2021).

SOC advances underwent similar development phases from RHE (Abaci et al., 2015; Mohammadi et al., 2016) to HSE and integration of additional cell types, components and vascularization (Cui et al., 2022). RHE-based SOC employed young and mature keratinocytes with different level of stratification and junctional tightness, exhibited stability above 24 h and were employed for in vivo irritation assays (Zhang et al., 2021). HSE-based SOC exhibited better barrier functions due to an improved cell viability and were used for transdermal/topical drug permeation studies (Fig. 6 B1–B7) (Sriram et al., 2018; Alberti et al., 2017) and wound healing (Li et al., 2015; Biglari et al., 2019) and skin microbiome investigations (Applied In Vitro Toxicology, 2015). A 3D vinyl-based bilayer tissue model made of an epithelial and a stromal component was reported by Valencia et al. (2021) using immortalized human skin keratinocytes (hKCs, HaCaT cell line) and primary human dermal fibroblasts (hFBs). A microporous (polycarbonate) membrane was again employed to separate the skin model from a blood vessel channel used to recapitulate dynamic perfusion and drug delivery. Varone et al. introduced two vacuum channels around the epithelium chamber to apply mechanical forces (Varone et al., 2021).

Hair follicles were incorporated in SOC models by Atac et al. (2013). Integration of explants in SOC can provide access to all cell types and diseased skin but suffer for limited availability and donor variability. Multi-organ on chips integrating skin with other models (e.g. liver, intestine and kidney) to investigate their crosstalk are the next frontier (Wagner et al., 2013a; Maschmeyer et al., 2015a, 2015b) (see Section 2.5). Microfluidic arrays of dermal spheroids were implemented by Chen et al. as a screening platform for skincare products ingredients (Chen et al., 2021).

2.4. Vascularization models for testing intravenous administration

The vascular system has a critical role for maintaining homeostasis and organ-specific functions (Pradhan et al., 2020). Tissue survival in vivo is entirely dependent on delivery of nutrients through blood vessels, while vascular dysfunctions are associated to various chronic or acute disorders. Furthermore, several therapeutic agents are directly administered intravenously instead than reaching the bloodstream across other biological barriers/organs. Compared to oral administration, this route allows shorter times until effect and, importantly, permits to overcome impediments related to low gastro-intestinal solubility and permeability (Pocock et al., 2017).

Thus, it is not surprising that the recapitulation of micro-tissues and organoid vascularization became focus of intense research as a key tool for providing suitable disease models with superior biomimetic performance in investigating pathophysiology and testing drug efficiency. In this respect, it is worth noting that vascularization additionally consents to increase lifespan of OOC models and, for this reason, it is often integrated in various microphysiological systems (as already mentioned in some examples before). On the other hand, on chip models are relevant for the investigation of specific diseases of the vascular system such as atherosclerosis and deep vein thrombosis (Benam et al., 2015).

Various techniques were exploited and, in some cases, combined to produce network of perfused microvessels, vascularized micro organs (VMO) and micro tumors (VMT) (Osaki et al., 2018a; Dellaquila et al., 2021; Lin et al., 2019). Vasculogenesis and angiogenesis are the biological processes responsible for in vivo formation of new blood vessels leading respectively to de novo formation of vascular system and growth of capillaries from pre-existing vasculature (Vailhé et al., 2001; Risau, 1997). Driving these processes in vitro provides an effective strategy for a (random) formation of vessels by seeding precursors, stem or endothelial cells inside extracellular matrix and exposing them to vascular growth factor (e.g. VEGF) (Sekine et al., 2013). This approach permits to generate random networks of sub-100 μm vessels but presents limitations when perfusable vascular lumens are the target.

In this case, microfluidics, soft lithography, 3D printing and bioprinting provide useful alternatives and support. For example, soft lithography allows to realize perfusable microchannel networks by replica molding following an appropriately engineered CAD design. In this case, the (already discussed) membrane-based layout is a widespread strategy upon the pioneering work of Ingber group (Huh et al., 2010a) and was employed in various organ-specific models including lung, gut, liver, kidney, hearth, brain and blood-brain barrier. In Fig. 7 A, the case of application to liver is reported (Du et al., 2017). In particular, in the liver-on-a-chip model by Du et al., the four major hepatic cell lines were grown in two membrane-separated chambers to recapitulate liver functions (namely from base to top: hepatocytes, hepatic stellate cells, the liver sinusoidal endothelial cells and Kupffer cells).

Other architectures are based on lateral/planar microchannels (e.g. interconnected by sub-networks of smaller sizes) (Dellaquila et al., 2021). External pumps with valves or hydrostatic pressure consent to drive the flow in the perfusable vascularized systems. In all these cases, the use of scaffolds with predetermined geometries enables high control on lumen sizes, network interconnections, flow rates and imposed shear stress. Direct micromachining of microfluidic networks was also performed by laser patterning techniques with advantages in realizing layer-by-layer architectures but at higher cost (Fig. 7 B).

Templating and sacrificial molding methods are another option (Fig. 7 C). In this respect, 3D printing offers a cost-efficient approach through the use of cytocompatible sacrificial templates in engineered tissues but presents limitations in terms of minimal sizes (no less than ≈100 μm) (Miller et al., 2012). As examples, in skin-on-a-chip field, Abaci et al. and Mori et al. (Abaci et al., 2016; Mori et al., 2017) exploited respectively micropatterned alginate sacrificial layers or nylon threads successively removed in order to obtain hollow channels to be covered by endothelial cells (Abaci et al., 2016; Mori et al., 2017). A combination of 3D printing for the device layout and 3D bioprinting of the cellular layers was exploited by some authors as a mean to achieve high structural control (Kim et al., 2019b).

In various reports, biological processes and engineered-based fabrication techniques have been successfully combined to exploit the advantages of both worlds (Dellaquila et al., 2021; Kim et al., 2013; Wang et al., 2016) leading to microfabricated vessel scaffolds by lining microfluidic channels with endothelial cells (Fig. 7). For example, Hughes and Lee group realized perfusable microvascular networks connecting microfluidic channels without noticeable leakage. The adopted strategy was to pass through different stages of vascular development from vasculogenesis, to endothelial cell (EC) lining, sprouting angiogenesis and anastomosis (Fig. 7 D) (Wang et al., 2016). Then, they employed this approach to support the in vitro growth of 3D (vascularized) microtumors and to investigate the effect of drugs targeting growth factors in terms of regressing the vasculature (Sobrino et al., 2016a). Tumor cell extravasation dynamics was also investigated

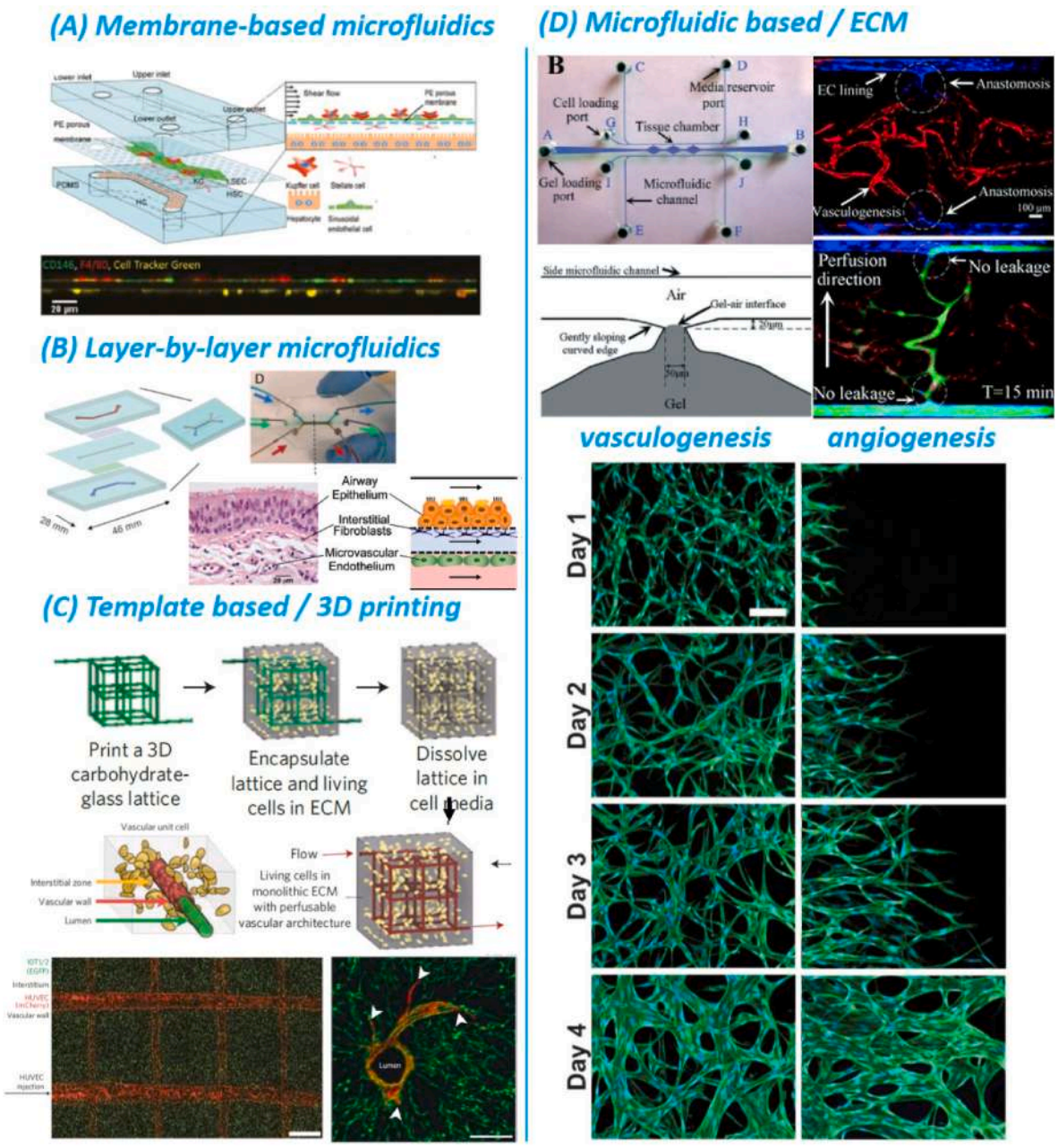

Fig. 7. Schematic representation of methods employed to vascularize 3D OOC models. These techniques can be divided into soft-lithography and 3D patterning approaches. **(A)** Membrane-based soft lithography technique in which a porous membrane is inserted among two microfluidic channels. Reproduced from Ref. (Du et al., 2017). **(B)** Layer-by-layer microfluidics consisting of assembled modular layers. Reproduced from Ref. (Sellgren et al., 2014). **(C, top)** Templating approaches in which a matrix is cast around the template. The template is subsequently removed, generating hollow channels, which can be seeded and perfused. **(C, bottom)** Three-dimensional printing (bioprinting) in which vascular and cell inks are used to generate a 3D tissue with embedded, perfusable vascular channels. Reproduced from Ref. (Miller et al., 2012). **(D, top)** ECM-based soft lithography in which microfluidic channels are filled with ECM (Wang et al., 2016). **(D, bottom)** Micrographs of vasculogenic and angiogenic vessel formation in the fibrin matrix as a function of time. Reproduced from Ref. (Kim et al., 2013).

using on-chip microvascular models (Chen et al., 2017) (see Section 2.2 for further details). Remarkably, vascularized OOC are suitable for screening the efficacy/toxicity of libraries of relevant compounds against multiple tissues in a more physiological environment. Finally it is worth mentioning that Pradhan et al. investigated how hemodynamic forces and vascular parenchymal mechanotransduction influences relevant pathways in organ-specific niches and pathophysiological states, a possible way toward developing mechanotherapeutics (Pradhan et al., 2020). A further option is to transfer tissues on chip, where further studies are then carried out.

In terms of bioavailability, blood organ barriers can however limit drugs in reaching their targets. For these reasons, numerous studies focused on the accuracy of microfluidic-based in vitro reproduction of these barriers in order to provide miniaturized and controllable platforms for investigating drug delivery and pharmacokinetics as well as nutrient/gas/waste exchange. The gut and lung cases were described before. Another important case is represented by the blood-brain barrier which is relevant for administering drugs to the brain and for developing therapies for neurodegenerative diseases (see Section 2.1 for details). Other examples of applications to liver and kidney are reported in Section 2.4 since these organs are key players in drug metabolism and clearance with impact on bioabailability and side effects/toxicity.

3. Microphysiological systems for (other) organs/disease studies and multi-organs platforms

3.1. Blood brain barrier and OOC for neurodegenerative diseases

The blood-brain barrier (BBB) separates bloodstream from brain tissue and is formed by specialized endothelial cells, pericytes and astrocytes up to neurons, as illustrated in Fig. 8 top (van der Helm et al., 2016; Osaki et al., 2018b). Its study attracted significant attention as the BBB represents a formidable challenge to access the central nervous system for delivery of pharmaceuticals and therapeutic antibodies against neurological disorders. Indeed, by implementing its neuroprotective function, the BBB tightly regulates transport of biomolecules and harmful compounds. It is characterized by low permeability to most chemical compounds and provides homeostasis for optimal neuronal function (van der Helm et al., 2016). To increase the throughput of present technologies and overcome their limitations, engineered microfluidic BBB models have been proposed. However, they must satisfy a number of criteria: high-fidelity in mimicking in vivo physiological microenvironment and relevant conditions/functions, possibility for investigating organ-level functions, stability for a prolonged period to permit real-time study, recirculating perfusion for drug permeability studies, and of course standardization and reproducibility (van der Helm et al., 2016).

Various proposed BBB-on-a-chip models rely on co-cultures of neurovascular endothelial cells and primary astrocytes on the two sides of a porous membrane (Wang et al., 2017). This approach was shown to better recapitulating in vivo conditions and to result in tighter junctions and lower barrier permeability than the case with only endothelial cells (Jeong et al., 2018). Moreover, it allows recirculation at physiologically relevant perfusion rates and the application of shear stress at in vivo levels. An example of this class of microfluidic BBB models is reproduced in Fig. 8 A1 (Wang et al., 2017) which summarizes all the main components and details of the layout used by Wang et al. for co-cultures of rat primary astrocytes and brain microvascular endothelial cells (BMECs) derived from human induced pluripotent stem cells (hiPSCs). Similarly, Park et al. combined hiPSC-derived human brain microvascular endothelium with primary human brain astrocytes and pericytes (Park et al., 2019). Notably, differentiation under hypoxic conditions enhanced barrier functionality with high levels of tight junction SLC and ABC proteins, functional efflux pumps and surface proteins modulated transcytosis capabilities for drug, peptide, nanoparticle and antibody.

When characterizing barrier-forming tissues, a crucial step is the assessment of barrier integrity and function, which should be maintained in time for the whole duration of the study. For this purpose, various in vitro techniques are available, from microscopy imaging of cell-cell adhesion proteins to measuring ionic currents, to flux of water or transport of molecules across cellular barriers (Arik et al., 2018). In their work, to evaluate barrier integrity, Wang et al. performed time lapse studies by immunostaining for the tight junction proteins, ZO-1 and claudin-5, while cell nuclei are stained in blue with DAPI as shown in Fig. 8 A2 (Wang et al., 2017). Recently, trans-endothelial electrical resistance (TEER) measurements (Fig. 8 A3) are attracting strong attention as an alternative electrical procedure for assessment of tight junction formation and comparison with in vivo conditions in various models including the blood-brain barrier (BBB), gastrointestinal (GI) tract, and pulmonary models (Srinivasan et al., 2015). Notably a tighter barrier was observed when using co-cultures.

To further analyze barrier function, permeability assays are commonly carried out using fluorescent tracers, large molecules (FITC-dextrans) and model drugs (caffeine, cimetidine, and doxorubicin) as well as permeability mediators with results compared with in vivo permeability coefficients values (Wang et al., 2017). In this respect, it is of particular interest an electrochemical permeability assay introduced by Wong et al. as a method to overcome the need for complex optical instrumentation and laborious manual sampling by using an electroactive tracer (Wong and Simmons, 2019).

Not all microfluidic BBB platforms with low permeability have been, however, implemented with the membrane-based approach. For example, Bang et al. established a 3D blood brain barrier model by the direct contact between a perfusable vascular network and astrocytes in an architecture comprising a vascular and a neural channel (Fig. 8 B1–B2) (Bang et al., 2017). These side channels were supplied by different media resulting in better barrier properties and viability with respect to the single medium cases. Notably, the vascular network permeability for FITC-dextrans was estimated to be similar to in vivo values and the authors also observed a good neurovascular interfacing and the presence of synapses.

Beyond facilitating the development of new treatments, the availability of such microfluidic models of tissue barriers can facilitate an improved understanding of their functionality and disruption which are associated to the pathophysiology of many diseases (Arik et al., 2018). For example, Brown et al. used a microfluidic model of the human neurovascular unit to investigate the inflammatory disruption of the blood-brain barrier, its metabolic consequences and repair mechanisms. Namely, a loss of barrier function associated to increased diffusion and reduced presence of tight junctions was observed upon inflammatory stimulation using lipopolysaccharides or a cytokine cocktail to mimic systemic and local infections. Then, the authors demonstrated how metabolite analysis can contribute to identify critical pathways in inflammatory response (Brown et al., 2016). Present limitations in BBB-on-chip field concern standardization of methods for quantification of relevant parameters such as barrier permeability and shear stress, making difficult a direct comparison in terms of performance (van der Helm et al., 2016).

Remarkably, microfluidic neurodegenerative diseases models for both the central and peripheral nervous system focusing on Alzheimer's disease, Parkinson's disease, and amyotrophic lateral sclerosis were implemented recapitulating their critical features with compartmentalized microenvironments for the co-culture of neurons, glial cells, endothelial cells, and skeletal muscle cells and the ability to reproduce chemical gradients and mechanical features (Osaki et al., 2018b).

To summarize, different (vertical) and planar architectures have been implemented with various cell lines co-cultured in order to model the BBB on chip. Other parameters to take into account in the chip design include membranes selection and ECM coating. The incorporation of physiological shear stress, inflammatory stimulation and the integration of sensors for TEER measurements provide advantages with respect to traditional methodologies.

3.2. Tumor models and organoids engineering for new drug development

The development of cancer-on-chip models is of particular interest for their potentials to recapitulate the cancer pathophysiology by reconstructing the highly complex tumor microenvironment (TME) composed by several factors, including extracellular matrix (ECM), blood vasculature, and multiple stromal cells, which control cellular function, proliferation and cancer metastasis.

Conventional in vitro models based on monolayer cultures are unable to accurately mimic the in vivo environment and, consequently, are less effective for drugs research. On the other hand, the use of animal models has limitations for high-throughput screening in preclinical drug testing because of high consumption of chemicals, time consuming operations, constraints in study of the mechanisms at play and species-specific differences. By combining modern microfluidic and tissue engineering technologies, tumors-on-chips (ToC) provide more biomimetic and high-throughput in vitro models. ToC can recapitulate the complex microphysiological features of disease microenvironments by enabling the production of three-dimensional models and replicating tumor and vasculature interactions, tumor angiogenesis and metastasis. As a consequence, they can accelerate drug development and screening.

In this scenario, tumor spheroids/organoids are considered the best

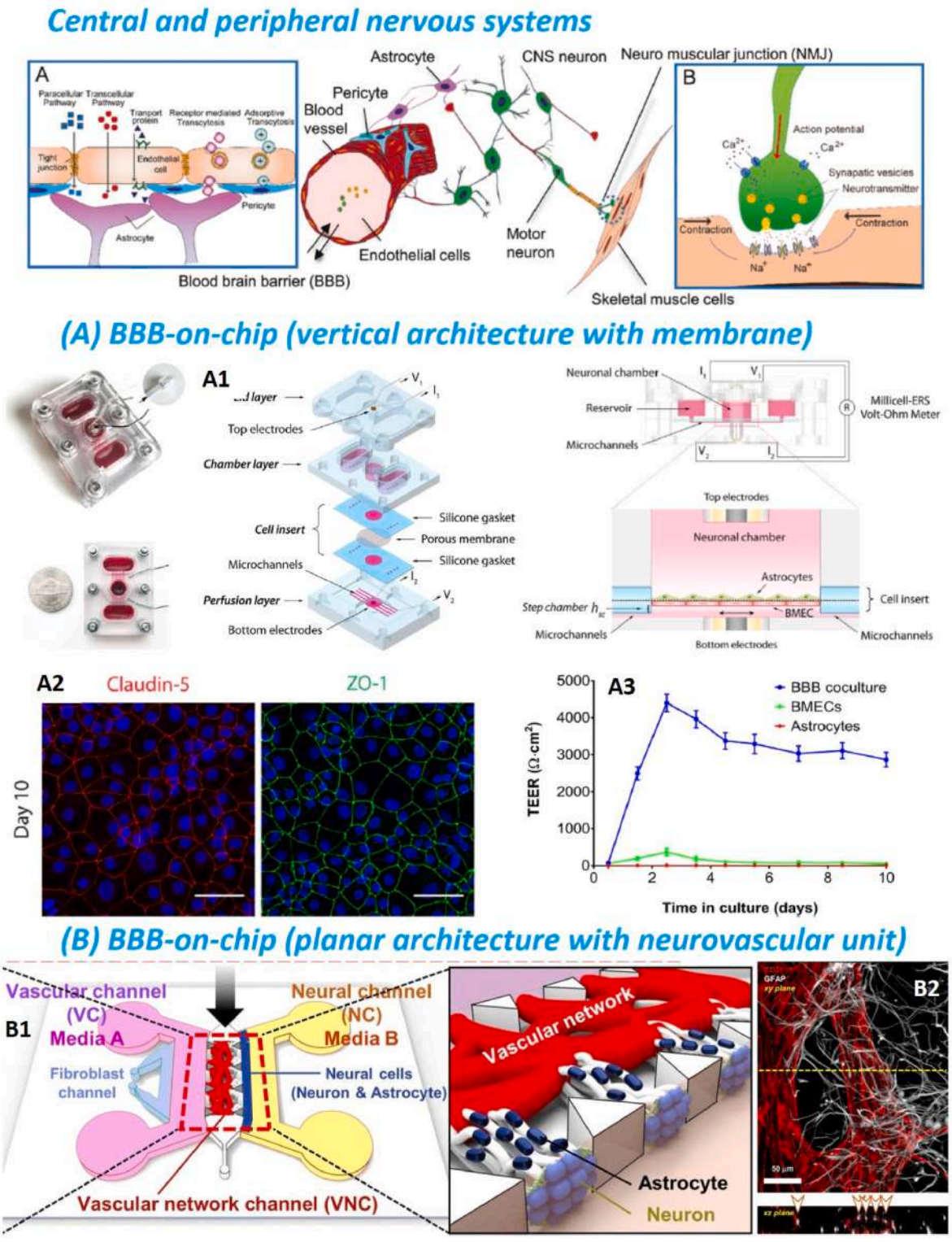

Fig. 8. (Top) The main players at the central and peripheral nervous systems (CNS and PNS involved in neurodegenerative diseases (Osaki et al., 2018b). **(top left)** At CNS level, the blood–brain barrier (BBB) separates bloodstream from brain tissue. It is characterized by tight junctions and a very low permeability with access through paracellular and transcellupar pathways. It involves different cell types: endothelial cells, pericytes, astrocytes and CNS neurons. **(top right)** At PNS level, motor neurons and muscle fibers form the neuromuscular junction, which is a chemical synapse. Muscle contraction is driven by signals transmitted by the motor neurons to the muscle in the form of acetylcholine release. Reproduced from Ref. (Osaki et al., 2018b) **(A1)** Vertical structure of the BBB-on-chip reported by Wang et al. and evaluation of barrier integrity **(A2)** by immunostaining for the tight junction proteins Claudin-5 and ZO-1 and **(A3)** by TEER measurements. Reproduced from (Wang et al., 2017); (**B1**) Planar microfluidic platform for neurovascular unit containing blood-brain barrier. **(B2)** Confocal microscopy image of the direct vascular network-astrocyte interface that confirmed direct contact on two axes, with contact points indicated in the xz plane through arrows. Reproduced from (Bang et al., 2017).

models for cancer research. They are self-assembled cancer cells aggregates with diameters from 100 μm to 1000 μm. Tumor spheroid formation attracted significant attention because they are able to better mimic the in vivo TME providing a more accurate platform for cancer investigation and therapeutic testing. Indeed, they are able to reproduce the extracellular matrix environment (ECM), cell–cell interactions and the presence of nutrients, metabolites and oxygen gradients (Kwapiszewska et al., 2014) beyond their 3D structure. Furthermore, they can be produced from a variety of tumor cell lines including human and patient-derived cells.

Conventional homogeneous spheroids formation is achieved with techniques such as hanging drop and rotating flask methods, and the use of external (e.g. electric field or magnetic) forces or non-adhesive surfaces. These techniques allow drug testing and performance analysis, and commercial systems are available on the market, such as Insphero, Aggrewells (Stem Cell Technologies) and Nucleon Sphera (ThermoFisher). However, they require frequent media exchange and are labor-intensive and time consuming. On the other hand, in microfluidic systems, procedures can be automated and the formation of tumor spheroids can be achieved from a small number of cells, with continuous infusion of the culture medium ensuring high cell activity, small sample and reagents volumes. This guarantees high sensitivity and integration, with advantages in terms of arraying the samples and testing various combinatorial treatments with high throughput.

Other studies addressed on chip investigation of tumor and vasculature interactions, tumor angiogenesis and metastasis. Among them, the self-assembly microvascular approach allows to recreate on chip tumor angiogenesis and to emulate metastatic cascade (Mollica et al., 2019) such as invasion/intravasation (Du et al., 2018), extravasion of tumor cell (Chen et al., 2016a, 2017; Song et al., 2018b) and perivascular niche (Xiao et al., 2019; Sobrino et al., 2016b; Phan et al., 2017; Marturano-Kruik et al., 2018). Indeed, typically in a metastatic cascade, first tumor cells invade the blood circulation passing the extracellular matrix and the vascular endothelium. Then cancer cells extravasate at the distant site travelling across the endothelium blood vessel to leave the circulation and colonize another tissue/organ giving rise to a new metastatic TME or secondary tumor formation (Xu et al., 2016; Lim et al., 2021; Zhang et al., 2022; Lin et al., 2020; Del Piccolo et al., 2021; Imparato et al., 2022) (Fig. 9 top).

In this respect, Du et al. (2018) reported a microfluidic co-culture system containing both breast cancer cells (MDA-MB-231) and noncancerous cells (MCF-10A or HDF-n), which was employed to investigate the influence of the tumor microenvironment on metastasis before intravasation into the vessels. A vascular endothelial layer was also recreated in order to mimic the semipermeable membrane function and the transendothelial nutrients transport in blood vessels. The authors demonstrated the ability of the developed tool to study the mechanism of tumor invasion into the stroma and to screen anti-metastatic drugs. Chen et al. (2017) instead presented a microfluidic platform with self-organized perfusable human microvascular networks formed over 4–5 days, after which the tumor was perfused and extravasation events were tracked over 72 h via standard confocal microscopy (Fig. 9 A). This assay allows a rapid quantification of tumor cell extravasation kinetics and can be used for the screening of therapeutic agents. As another example, Xiao. et al. (Xiao et al., 2019) reproduced on-a-chip the microvasculature as a perivascular niche model to evaluate the ex vivo dynamics of brain tumor stem-like cells (BTSCs) derived from glioblastoma patients. They found that the degree of colocalization between tumor cells and microvessels depends on the genetic and pathologic subtypes of the tumor samples and varies significantly across patients. These findings demonstrate the potential of the developed assay for ex vivo analysis of tumor cell dynamics and heterogeneity, representing a new route to study patient-specific tumor cell functions.

As described above, considerable efforts were dedicated to combine tumor cells and microvasculature on chip with the aim to achieve a more in deep understanding on the angiogenesis processes, the interaction of the cancer cells with the microvasculature and the metastasis cascade dynamics. However, the aforementioned models do not recapitulate the pathophysiology of vascularized solid tumor tissue, but it is known that this is a critical feature in cancer treatment. For this reason, novel technologies were developed to culture 3D solid tumor tissue (or tumor spheroids) with microvasculature on-a-chip (Lee et al., 2018a; Chung et al., 2017; Ayuso et al., 2018; Nashimoto et al., 2020; Haase et al., 2020).

In this respect, Nashimoto et al. interconnected a spheroid to a perfusable vascular network inducing angiogenic sprouts from the microchannels up to reaching vessel-like structures in the spheroid (Nashimoto et al., 2017) (Fig. 9 B1). Intriguingly, they demonstrated the presence of a continuous interconnection available to deliver biomolecules and drugs. The constructed vascular network allowed long-term perfusion culture of the tumor spheroids which result in a significant enhancement of the proliferation activities of tumor cells and in a non-conventional dose-dependent response to the anticancer drug, highlighting the importance of vasculature network flow in evaluating tumor activities in a drug screening platform (Nashimoto et al., 2020) (Fig. 9 B2–B4). This achievement allows to mimic in vivo TMEs and represents an important achievement for all the studies on spheroids/organoids/tumoroids. Using a vascularized tumor model based on microtumors arrays with independently-addressable elements, a blinded screen of both anti-cancer and anti-angiogenic drugs was performed by Phan et al. (2017) (Fig. 9 C). Further efforts may be necessary in this direction to develop more powerful tools for fundamental studies in tumor angiogenesis and drug testing targeting a clinical personalized therapeutic treatment.

3.3. Biomechanical structures - bone-on-a-chip and heart-on-a-chip

Biomechanical structures represent key components of the human body and include bones, muscles and tendons. Several 2D models for bones and cartilage employ a single type of cells (chondrocytes for the cartilage; osteoblasts, osteocytes, and osteoclasts for the bone) (Hodgkinson et al., 2022) with intrinsic limitations. Another important aspect is that a reliable in vitro model must allow to investigate the influence of mechanical cues. This can be achieved in different ways. An option consists in seeding bone cells on 2D membranes which are pneumatically or electromagnetically deformed to introduce cyclical cell stretching. In microfluidic systems, shear stresses can be recapitulated by means of fluid flow. Among the co-cultures models, it is worth mentioning the work by Middleton and coworkers who investigated osteocyte-osteoclast signaling under shear stress stimulation (Middleton et al., 2017). 3D models were implemented using different scaffold materials, prevalently natural hydrogels (such as collagen, gelatin, hyaluronic acid, alginate) and synthetic polymers (e.g. polyethylene glycol, PNIPAM, PDLLA). The first class presents advantages in terms of biocompatibility, permeability, similarity to natural tissues, presence of motifs for cell adhesion, non- or low-immunogenicity. Furthermore, they are low cost and they properties can be tuned, e.g. by chemical modification (e.g. ECM stiffness is relevant for osteoarthritis pathogenesis and progression (see Section 3.3 for details on Materials for OOC). Bone models were also engineered using hydroxyapatite as a constitutive material resembling bone mineralization products and favourable for proliferation and osteogenic differentiation of the human foetal osteoblast cell line (hFOB) (Tang et al., 2021). In particular, Tang et al. produced hydroxyapatite microfluidic chips by ceramic stereolithography with a diffusive mixer to achieve a concentration gradient of the model drug doxorubicin hydrochloride (DOX) and evaluate its half maximal inhibitory concentration (IC50) (Tang et al., 2021). Hydroxyapatite-based nanocomposites are attractive materials for bone tissue engineering and their cytocompatibility was demonstrated with respect to the MG63 osteoblast-like cell line (Scialla et al., 2017). Recently, vascularized bone-on-chip models attracted attention (Whelan et al., 2021) and a neuro-vascularized bone chip was implemented by

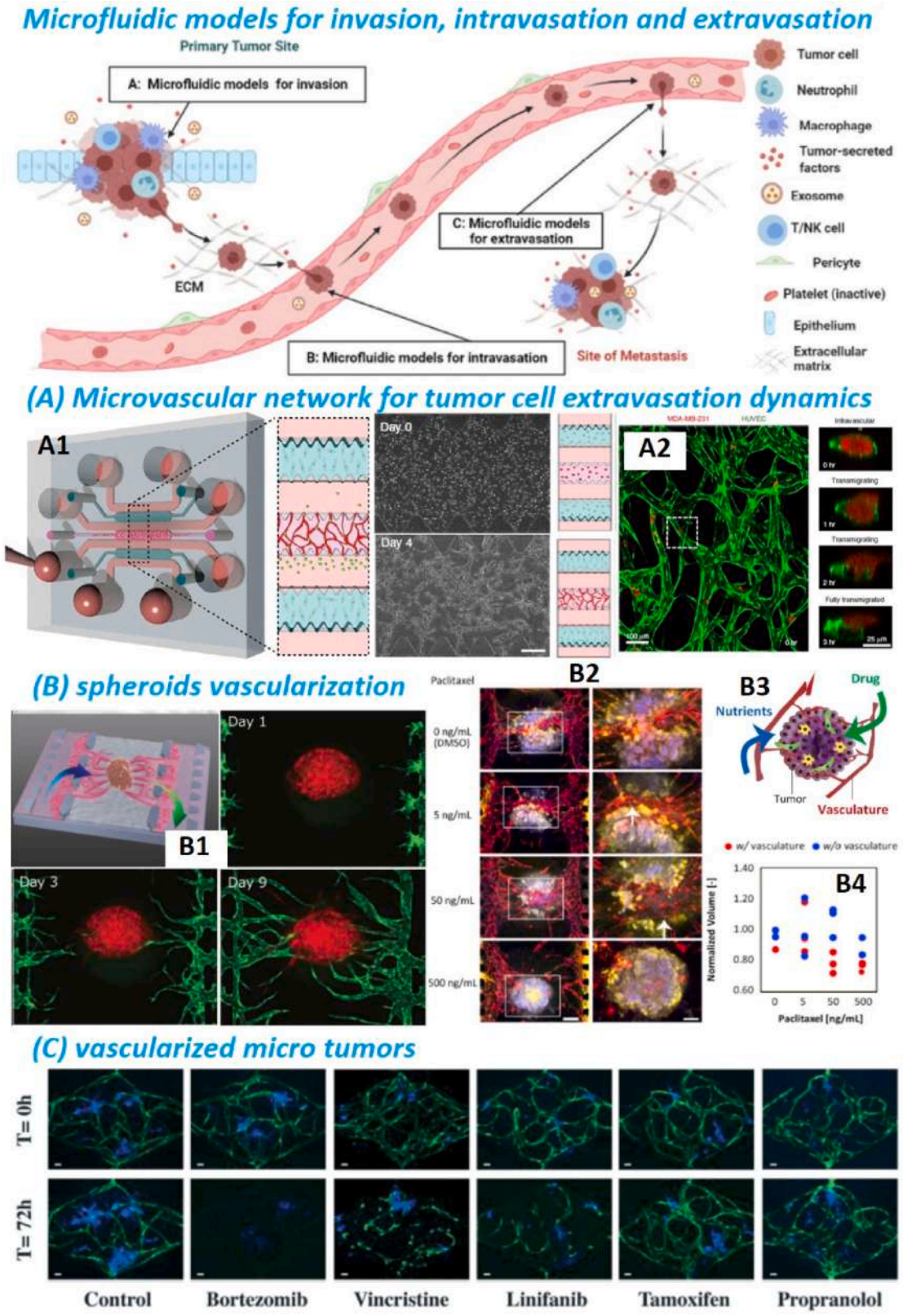

Fig. 9. (Top) *Microfluidic models including metastatic steps from invasion to intravasation and extravasation. Reproduced from Ref.* (Zhang et al., 2022) ***(A1)*** *Microfluidic platform with self-organized perfusable human microvascular networks formed over 4–5 days.* ***(A2)*** *Confocal image of a region of tumor-perfused (red) microvascular network (green) and cross-sectional views of a transmigrating tumor cell (right sequence) with extravasation scoring. Reproduced from Ref.* (Chen et al., 2017). ***(B1)*** *Schematic diagram and fluorescent micrograph of a sferoid interconnected to a perfusable vascular network inducing angiogenic sprouts. Reproduced from Ref.* (Nashimoto et al., 2017)**.** ***(B2)*** *Immunofluorescence images of the tumor spheroid with the vasculature under drug administration at different doses.* ***(B3)*** *Tumor vasculature for nutrients and drugs.* ***(B4)*** *Spheroid volumes as a function of drug concentration calculated from sequential histological sections Reproduced from Ref.* (Nashimoto et al., 2020). ***(C)*** *VMT arrays for drug screening with ECFC-EC formed vascular networks around HCT116 colorectal cancer cells and evaluation of drug efficacy on tumor growth and the associated vasculature quantified after 72 h (reproduced from* (Phan et al., 2017)*).*

Neto et al. with three channels comprising nerve, vascular and bone unit in order to investigate the response to inflammatory bone conditions and its effect first on the vascular unit and then on the nerve unit (Neto et al., 2102) (Fig. 10 A1-A2). This platform can provide a useful tool for drug development and the authors investigated anti-inflammatory drug nanodelivery by means of nanoparticles. In another study, bone regeneration was also studied on chip (Galvan-Chacon et al., 1002).

Muscles are the other major biomechanical structures beyond bones. In this respect, heart-on-a-chip models assume particular relevance since cardiac pathologies have high impact on worldwide morbidity and mortality rates. Furthermore, there is a high incidence of cardiovascular drug toxicity combined with the severity of adverse drug reactions in late-stage drug development (Savoji et al., 2019). For these reasons, human heart muscle on chip models have been developed to mimic healthy and pathological cardiac tissues and provide high-throughput tools alternative to animal models for testing cardiovascular drugs, cardiotoxicity and cardioprotective efficacy in preclinical trials (Meyer et al., 2019). In these studies, the cardiac/myocardial mechanics and heart muscle contractility are central indicators and contractile force development can be a phenotyping issue in cardiomyocyte-on-a-chip models (Meyer et al., 2019). Microcantilevers are a hallmark of cardiac OOC. In a pioneering work, Legant et al. reported 3D myotubes attached to MEMS microcantilevers as tissue gauges to measure the microtissue-generated forces (Legant et al., 2009). Few years later, Agarwal et al. recapitulated heart ventricle architecture on flexible cantilevers of soft elastomers, whose deflection was used to evaluate the generated diastolic and systolic stresses (Agarwal et al., 2013). The integration of flexible strain gauge sensors is a characteristics of the architecture from Parker group to monitor the contractile stress and beat rate of the reconstituted cardiac tissue (Lind et al., 2017a) and how they are influenced by administration of bioactive compounds and drugs (see also Section 3.2 for discussion on sensors for OOC). The addition of endothelial barrier model then permitted them to test the delivery through the blood vessels toward heart musculature (Lind et al., 2017b). A dose–response analysis on the effect of 12 cardiac and cardiotoxic drugs was instead carried out on a model of the ventricle laminar structure reconstituted by Lind et al. using cardiomyocytes derived by human induced pluripotent stem cells (Lind et al., 2017b). In a recent

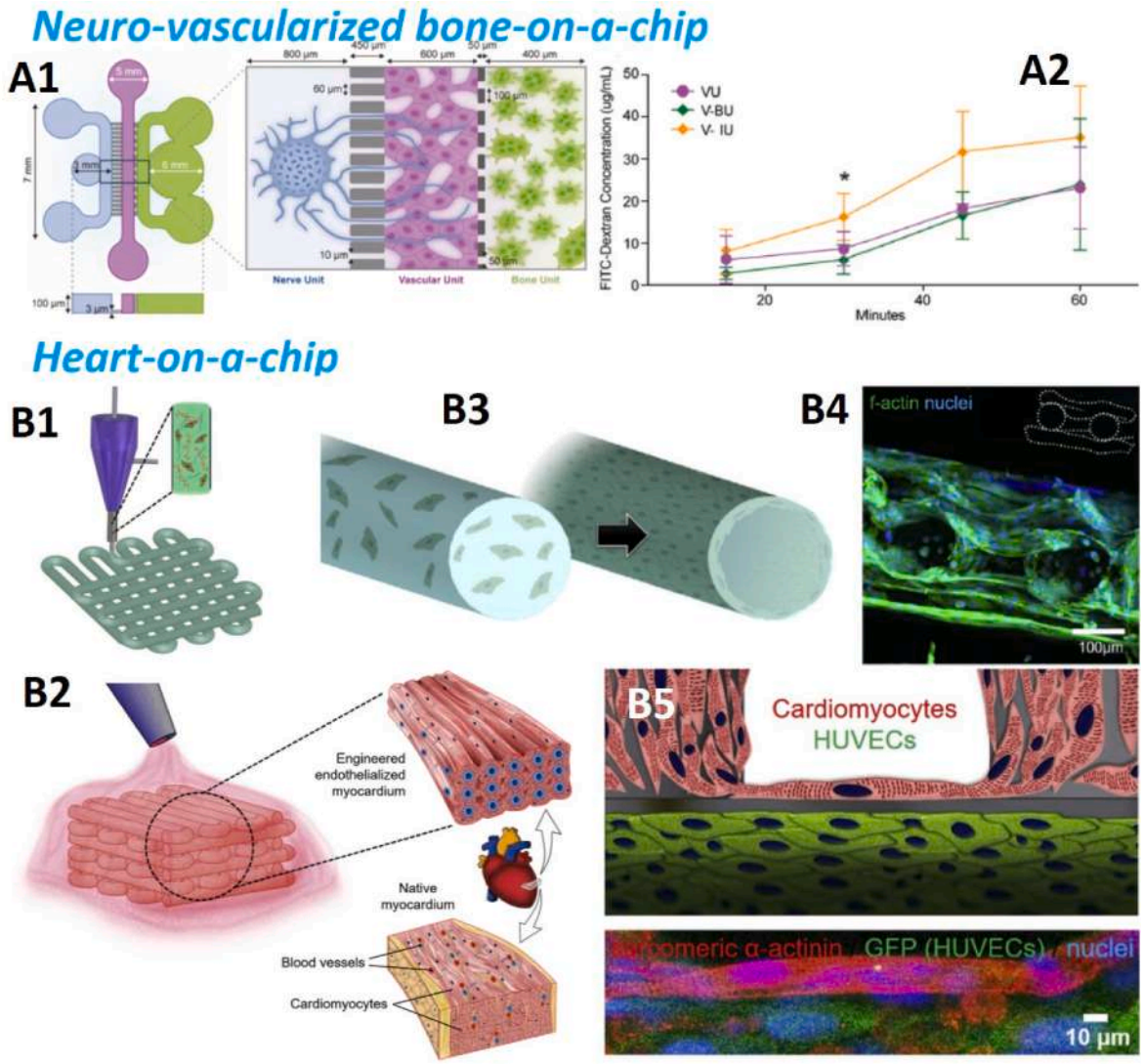

Fig. 10. **(A1)** *Model of neuro-vascularized bone chip. Reproduced from Ref.* (Neto et al., 2102). ***(A2)*** *Permeability of the endothelial barrier evaluated at the vascular unit adjacent to the bone inflammatory unit (V-IU)—osteoclasts under IL-1β exposure—and compared to vascular unit adjacent to the physiological bone unit (V-BU)—osteoclasts in standard culture conditions.* ***(B1–B2)*** *Schematic diagrams of the process for fabricating endothelialized myocardium by 3D bioprinting.* ***(B3)*** *Schematics of the assembly of human umbilical vein endothelial cells encapsulated in bioprinted microfibers into a layer of endothelium.* ***(B4)*** *Confocal fluorescence micrograph indicating the formation of the endothelium by human umbilical vein endothelial cells.* ***(B5)*** *Schematic and confocal fluorescence images of an endothelialized myocardial tissue realized by seeding neonatal rat cardiomyocytes on to the bioprinted endothelialized microfibrous scaffold. Reproduced from Ref.* (Zhang et al., 2016).

work, Ren et al. validated the maturation and phenotypic changes of cardiomyocytes cultured in well-aligned structures and successfully reproduced their synchronous beating upon electrical pulse stimulations (Ren et al., 2020). DOX-induced cardiotoxicity and the cardioprotective efficacy of CAR and IVA drugs were then assessed.

In terms of real time monitoring, transepithelial electrical resistance (TEER) sensors and multi-electrode arrays (MEAs) were used for evaluating tissue barrier function and recording cardiac activities (see Section 3.2) (Maoz et al., 2017). Photonic crystals provided alternative self-reporting monitoring tools of cardiomyocytes activity (Shang et al., 2020). Furthermore, bioprinting is starting to have a significant impact on the field. Indeed, Zhang et al. fabricated endothelialized myocardium model capable of spontaneous and synchronous contraction by printing endothelial cells within microfibrous hydrogel scaffolds and then seeding cardiomyocytes (Zhang et al., 2016) (Fig. 10 B1–B5). An aorta smooth muscle-on-a-chip was implemented by Abudupataer and coworkers (Abudupataer et al., 2021).

A further target for of large interest is represented by OOC models for amyotrophic lateral sclerosis (ALS) and neuromuscular development and disease which were developed combining human iPS-derived muscle cells and optogenetic motor neurons (Osaki et al., 2018c; Arjmand et al., 2022; Fralish et al., 2021). However, they are not discussed here for space constraints. In general, mechanobiology and mechanotransduction attracted large interest for the relevance in many biological processes. For this reason, biomechanical aspects have been also investigated in lungs and gut as discussed above (e.g. simulating breath and peristaltic stimuli). In this respect, OOC platforms provide advanced tools for investigation under well controlled and engineered conditions.

3.4. Metabolism-on-chip – liver, kidney and multi-organ models

Beyond the intestine, liver, kidney and pancreas on chip models were investigated. They are relevant for considering the role of drug metabolism/clearance beyond absorption, as well as for assessing potential organ damage and for evaluating multi-organ interactions (see Section 2.5) (Bovard et al., 2018; Maschmeyer et al., 2015a; De Gregorio et al., 2020; Foster et al., 2019; Christoffersson et al., 2019; Tan et al., 2019; Decsi et al., 2019; Deng et al., 2019; Theobald et al., 2018, 2019; Lee and Sung, 2018; Ong et al., 2019; Vernetti et al., 2017; Bavli et al., 2016; No et al., 2015; Bale et al., 2014; Esch et al., 2014; Shintu et al., 2012a; Zhang et al., 2009; Fabre et al., 2020; Phillips et al., 2020; Peel et al., 2019; Musah et al., 2017a, 2018; Wilmer et al., 2016; Jang et al., 2013; Miller and Shuler, 2016a).

3.4.1. Liver-on-a-chip

The liver is responsible for various functions including the production of bile, serum proteins (albumin), and lipoproteins, and it has a key role in the metabolism of amino acids, lipids, and carbohydrates taken with food. It is also involved in the detoxification process of endogenous (bilirubin) and exogenous products such as drugs. The detoxification process can lead to drug-induced liver injury (DILI). Animal models and in vitro cell culture models were used to evaluate drug-induced damage to the liver. However, due to the species-specific differences that exist between animals and humans and due to the low sensitivity of in vitro models, neither type has led to good results in the prediction of DILI (Ware and Khetani, 2017; Jang et al., 2019). In this respect, Organ-on chips (OOC) can again provide useful tools to mimic the functional and structural unity of the liver, including physical and chemical stimuli (Gough et al., 2021).

A multispecies liver-on-chip could be helpful to understand toxicities detected in animal models in order to better determine human safety. For this reason, Jang et al. (2019) realized a liver-on-chip to study the different types of toxicity in the liver of dogs, rats, and humans when they are treated with different drugs. Their chip was composed of a top parenchymal channel, where primary rat, dog or human hepatocytes were seeded on a porous ECM (extracellular matrix)-coated membrane. Then in the bottom vascular channel below the membrane, sinusoidal endothelial cells (LSEC), Kupffer cells and stellate cells were seeded (Fig. 11 A). To verify if this liver-on-chip could be helpful to predict species-specific DILI responses, the authors evaluated the hepatotoxic effects caused by bosentan, an endothelin receptor antagonist vasodilator, that induces cholestasis in humans but not in dogs or rats, using the three species models. As shown in Fig. 11 B, the administration of Bosentan at 1, 10 and 100 μM led to a decrease in albumin secretion in dog and human chips but not in rat chip. Moreover, the plasma concentration of bosentan that has been associated with DILI in humans is similar to the concentration in the human liver-chip at which they observed toxicity. The chip was also more sensitive compared to culture plates and this could be due to the presence of a fluid flow and better hepatocyte functionality. In another study, Jang et al. studied the toxic effect caused to the liver by the generic analgesic acetaminophen (APAP), which through its toxic and reactive metabolite N-acetyl-p-benzoquinone exhausts cellular glutathione and leads to oxidative stress in the cells. This process was observed through a cellROX fluorescent probe that binds to reactive oxygen species (Jang et al., 2019).

Hepatotoxicity tests were performed by Bircsak et al. (2021) using a multiwell microfluidic plate, Mimetas OrganoPlate® 2-lane (Fig. 11 C). In this case, the liver-on-chip is present in OrganoPlate 2-lane and consists of an organ channel where they seeded clusters of pluripotent stem cell (iPSC)- derived hepatocytes (iHep) on an extracellular matrix, and a perfusion channel where they seeded HMEC-1 endothelial cells and differentiated THP-1 into macrophages. Cells were shown to remain viable for 15 days by secretome measurements (albumin and urea secretion) and image-based analysis. To demonstrate ability to discover hepatotoxicity, the authors treated the cells with troglitazone (180μ M) as a hepatotoxin for positive control, and 0.5% dimethyl sulfoxide (DMSO) as vehicle control. Then, similar conditions with 72 h exposure time and the same assays were employed to validate the liver toxicity of a library of 159 compounds by means of a Toxicological Prioritization Index (ToxPi score), which is a dimensionless weighted linear combination of %live iHep, urea, iHep nuclear size and albumin. Among 159 compounds, 39 were found to be toxic and 34 of them showed a decrease in iHep viability compared to vehicle control (DMSO). Then, for dose-response evaluation, the authors considered 21 compounds from the previous screening and these studies confirmed all true negative and true positive compounds, except hyproniazide. These results suggest that the liver-on-chip created in the OrganPlate detects the hepatotoxicity of most compounds and it is possible to perform more chronic exposure analysis with this platform using several time points and additional readings (Bircsak et al., 2021).

Another intriguing study by Tsamandouras et al. (2017) described hepatic drug metabolism changes in the human population using physiological microsystems with hepatocytes taken from different donors. For each donor, they analyzed the metabolic depletion profiles of six different drugs and confirmed that there is an inter-donor variability by comparing the expression levels of metabolism-related genes and other liver functions. Notably, TEER measurements and pH changes of HepG2 hepatoma cell line using a chip-embedded non-toxic sensor were employed by Farooqui et al. (Farooqi et al., 2021) for monitoring drug toxicity on cells exposed to various concentrations of drugs such as doxorubicin, epirubicin and lapatinib. Using this liver-on-chip, the authors demonstrated ability to provide real-time data on drug-induced liver injury in vitro (Fig. 11 D).

3.4.2. Kidney-on-a-chip

The kidneys have the task of filtering metabolic waste products from the blood and expelling them through the urine. Through their functional unit, the nephron, the kidneys maintain the correct hydro-saline balance in the body. Furthermore, they play a key role in drug elimination and therefore may be susceptible to drug-induced nephrotoxicity, which can lead to acute or chronic kidney injuries (Li et al., 2017; Cohen et al., 2021). Drugs that can cause nephrotoxicity include antimicrobial,

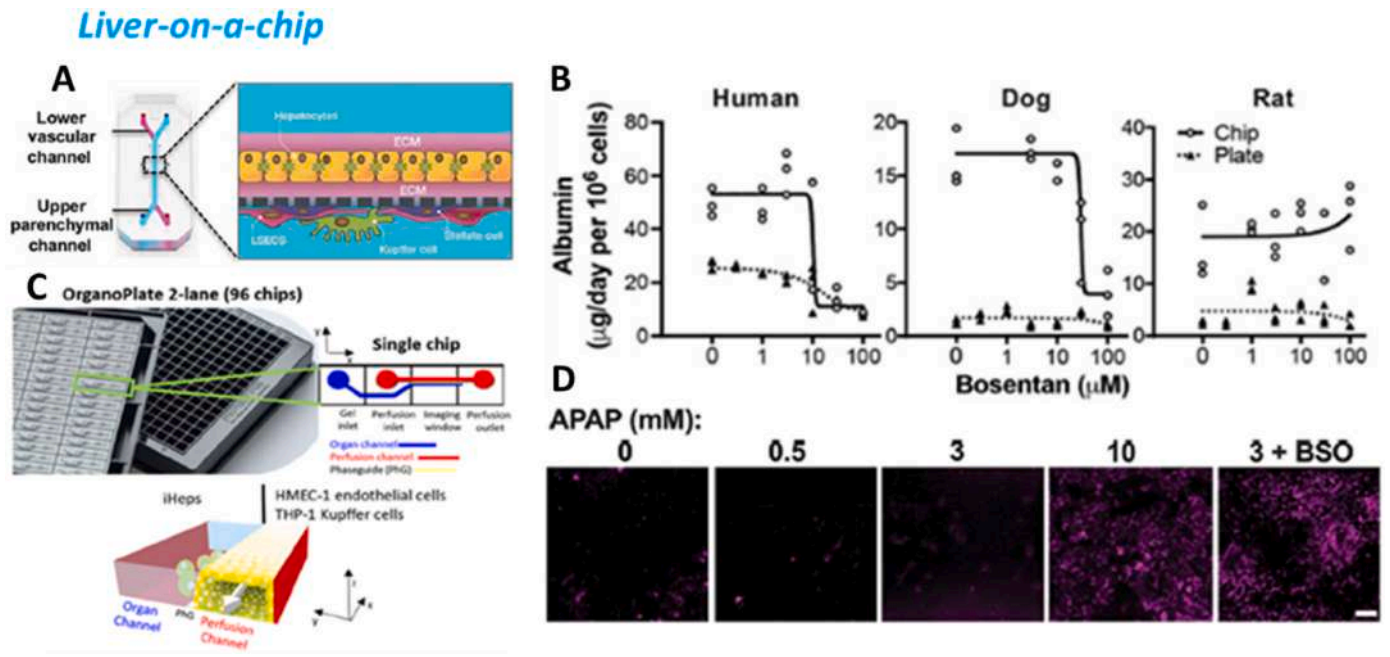

Fig. 11. Liver-on-chip. **(A)** Liver-on-chip diagram showing which hepatocytes are seeded in the upper channel and Kupffer cells, Stellate cells and LSEC are seeded in the bottom channel. Reproduced from Ref. (Jang et al., 2019). **(B)** Species-specific drug-toxicities in a rat, dog and human liver-chip. Albumin secretion after daily administration of Bosentan at 1,3,10, 30 and 100 μM for 3 days in human chips with two kinds of cells (hepatocyte and LSEC), and plates only with hepatocyte monoculture, and for 7 days in dual-cell dog and rat chips and plates. Reproduced from Ref. (Jang et al., 2019). **(C)** OrganPlate 2-lane. Image of OrganPlate 2-lane with 96 chips and schemes of organ channel and perfusion channel separated by a phaseguide(PHG). Reproduced from Ref. (Bircsak et al., 2021). **(D)** Detection of liver injury caused by acetaminophen(APAP). Images of ROS intensity after daily administration of APAP at 0.5, 3 and 10 mM in human chips. Reproduced from Ref. Jang et al. (2019).

chemotherapeutic, immunosuppressive and analgesic agents (Perazella, 2009). Organ-on–chip (OOC) technology can provide useful tools to reduce the nephrotoxic potential of novel drugs by mimicking organ functions and the complexity of the native tissue better than animal models and 2D culture models due to the presence of a fluid flow, pressure and a co-culture of various types of cells (Ashammakhi et al., 2018).

For example, Yin et al. (2020) employed a kidney-on-chip model to evaluate nephrotoxicity induced by some nephrotoxic drugs such as cisplatin (DDP), gentamycin (GM) and cyclosporin A (CsA). Specifically, they developed a microfluidic platform, where renal proximal tubule epithelial cells (RPTEC) were seeded in the upper layer on a polycarbonate (PC) membrane coated with extracellular matrix (ECM) collagen, while peritubular capillary endothelial cells (PCECS) were seeded in the bottom layer on another PC membrane coated with ECM collagen (Fig. 12 A-B). Their configuration comprised a peristaltic pump that controls the flow rate of the cell culture medium into the chip, a temperature control to maintain an optimal culture medium temperature and matching catheters. The effects of different concentrations of DDP, GM and CsA were evaluated on the kidney-on-chip and compared with results from the Petri dishes (in static condition) with a live/dead assay and a cell counting kit-8 (CCK-8) (Fig. 12 C). Remarkably, Yin et al. demonstrated that the number of live cells was higher in the fluidic condition of the chip than in the static group proving that the microfluidic system can be used for long-term cell culture and nephrotoxic drug screening (Fig. 12 D) (Yin et al., 2020).

In another study, Vormann et al. (2021) used three-lane OrganPlate, purchased by Mimetas, to create a 3D microfluidic platform for the detection of drug-induced kidney injury (DIKI) in the development of new drugs (Fig. 12 E-F). This platform presents: (i) an upper perfusion channel, where they seeded the human primary renal proximal tubule epithelial cells (RPTEC) and human immortalized proximal tubular epithelial cells with organic anion transporter 1 (CiPTEC-OAT1), (ii) a central channel loaded with extracellular matrix gel composed of collagen I and (iii) a bottom perfusion channel where culture medium was added. The channels were divided by structures called Phaseguide that work like pressure barriers. Afterwards, the cells were subjected to a treatment with four nephrotoxic compounds (tenofovir, cyclosporin A, tobramycin and cisplatin) and various assays were carried out to verify the damaging effect of these drugs on the kidney. Cell viability was determined with the cell counting kit-8; instead membrane integrity was observed with lactate dehydrogenase (LDH) activity and with the β-N-acetylglucosaminidase (NAG) – assay kit. They also evaluated gene expression of toxicity and nephrotoxicity markers and performed detection of miRNA in medium cell culture and drug transporter assays. After having chosen certain concentrations of nephrotoxic compounds, these have been shown to cause a decrease in Ci PTEC-OAT1 cell viability and an increased release of LDH for tobramycin and cyclosporin A at the highest concentration tested. With the same concentrations of nephrotoxic compounds administered to the RPETC, reduced cell viability was instead seen only after exposure to tobramycin, thus resulting in the RPETC being less sensitive than the CiPTEC-OAT1 (Vormann et al., 2021).

In ref. Kim et al. (2016), Kim et al. demonstrated the nephrotoxic effects of the antibiotic gentamicin with cell injury markers, such as cell viability and membrane permeability, and they also compared the nephrotoxicity of the gentamicin, using different systems that simulate the pharmacokinetics of continuous infusion and bolus injection in humans. Of the two systems, the one that causes less nephrotoxicity is the one that mimics a once-daily bolus injection. This approach could be used in a large range of drug-induced nephrotoxicity studies. Other researchers used the kidney-on-chip approach to demonstrate the non-toxicity of a compound. For example, the microfluidic platform in ref. (Li and Tian, 2018a) presented human embryonic kidney cells encapsulated in gelatin methacryloyl (GelMA) to simulate the microenvironment and the main functions of the kidney. By administering 30 μM of kaempferol to the embryonic kidney cells for 12h, Li et al. did not notice any cell damage thus demonstrating the non-toxicity of

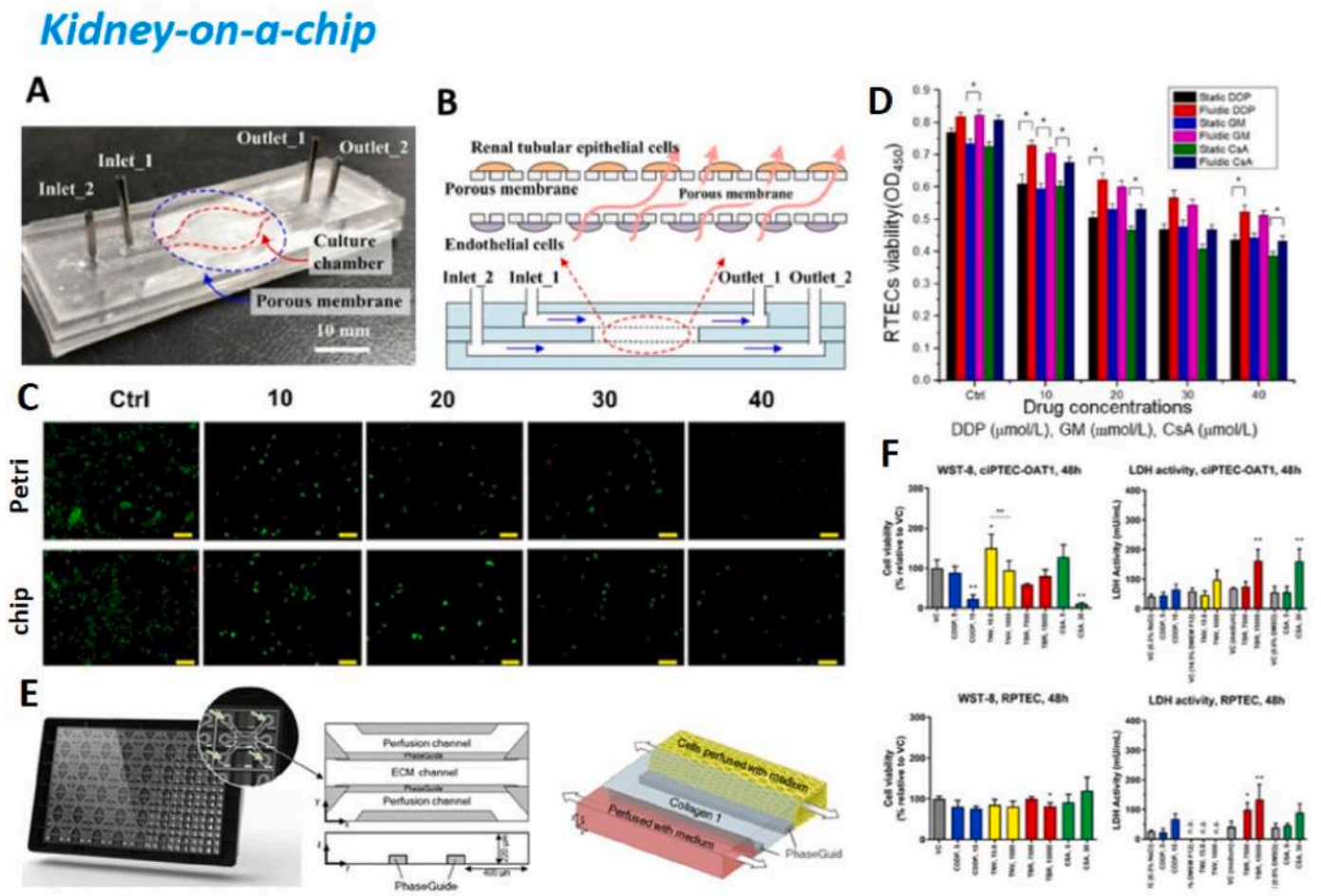

Fig. 12. **(A–B)** Image and scheme of a microfluidic kidney-on-chip made of three PDMS layers, two membranes, two inlets and two outlets. Reproduced from Ref. (Yin et al., 2020). **(C)** Live/dead cells (RPTECs) assay: live and dead cells (RPTECs) were labelled in green and red respectively. They used different concentrations (10,20,30 and 40 μmol/L) of DDP, under static conditions on Petri dishes and fluidic conditions on chip. Reproduced from Ref. (Yin et al., 2020). **(D)** Statistical analysis: CCK-8 of DDP, GM and CsA under static and fluidic conditions using a microplate reader (*p < 0.05, **p < 0.01). Reproduced from Ref. (Yin et al., 2020). **(E)** Scheme of the Mimetas kidney-on-chip. **(F)** Release of LDH and cell viability upon exposure to model nephrotoxicants cisplatin(CDDP), Tenofovir (TNV), Tobramycin (TBR) and Cyclosporin A (CSA) in RPTEC and in ciPTEC-OAT1 after 48 h *p < 0.05, **p < 0.01. Reproduced from Ref. (Vormann et al., 2021).

kaempferol, a bioactive metabolite from spearmint.

3.5. Multi-organs on chip platforms

Multiple organs on chip platforms (MOC) are the ultimate frontier in OOC research where different organs compartments are interconnected into miniature 'body-on-a-chip' microphysiological systems (MPS). The ambition is to recapitulate organ-organ interaction/crosstalk, physiological relations, methabolic pathways, significant biological barriers and whole-body drug response with an in vivo-like sequential organ-to-organ transfer of media. Intestine models account for absorption and metabolism of drugs, liver for their metabolism and kidney for clearance/excretion to enable a more appropriate evaluation of systemic effectiveness, accuracy and safety of drugs (Maschmeyer et al., 2015b). In this section, we describe this research keeping the focus on drug development from oral-administered (in digestion-on-chip) to inhaled (e.g. lung/liver models) and transdermal-administered drugs (integrating skin). Then some examples of MOC platforms for assessing drug availability and cytotoxicity on tumors, brain and heart are discussed, including applications for brain metastasis studies.

The bioavailability of two orally-administered small molecules (omeprazole and verapamil) was analyzed by de Haan et al. (de Haan et al., 2021). Specifically, the authors employed a three-stages compartmentalized chip to mimic the digestion chain representing mouth, stomach and intestine. For this purpose, three y-shaped micromixers were connected in series adding sequentially saliva, gastric juice and intestinal juice to the previously-treated sample. Finally, the output chime and an additional cell culture matrix were inputted in a fourth micromixer, whose outlet was connected to a flow-through transwell that contains a co-culture of human colorectal adenocarcinoma cell line (Caco-2) and human colon adenocarcinoma mucus-secreting cell line (HT29-MTX-E12). Mass spectrometry (MS) was used for analysis. By means of this flow-based digestion-on-chip, the break down of omeprazole upon exposure to gastric acid was observed, while it arrives undamaged at the cell barrier if added in a way that emulates an enteric lining. Conversely, verapamil was not affected by digestion. A decreased absorption of verapamil was also noted when dissolved in apple juice as matrix (de Haan et al., 2021).

Toxicity studies on inhaled substances were instead the target for Bovard et al. (2018), who combined lung and liver on a chip consisting of a fluidic plate and a reservoir made of polyetheretherketone (PEEK), a nonabsorbent material for small molecules. In the lung compartment, normal human bronchial epithelial (NHBE) cells were cultured at the air-liquid interface (ALI), while the liver compartment consisted of HepaRG liver spheroids. The aim was to mimic the human physiological response that occurs upon inhalation of substances, which are metabolized by both lung and liver CYP enzymes. In presence of liver spheroids, aflatoxin B1 (AFB1) toxicity decreased compared to NHBE lung cells

alone due to crosstalk between the two cell types. Thus such lung/liver MOC platform may be useful for evaluating the toxicity of new inhaled drugs used in the treatment of lung diseases (Bovard et al., 2018). Both inhalation- and intravenous administration were instead the target of comparison in terms of effectiveness and potentially toxicity in the study by Miller and coworkers, whose multi-organ platform integrated lung (including ALI), liver and breast cancer in a single chip (Miller et al., 2020). The cultured cell lines were A549 for the lung, HepG2 C3A for the

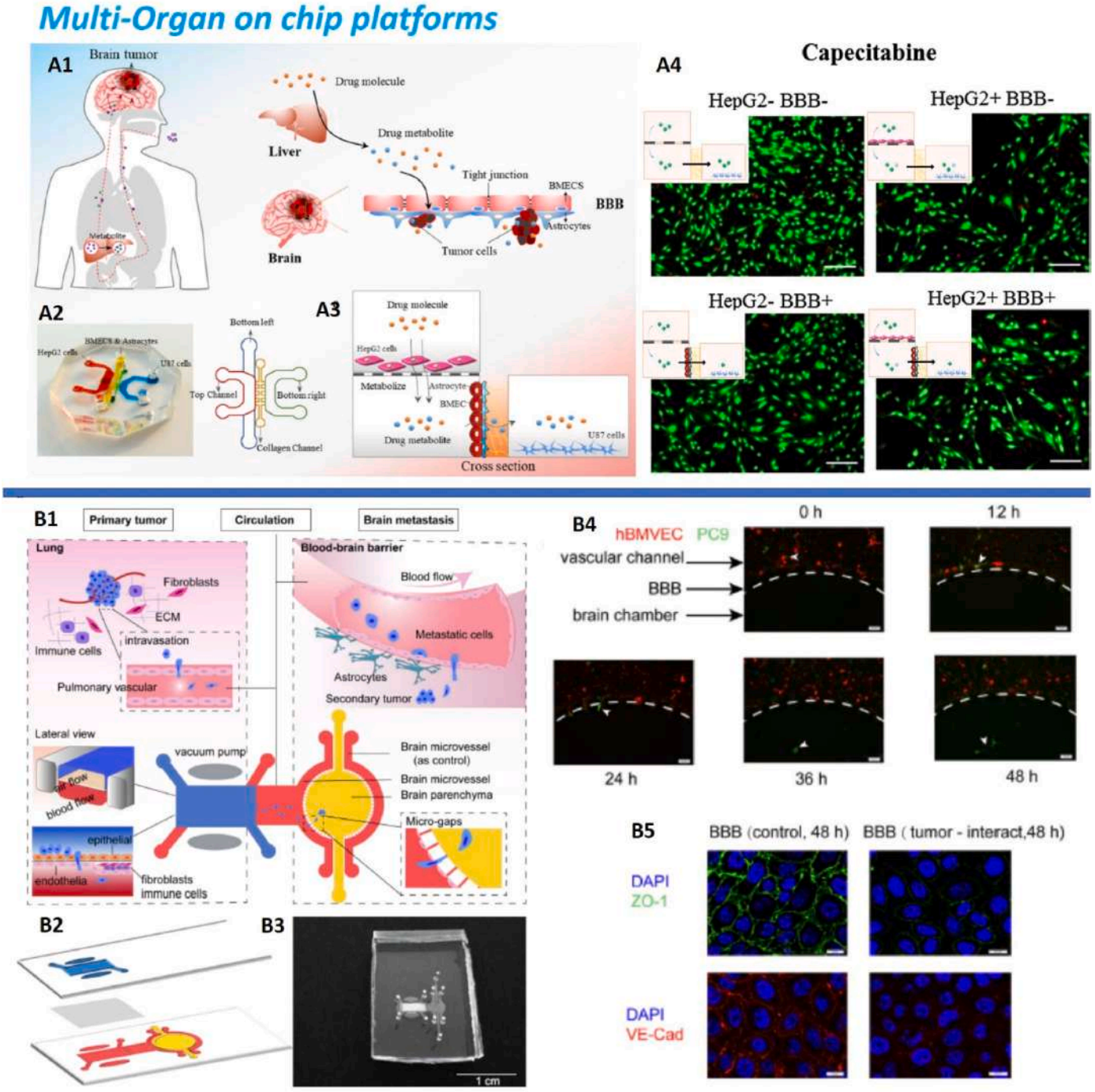

Fig. 13. **(A)** Multi organ-on-chip (liver and brain) platform: **(A1)** Pathway for oral drugs administration to brain tumors through liver metabolic activity and across the BBB. **(A2)** The MOC assembled by Li et al. to recapitulate this process using HepG2 cells in the top (liver) channel, brain microvascular endothelial cells (BMECS) and cerebral astrocytes in the bottom left and U87 cells in bottom right channels. **(A3)** MOC cross-sectional view. **(A4)** U87 cell viability in presence/absence of the liver compartment and the BBB upon administration of 80 μM CAP for 2 days. Live cells stained green, dead cells in red. Bar: 50 μm. Reproduced from Ref. (Li et al., 2021). **(B)** MOC device for the investigation of lung cancer-derived brain metastasis. **(B1)** Pathological process and its recapitulation on chip by Liu et al. (Liu et al., 2019a) through an upstream lung and downstream brain compartment. **(B2)** Structure of the MOC consisting of two PDMS layers and a membrane and **(B3)** its realization, scale bar 1 cm. **(B4)** Extravasation of PC9 lung cancer cells (green) through the BBB (red) in time-lapse images; scale bar, 50 μm. **(B5)** Confocal imaging of the expression of the tight junction zonal occludin-1 (ZO-1, green) and vascular endothelial -cadherin(VE-Cad, red) proteins in the control BBB (left) and in the BBB after tumor cells extravasation (right), evidencing a decrease in tightness upon vascular interaction with tumor cells; Scale bar, 20 μm. Reproduced from Ref. (Liu et al., 2019a).

liver, and MDA MB231 for breast cancer, while curcumin, a natural compound from plants of the Curcuma longa species, represented the investigated drug. Inhalation therapy has the potential to be more economical if applied at home by the patient in contrast to intravenous therapy needing access to a clinical setting. Furthermore, for the same reason, it can be administered more frequently using lower drug level, as a way to reduce toxicity. In their study, the authors emphasized the importance of recirculating flow for more appropriate MOC platform and reported a small influence of curcumin administration on lung and liver viability while its effect was higher on breast cancer cells.

In order to better testing systemic transdermal administration and subsequent drug metabolism, skin models were also integrated in multi-organ-chip. Marx group pioneered this field and in a first study realized a MPS combining skins with liver (Wagner et al., 2013a). Successively, they improved this platform merging skin (with an air–liquid interface), reconstructed human intestinal barrier, liver (spheroids), kidney (in the form of a membrane covered by human proximal tubule epithelial cells) and vasculature mimicked with endothelial cells (Maschmeyer et al., 2015a, 2015b).

Multi-organ platforms have been also realized for predicting anti-tumor drug response. In the case of brain cancer treatments, in addition to the liver involved in drug metabolism, a key role is played by the blood-brain barrier, which selectively regulates the passage of chemicals to and from the brain. As an example, Li et al. (2021) developed a multi-organ device to evaluate how the BBB and liver metabolism influence the availability and cytotoxicity of drugs used to treat glioblastoma (Fig. 13A). Their biomimetic liver-brain chip consisted of microfluidic channels to create three compartments: the left one with human hepatocarcinoma cells (Hepg2) to mimic the liver, the right one with U87 cell to account for the glioblastoma. In between, a porous membrane and type I collagen were placed and rat brain microvascular endothelial cells (BMECS) and astrocytes were co-cultured to recapitulate the BBB. In this way, the chip recapitulated the drug pathway to reach both the liver and the brain upon oral administration. The brain-blood interface was characterized by TEER measurements and through the expression of proteins that constitute occluding junctions, such as ZO-1. Three anticancer drugs were tested in this study, namely Capecitabine, Temozolomide and Paclitaxel. Liver metabolism had limited effect on Temozolomide while resulted in a 30% enhancement of the Capecitabine cytotoxicity on U87 cells. The BBB instead reduced Paclitaxel cytotoxicity by 20%, but Temozolomide and Capecitabine effects were not significantly influenced. In conclusion, this chip allowed to evaluate how the efficacy of a drug targeting the brain is affected by both liver metabolism and the ability to cross the blood-brain barrier (Li et al., 2021).

A similar multi organ on-chip architecture was realized to assess the cardiac safety of an antidepressant drug (clomipramine) which is first metabolized by the liver. After administering 1 μM of drug in an upper compartment containing liver organoids, Yin et al. observed a reduced cell viability and an increased cardiocytotoxicity in the cardiac organoids located in the lower compartment (Yin et al., 2021). Clomipramine also caused a reduction in intracellular calcium flux in the cardiac organoids monitored through a fluorescent Ca^{2+} indicator dye (Fluo-4 AM). Thus, the multi-organ chip permitted to predict the drug side effects both at the level of the main organ involved in its metabolism (the liver) and at the level of the target organ, in this case the heart.

Coming back to cancer, metastasis formation is a key aspect to be addressed. It was discussed in Section 2.2 in terms of interaction of cancer cells with the microvasculature. However, multi-organ models can contribute to gain further insight on the process. Liu et al. (2019a) implemented a platform for studying brain metastasis (BM) from primary tumor growth to its spreading by integrating an upstream lung compartment and a downstream brain including a functional BBB. In Fig. 13B, the metastatic process and the MOC platform are illustrated. The lung model encompassed bronchial epithelial cells, fibroblasts, immune cells, pulmonary vascular endothelial cells, and tumor cells, and employed vacuum channels to account for breathing movements reconstituting the tumorigenesis and cancer intravasation. The brain model consisted of a brain parenchyma chamber surrounded by two vascular channels: (1) the left one connected to the upstream chamber in order to provide a pathway for metastatic cells, (2) the right one unconnected as a control. For cell co-culturing and tumor extravasation, the brain parenchyma compartment was interconnected to the vascular channels by micro-gaps. In their systematic study, the authors employed lung cancer cell lines with differing metastatic abilities and identified the Aldo-keto reductase protein family 1 B10 as a diagnostic biomarker showing higher expression in case of lung cancer BM and a prospective therapeutic target if silenced to limit BBB extravasation.

In order to account for drug absorption, metabolism and clearance, Vernetti et al. reported a five organs platform including jejunum, liver and kidney models (respectively) in addition to skeletal muscle and neurovascular models (Vernetti et al., 2017). The authors observed an organ-specific processing consistent with clinical data in their study of terfenadine for pharmacokinetics and toxicity; trimethylamine (TMA) as a potentially toxic microbiome metabolite; and vitamin D3. Furthermore, trimethylamine-N-oxide (TMAO) resulted able to cross the BBB. Co-culturing endothelial cells, fibroblasts and pericytes with (circulating) immune cells was also considered to investigate immune responses and its influence on disease progression and drug-induced response within an in-vivo mimicking microenvironment (van Dijk et al., 2020; Sun et al., 2019). The microbiota-gut-brain axis attracted large interest too (Raimondi et al., 2019, 2020).

4. Technologies and materials for organs-on-chips

4.1. Microfluidic tools for organs-on-chips and drug research

A number of microfluidic tools have been optimized for Organs-on-Chips. A paradigmatic example concerns application to cancer field, where most of the tools were employed, from vascularization techniques and perfusable channels to administer nutrients and drugs (already discussed in Section 1.4) to microwell arrays, gradient generators and droplet microfluidics (described here). Thus we will draw this section by discussing the main microfluidic components to facilitate high-throughput drug screening with focus on the exemplary case of anti-cancer drug research.

In particular, we can distinguish systems based on (i) microwells or U-shaped microstructures, or (ii) emulsion/droplets. Within the first category, the cancer cells are injected into the chip through a microchannel and captured by microwells arrays or U-shaped microstructures allowing their aggregation and tumor spheroid formation. This type of microfluidic chip is suitable for long-term culture, due to the continuum turnover of the culture media injected into the chip through the microchannel. For example, Khot et al. (2020) used a 3D printed master to fabricate cell culturing wells in a PDMS layer sandwiched between two transparent PMMA layers, for direct microscope inspection (Fig. 14 A-F). Using this device and culturing under static conditions, they reported on-chip generation of around 250 μm 3D spheroids from human colorectal HT29 adenocarcinoma cell line. Then they demonstrated that seeding the cells through a port placed directly above the cell culturing wells improves the efficiency of 3D spheroids formation up to 100%, with respect to 68% observed in the case of flow-driven cell seeding. Following the culturing process, the HT29 spheroids were treated and analyzed on chip, through the perfusion of anti-cancer 5-Fluorouracil and the use of fluorescence microscopy for subsequent cell viability imaging confirmed by a Lactate dehydrogenase assay on the supernatant. In addition, in this work, two different methods were proposed for administering cytotoxic treatment in the microfluidic devices, specifically limited-perfusion and continuous flow. In the first setup, allowing single endpoint experiments, single 3D spheroids were treated with 5-Fluorouracil under fluid flow (25 min at 20 μL/min) and then incubated under static conditions (for 24 h). In the second setup, spheroids

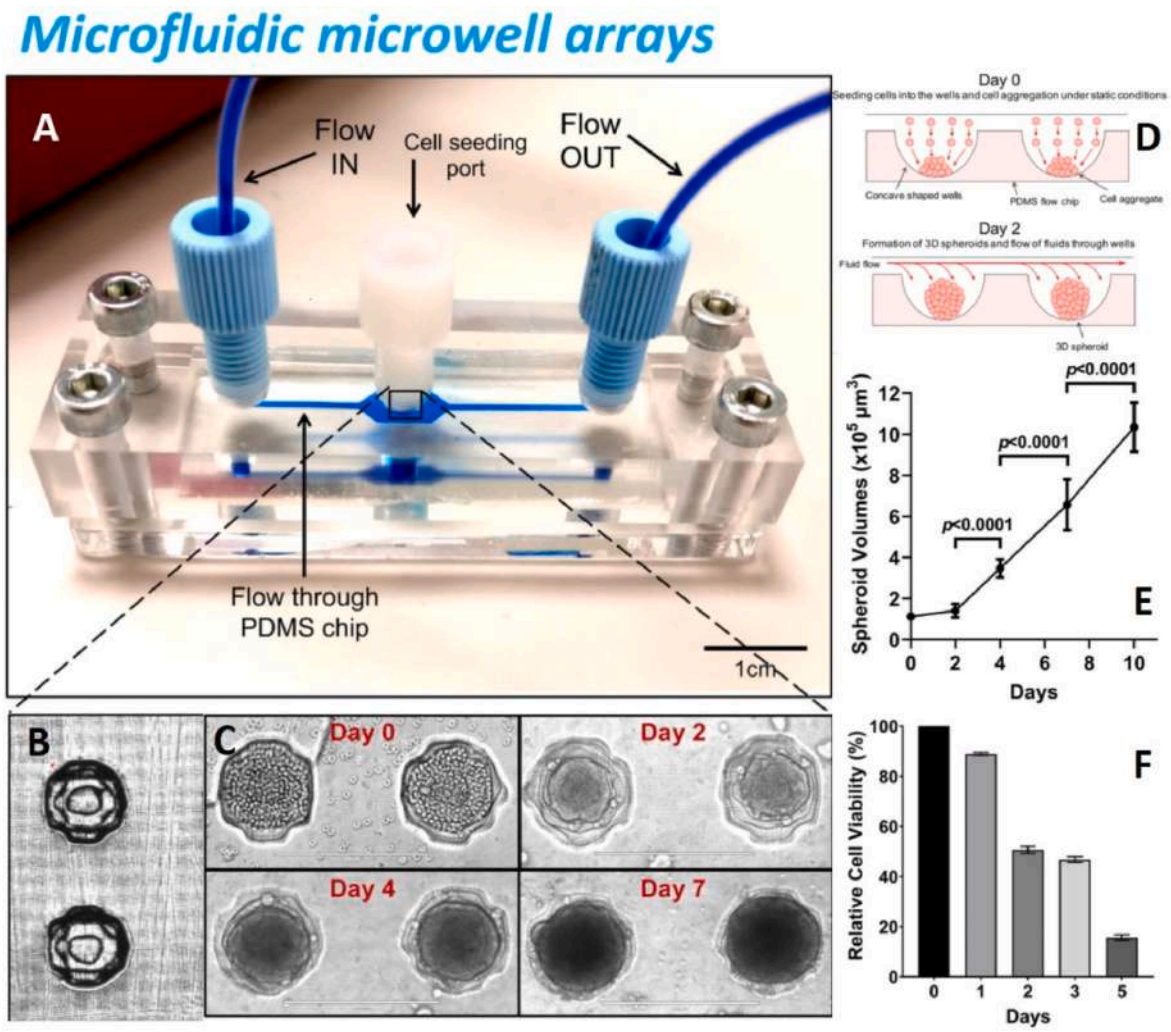

Fig. 14. **(A)** The PDMS 3D cell culturing microfluidic device developed by M. I. Khot et al., embedded between two PMMA layers and using standard UNF 1/4–28 flangeless fluidic fittings. Scale bar = 1 cm. **(B)** Optical microscopic image of the 3D cell culturing wells in the center of PDMS chip. **(C)** Progressive growth of 3D HT29 spheroids in images taken at days 0, 2, 4 and 7. Scale bar = 400 μm. **(D)** Scheme of the designed platform with concave shaped wells to favor cell aggregation at day 0. Then cell aggregates were cultured under static conditions to form 3D spheroids in the following two days and finally fluid flow was applied. **(E)** Progressive growth of HT29 spheroids cultured under static conditions for 10 days in the microfluidic devices. **(F)** The spheroids were treated with 5-FU (200 μM) through continuous perfusion at 20 μL/min for 5 days, and to monitor their chemosensitivity the supernatant was collected at the different time-points to perform a Lactate dehydrogenase (LDH) assay as reported in the histogram. Adapted from Ref. (Khot et al., 2020).

on multiple devices were treated in parallel under continuous perfusion (up to 5 days at 20 μL/min) using a multichannel pump to better mimic systemic circulation in the body. Similar microfluidic chamber arrays were employed for on chip high throughput screening in other sectors/assays, such as screening of transient receptor potential channel modulators (Ai et al., 2020a), screening of species differences in metabolism (Ai et al., 2020b), screening of aggregation models (Mondal et al., 2016), whole-organism behavior-based chemical screening (Chung et al., 2011) and single-embryo screening (Popova et al., 2018).

When the target is high-throughput screening, the use of gradient generators can be very effective. In this respect, Y. Fan et al. (2016) developed a 3D brain cancer chip by using photo-polymerizable poly (ethylene) glycol diacrylate (PEGDA) hydrogel for high-throughput drug screening and prolonged drug release. The relevance of their device lies in the easy fabrication of the microfluidic device by simply a few seconds of photolithography without replica molding and plasma bonding which are instead required in the case of common PDMS microfluidic devices. 3D spheroid formation of glioblastoma multiforme cells (GBM, U87) was achieved into the microwell arrays and the authors investigated a combinatorial treatment with Pitavastatin and Irinotecan exploiting the integration of gradient generators on the chip (Fig. 15A–D).

Tumors, however, are complex tissues typically made of multiple cell types (e.g. cancer and stromal cells). Therefore, heterogeneous spheroids should be generated to explore mutual cell-cell interactions in both spheroids formation and anti-cancer drug screening response. In this respect, Yang et al. (2019) reported the generation of heterospheroids consisting of MCF-7 (breast cancer) and L929 (fibroblast) cells, cultured for a long time in a microfluidic system and treated with Doxorubicin and Paclitaxel. Their device layout consisted of two (microwell and microfluidic) modules. Specifically, the microwell arrays were realized in PEGDA hydrogel, while the microfluidic module was realized in PDMS. Their drug screening study showed that heterospheroids of cancer and fibroblasts cells are characterized by a higher drug-resistance than homospheroids and combinatorial drugs are more effective than single drugs. In another study, Mazzocchi et al. (2018) demonstrated the generation of 3D spheroids in a microfluidic device from cells derived by two mesothelioma biopsies to provide patient-specific models. In general, the microwells arrays approach is suitable for studies on a wider range of drugs, drug combinations and doses, and could represent a powerful tool to adjust patient-specific cancer treatments.

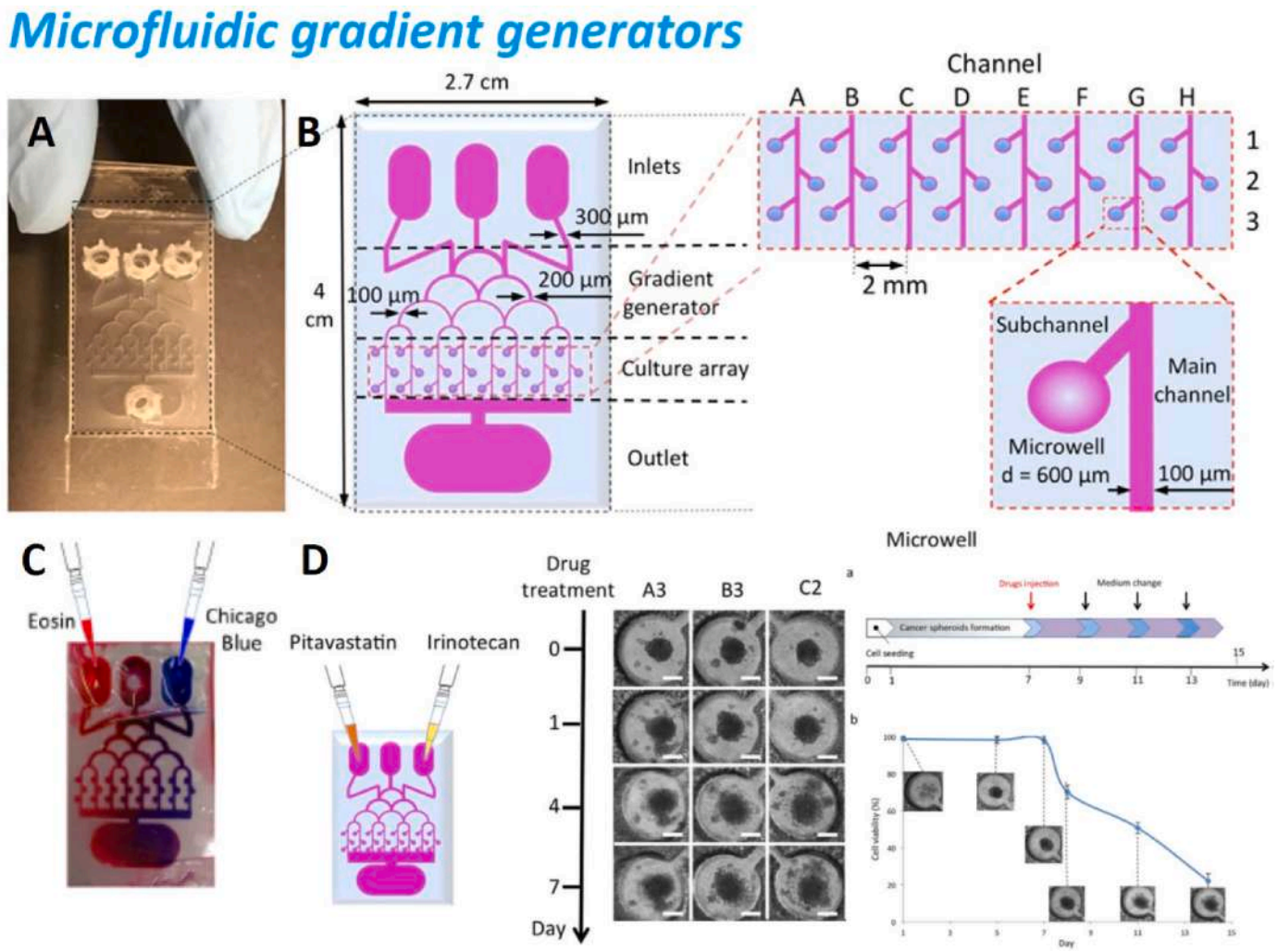

Fig. 15. (A–C) Gradient generator microfluidic chip designed by Fan et al. (Fan et al., 2016) and including individual culture chambers for brain cancer high-throughput combinatorial drug screening, performed with Pitavastatin and Irinotecan on cancer spheroids. **(D)** Time-lapse images and cell viability of U87 cancer spheroids upon continuous drug release. Scale bar, 200 µm. Adapted from Ref. (Fan et al., 2016)

Very promising for cancer research and drug development is the U-shaped microstructures technology reported by W. Liu et al. (2019b), who proposed a microfluidic strategy for large-scale and high-throughput in vitro anti-cancer investigation. An extraordinary large number of heterotypic 3D tumors (total of 672 tumors) with tissue-biomimetic phenotypes were produced in a single microfluidic device. Moreover, on-chip optical and fluorescent imaging were employed to analyze various 3D tumors characteristics such as growth dynamics, viability and apoptosis during cultivation and drug administration. These characteristics are advantageous for standardizing carcinogenesis, tumor progression and drug development studies by means of biomimetic organ-on-chip systems.

Within the second category, droplets microfluidics is exploited. Usually, droplets are generated in a flow-focusing microfluidic device with two incompatible solutions injected in a microfluidic T-junction. At the cross junction, when the solution containing cells in aqueous medium meets the other solution, usually oil, emulsion droplets are spontaneously formed with cells trapped inside, due to their different interfacial properties. Then the droplets can be incubated to favor cells aggregation and tumor spheroid formation. With respect to microwells and U-shaped microstructures, the key advantage with droplets is the large number of microenvironments generated (tens of droplets per second) where cells can be encapsulated with high control on their number and in a rapid and efficient manner. In this frame, Lee et al. (2020) reported a T-junction microfluidic system for large scale generation of cancer-cells embedded in micro-droplets with high generation frequencies (70 Hz) and a generation yield of about 20% higher than previously reported (Kwak et al., 2018). Notably, they demonstrated the fabrication of brain tumor spheroids with diameter tunable between 100 and 130 µm by varying cell concentrations and as proof-of-concept they evaluated photothermal therapy and drug screening responses on brain tumor spheroids.

To resemble the real tumor complexity and microenvironment, cell-laden hydrogel droplets were generated and investigated. In particular, Sabhachandani P. et al. (Sabhachandani et al., 2016) described the generation of cell-laden alginate droplets in a microfluidic device which combines a T-junction for droplet formation and a docking array which can house 1000 droplets for gelation and spheroid formation and on chip drug screening (Fig. 16 A-D). They demonstrated the generation of three spheroids models, drug resistant or drug sensitive breast cancer spheroids (MCF7) and co-culture spheroids consisting of drug sensitive breast cancer cells and fibroblast cells (HS-5). With this technology, they carried out on-chip cytotoxicity experiments using doxorubicin and paclitaxel chemotherapeutic drugs. Jang M. et al. (Jang et al., 2017) used a flow focusing microfluidic platform to generate two different types of 3D in vitro gastric cancer models by using the AGS (intestinal type) and Hs746T (diffuse type) cell lines encapsulated in Type 1 collagen beads (as ECM hydrogel). During droplets formation, the syringe filled with

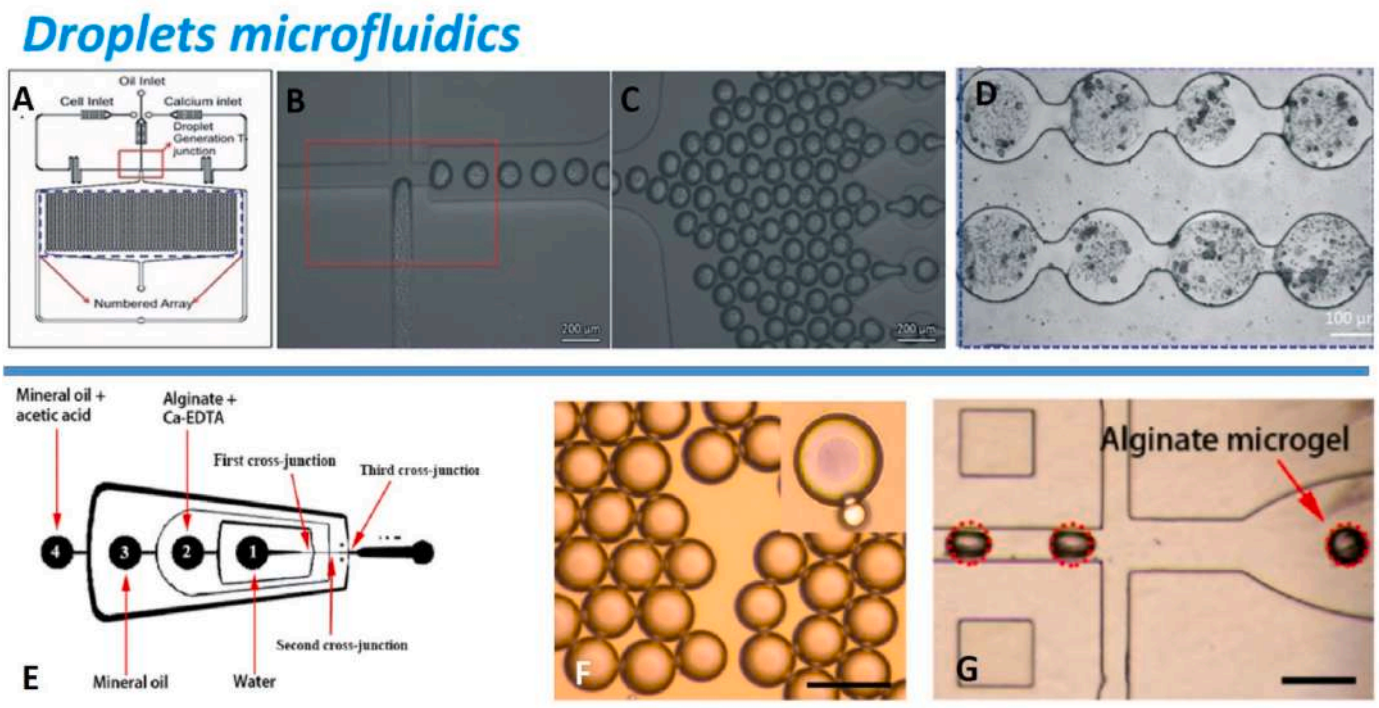

Fig. 16. **(A)** Layout of the microfluidic device for spheroid generation and docking array reported by Sabhachandani et al. (Sabhachandani et al., 2016). **(B)** T-junction for cell-laden alginate droplet formation. Scale bar: 200 μm. **(C)** Droplets entering the docking array after generation but before gelation. Scale bar: 200 μm. **(D)** Docking array with gelled cell-laden alginate spheroids. Scale bar: 100 μm. Adapted from Ref. (Sabhachandani et al., 2016). **(E)** Schematic of the flow-focusing device reported by Sun et al. (Sun et al., 2018) for producing core−shell alginate particles for encapsulating different cells in their core and the shell region. **(F)** Monodispersed core−shell alginate particles collected in mineral oil. **(G)** Cross-linking of alginate and microgel formation due to the injection of mineral oil containing acetic acid which triggers the release of Ca^{2+} from Ca-EDTA. Scale bars are 200 μm. Adapted from Ref. (Sun et al., 2018)

collagen solution was kept at low temperature by means of an ice bag, since collagen gels at 37 °C. Drug screening assays were then performed with 5-fluorouracil on the cultured microtumors. Another employed extracellular matrix component was matrigel, which is characterized by similar temperature dependent properties as collagen type I. Wu et al. (2020) demonstrated the generation in matrigel droplets of tumor spheroids derived from patients' breast tumor tissues. A combined approach was proposed by Karamikamkar et al. (2018), who produced breast cancer spheroids with alginate and collagen as ECM components, since the alginate helps to maintain the spherical shape of beads due to its fast gelling properties with respect to collagen I which gels more slowly and is temperature-sensitive. To reproduce the tumor complexity, Sun et al. (2018) developed a microfluidic layout based on the flow-focusing principle for the preparation of core−shell alginate particles, which permitted the encapsulation of stromal fibroblast cells in the shell and tumor cells in the core (Fig. 16 E-G).

To summarize, today several microfluidic tools are at the disposal of researchers for the implementation of OOC platform and to facilitate high throughput investigations. They include vascularization techniques and perfusable channels, microwell arrays, gradient generators and droplet microfluidics. Beyond them, it is worth mentioning also the availability of microfluidic separation tools to isolate specific cell types or molecular analyte for their further analysis or on chip culture (Nagrath et al., 2007; Chen et al., 2014; Wu et al., 2017; Contreras-Naranjo et al., 2017). Furthermore, microfluidic tools can be employed also for the production of drug nanoformulations and injectable liposomes with therapeutic applications (Zizzari et al., 2017; Shah et al., 2008; Shum et al., 2008). Although their discussion is not covered by this review, the interested researchers can find detailed reviews in literature for further readings.

4.2. Sensor integration for real-time analysis

Organs-on-chips provide effective microphysiological systems for biomedical studies and drug development. However, to take full advantage of their capabilities and accelerate research, they should be combined with efficient analytical methods. In this respect, we can distinguish among (1) endpoint analysis, (2) effluent collection and supernatant based assays, (3) in situ microscopy and imaging characterization and (4) real time analysis with integrated on-chip sensors. Concerning the first two categories, the small volumes in OOC platforms pose some challenges in the use of traditional methodologies such as a possible reduction in the low signal-to-noise ratios (Bennet et al., 2021). Within the third category, fluorescence and confocal microscopy provide powerful tools for investigating cellular arrangement, interactions and processes using appropriate fluorescent staining or tracers (as shown in the previous sections) but additional analytical assays may be required for further insight. In this respect, a recent trend consists in the on chip integration of in-line miniaturized sensors to replace off chip assays on manually extracted samples. This approach offers great opportunities for enabling continuous and automated data collection and in-situ monitoring of functional indicators and biological responses (Marrero et al., 2021a; Young et al., 2019). It also facilitates real-time decision making. The range of monitorable parameters include barrier integrity, oxygen concentration and inflammation response (e.g., cytokines production) as well as electrical and mechanical signals (Li and Tian, 2018b; Soucy et al., 2019). As a consequence, it is worth spending some words to present the most relevant sensing technologies.

Miniaturized (bio)sensors are widely employed in diagnostics and automated lab on chip platforms, exploiting their high selectivity and sensitivity and integration in portable measurements systems (Arndt et al., 2004; Nguyen et al., 2015; Haes et al., 2004; Baselt et al., 1998; Rizzato et al., 2020). In this respect, electrochemical/impedance

read-out is particularly attractive for miniaturization. Electrochemical sensors in OOC models permit to monitor microenvironment conditions (such as pH and temperature) and analyze metabolic parameters (respiration rate, lactate levels and glucose consumption). Enzyme, protein, aptamers and antibodies can be immobilized on the sensor surface as recognition elements to detect specific markers. For example, oxygenation is an important physiological parameter that impacts on cell metabolism and functionality of a tissue (Atkuri et al., 2007). In the gut, intestinal cells are subjected to different oxygen concentrations: low in the lumen center and high in the intestinal mucosa. Changes in oxygen distribution can be a symptom of bacterial infection and/or gut inflammation (Zeitouni et al., 2016). Amperometry with miniaturized electrodes permits to monitor dissolved oxygen levels by measuring the current produced via oxygen reduction reactions. For this purpose,

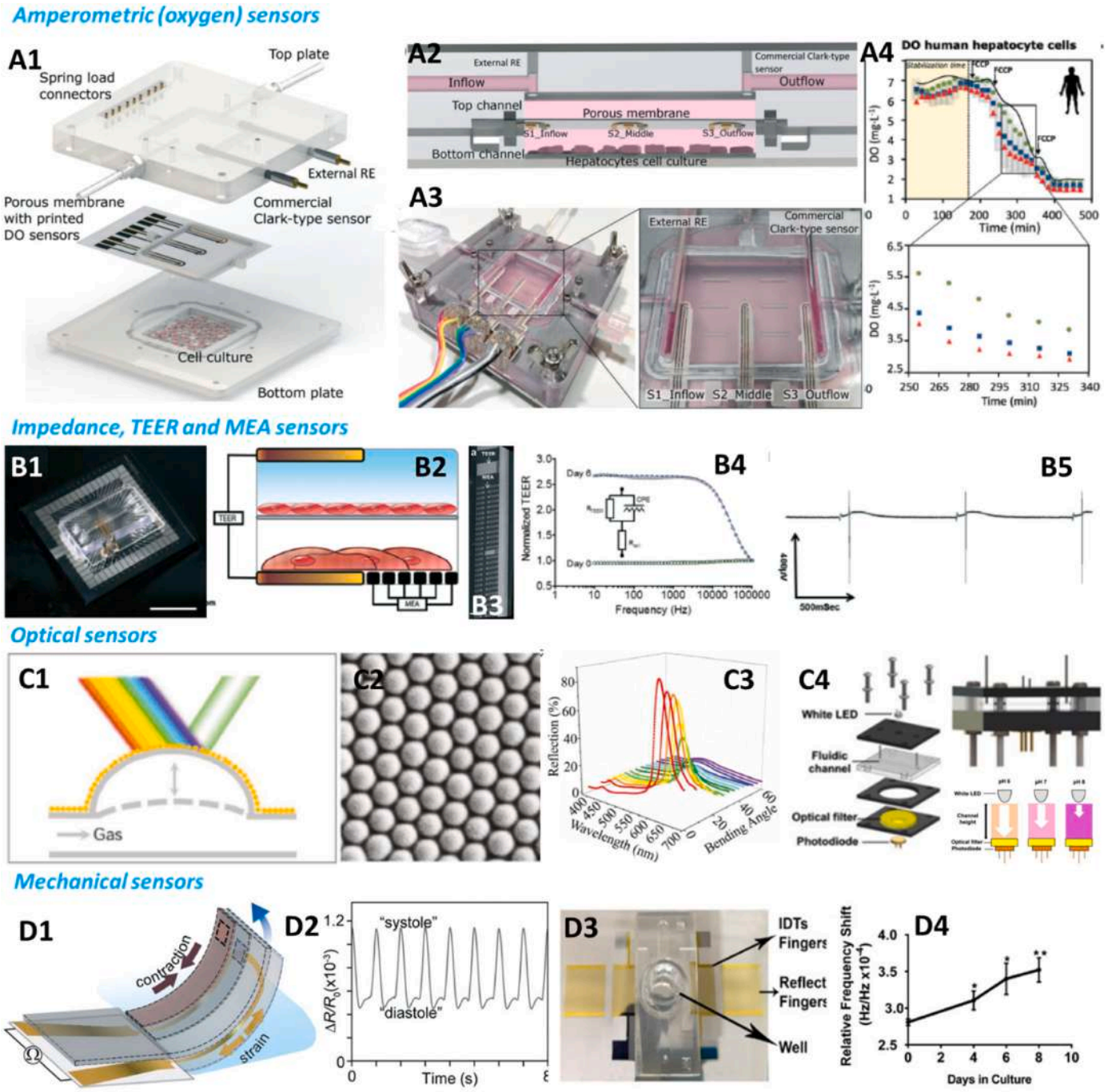

Fig. 17. ***(A1-A4)*** *Schematic of the OOC system with the three printed electrochemical sensors along the microfluidic channel and sensor characterization data without primary cells, with primary rat hepatocytes cell culture, and with primary human hepatocytes* (Moya et al., 2018). ***(B1)*** *Transepithelial Electrical Resistance- Multi-Electrode Array chip.* ***(B2)*** *Schematic of experimental setup with endothelial layer grown on the top of membrane and cardiomyocytes on the top of MEA and among the two sets of TEER electrodes.* ***(B3)*** *Scanning electron microscope (SEM) image of the bottom layer electrodes.* ***(B4)*** *TEER measurements as a function of frequency* ***(B5)*** *MEA trace of single electrode* (Maoz et al., 2017). ***(C1)*** *Schematic diagram of sectional view of the pulmonary alveolus which activity is monitored using photonic nanoparticles* ***(C2–C3)*** (Zhu et al., 1002).***(C4)*** *Optical* pH *sensing in cell culture medium and sensor characterization data.* (Shaegh et al., 2016).***(D1)*** *Cantilever strain-gauge sensor* ***(D2)*** *Micrograph of the sensor and typical response curve.* (Lind et al., 2017b) ***(D3-D4)*** *Surface acoustic wave sensor for detection and quantification of viability and growth of cells* (Wang et al., 2015).

Moya et al. (2018) integrated multiple ink-jet sensors in a thin and porous membrane inside a Liver-On-a-Chip device (Fig. 17 A). In tumor microtissues, instead, metabolic parameters provide information on cell growth and viability and in ref. (Misun et al., 2016) an amperometry sensor was implemented to monitor glucose and lactate levels secreted by a 3D human colon cancer microtissue.

Electrochemical impedance spectroscopy (EIS) is a related transduction technique based on changes in the electrical properties near the electrode surface. From its introduction by Giaver and Keese (Giaever and Keese, 1993), this method has been employed in lab-on-chip for facilitating several cell-based assays, including monitoring motion, attachment, growth, proliferation, spreading and differentiation of cultured cells (Arndt et al., 2004; Wegener et al., 2000; Bagnaninchi and Drummond, 2011), quantifying cell viability and heterogeneity (Han et al., 2007; Swami et al., 2021), assessing cell migration and invasive activities (Rodriguez et al., 2005; Primiceri et al., 2011; Keese et al., 2002) and evaluating the effects of biochemical compounds and cytotoxicity (Xiao and Luong, 2003; Primiceri et al., 2010; Kustermann et al., 2013; Ramis et al., 2013). Furthermore, upon electrode functionalization with suitable recognition probes, EIS sensors consent the detection of biorecognition events (Katz and Willner, 2003; Chiriacò et al., 2013, 2015, 2016; Buja et al., 2022). Recently, Sorafenib efficacy in hepatocellular carcinoma treatment was assessed on chip through EIS sensors integrated in a miniaturized platform for cell proliferation assays and drug screening (Piccinno et al., 2021). Within OOC field, in ref. (Ortega et al., 2019), Ortega et al. used EIS sensors functionalized with enzyme-linked secondary antibodies to detect interleukin (IL)-6 and tumor necrosis factor (TNF), reaching limit of detection of the order of ng/ml. Zhang et al. monitored liver and heart in a multi-OOC platform (liver and heart) achieving a two orders of magnitude lower limit of detection (LOD) (Zhang et al., 2017). Moreover, impedance spectroscopy has been exploited to measure tumor spheroid size on-chip (Schmid et al., 2016) and to study tumor spheroid viability throughout drug testing assays (Wu et al., 2018).

The transepithelial/transendothelial electrical resistance (TEER) can be very useful to monitor in real time the integrity and the functionality of cellular barriers in OOC models such as the BBB, the intestinal epithelial barrier in gut-on-a-chip or the air-liquid interface in lung-on-a-chip. In ref. (Maoz et al., 2017), Maoz and coworkers employed TEER measurements to simultaneously detect dynamic alterations of vascular permeability in heart-on-a-chip device. In the same chip, multi electrodes arrays (MEA) were integrated to measure field potentials of cardiomyocytes (Fig. 17 B). In general, the electric/electrochemical techniques described above require electrode integration in the chambers/channels housing living cells or in contact with fluids passing through the cell compartments.

Optical biosensors provide another, convenient in-situ monitoring approach (Kavand et al., 2107). Refractive index changes near the sensor surface (due for example to cellular response or analyte secretion) are measured in surface plasmon resonance (SPR) (Nguyen et al., 2015; Haes et al., 2004; Colombelli et al., 2021; Rizzato et al., 2018), optical waveguide light mode spectroscopy (OWLS), photonic crystals (PC) and resonant waveguide grating (RWG). In ref. (Li et al., 2018), SPR based on nanoholes arrays were integrated in a microfluidic platform to detect vascular endothelial growth factor. Photonic crystals and structures fabricated by colloidal lithography were used as self-reporting tools for cardiomyocytes activity or microphysiological breath (Shang et al., 2020; Zhu et al., 1002) (Fig. 17 C1–C3). Optical waveguides were fabricated in flexible PEG-based hydrogels to stimulate drug release from optogenetically engineered bacteria (Feng et al., 2020), whereas resonant waveguide grating biosensors have been used to study the role of plasma proteases on endothelial cell layers (Debreczeni et al., 2020).

Optical sensors have been also developed to investigate cell and tissue metabolism using sensitive opto-chemical tracer molecules. These sensors represent a valid alternative to electrical sensors to measure microenvironmental parameters such as pH and oxygen levels. Optical oxygen sensors exploit photoluminescence quenching produced by oxygen-sensitive dyes. Fluorophores based ruthenium- and metalloporphyrin were largely diffused due to their very high quenching constants (Kavand et al., 2107). For example, Shaegh et al. realized a bioreactor with integrated LED and photodetectors for monitoring of pH and oxygen levels (Shaegh et al., 2016). By means of a similar approach, Khalid et al. measured the absorption light variation in cell media in the presence of phenol red to monitor pH in a lung cancer-on-a-chip platform (Fig. 17 C4) (Khalid et al., 2020).

Mechanical sensors is another class which attracted attention due their potential applications in monitoring different physiological signals, mechanical (strain, pressure) or biological (for example detection of metabolic biomarkers) (Ferrari and Palma, 2020). These sensors are used in OOC to study tissue stiffness and monitor dynamic deformations typical of the striatal muscular tissues (skeletal and cardiac muscle tissues). For example, Lind et al. developed some cantilevers that contained flexible thin-film strain gauges to detect beat rate and contractile stresses of the cardiac cells (Lind et al., 2017b) (Fig. 17 D1-D2). In ref. (Sidorov et al., 2017), Sidorov et al. designed a platform to grow 3D cardiac tissue constructs (ECTCs) and to perform measurements of their mechanical and electrophysiological parameters to evaluate the ECTCs functionality in both normal and pharmacologically modified conditions, using cantilever probes.

Between mechanical sensors, surface acoustic wave are widely used since they are very sensitive toward mass loading, viscosity and conductivity variations occurring on the surface (Chiriacò et al., 2018; Rizzato et al., 2017; Rizzato et al., 2023), being the mechanical excitation strongly localized in the surface region (Maruccio et al., 2018). For example, Wang et al. used a shear horizontal-surface acoustic waves (SH-SAW) device comprising two pairs of resonators for detection and quantification of viability and growth of cells (Wang et al., 2015) (Fig. 17 D3-D4). The same authors included SAW sensors in a gravitation microfluidic platform system for monitoring the proliferation and metabolism of tumoroids (Wang et al., 2020). Liu et al. (2018) realized an integrated system of metal-enhanced fluorescence with SAW for cancer biomarker detection.

In some cases, gas sensors can provide other suitable monitoring and diagnostic tools as demonstrated by the increasing interest in their use for volatilomics and metabolomics (Milone et al., 2023; Serasanambati et al., 2019; Dummer et al., 2011; Phillips et al., 2012; Einoch Amor et al., 2019; Di Natale et al., 2003; Murdocca et al., 2021; Mougang et al., 2021). Finally, some authors developed and integrated sensors in OOC devices, equipped with miniaturized models of laboratorial instruments. For example, a 3D-printed digital fluorescence type microscope was incorporated in a lung-cancer on chip platform for the visual monitoring of the cells on the chip (Khalid et al., 2020). In ref. (Mermoud et al., 2018), Mermoud et al. presented microimpedance tomography system integrated in a flexible printed circuit board to control cell activity and membrane movements in a breathing lung-on-chip.

In summary, the integration of miniaturized sensors for in situ, automated monitoring of relevant cellular and physiological parameters represents an important frontier for further increasing the throughput and content of OOC platforms.

4.3. Materials for organs-on-chips devices

Different materials are used to develop organs-on-chips depending on the specific features required in mimicking the in vivo structural and/or biochemical environment (Table 1). In this paragraph, the advantages and disadvantages of the most popular materials explored in the design of OOC are discussed.

Glass is the oldest material employed in microfluidics. It is transparent, resistant to mechanical stress, hydrophilic, biocompatible and possess a low drug absorptivity. The major disadvantages which led to the experimentation of other materials concern its low gas permeability that does not allow long-term cell studies and the high cost of fabrication

Table 1
Materials for OOC platforms.

Categories	Materials	Advantages	Limitation	Applications
Glass		• transparency, • resistance to mechanical stress • hydrophilicity • biocompatibility • low drug absorptivity	low gas permeability,	• OOC substrate
Elastomers	PDMS	• flexible • optical transparent, • gas permeable • biocompatible, • low autofluorescent, • deformable, • ease of use, • low cost, • very useful in prototyping new devices	• hydrophobicity • incompatibility with organic solvents • tendency to adsorb protein and small analytes • leaching un-crosslinked oligomers	• OOC substrate • to mimic biological processes involving a mechanical deformation, (breathing (Huh et al., 2010b; Huh, 2015) and gut peristalsis (Kim et al., 2012)) • porous membrane to measure mechanical properties of monolayer cells (Huh et al., 2010b) • to produce microwell arrays to induce 3D cell aggregation (Lee et al., 2018b).
Thermoplastics	polystyrene (**PS**), polycarbonate (**PC**) polyurethane (**PU**)	• optically transparent, • more rigid than elastomers and • resistant to the diffusion of small molecules,	• lowly gas-permeability • inflexible • dissoluble in most organic solvents	• cell growth and adhesion (Lee et al., 2019) • Membranes (Pocock et al., 2017; Shah et al., 2016). • heart valves, pacemakers, haemodialysis membrane and artificial heart (Piccin et al., 2007) • membrane (Pourmand et al., 2018)
	polymethylmethacrylate (**PMMA**)	• moderate resistant to alcohol.		• OOC substrate
	polyethylene glycol diacrylate (**PEGDA**)			• microfluidic valve and pump (Rogers et al., 2011, 2014)
Thermosets		• optically transparent • resistant to heat degradation and to chemical attack of most solvents	• rigidity • high cost	• negative photoresists (es. SU-8) for microchannels fabrication • high-aspect ratio and free-standing microstructures
Paper		• low cost, • lightweight • ease to use	• limited detection method • difficulty to integrate microcomponents such as valves.	• cell growth
Natural Hydrogel	**Collagens**	• biocompatible, • permeable to gas, water and solute • low-cost • similar to natural soft tissue	• weak mechanical properties • limited long term stability • batch-to-batch variability	• ECM models (Hassan et al., 2020) • cell adhesion, growth and differentiation, tumoroids (Tasoglu and Demirci, 2013; Elomaa and Yang, 2017; Fedorovich et al., 2012; Roseti et al., 2017) • artificial microvessels (Liu et al., 2015)
	Gelatin matrigel	• non- or low- immunogenicity • alginate and gelatin have tunable properties • collagen present motifs for cell adhesion		• cell growth • ECM models • cell adhesion, proliferation • formation of functional organoids (Hoang and Ma, 2021).
	Fibrin			• vascular network engineering • scaffold for cell encapsulation • component of ECM
	Alginate			• microfluidic channels (Choi et al., 2007)
Synthetic Hydrogel	**PEG** and its derivative **PCL**	• biocompatible, • permeable to gas, water and solute • low-cost • tunable mechanical properties and degradation rate	• absence of cell adhesion ligands on the surface	• tissue engineering • drug delivery and bone tissue scaffold

processes (Ding et al., 2020). For these reasons, the use of polymeric materials became a mainstream. Launched many years after glass chips, polymeric-based devices can today be divided into three major groups: elastomers, thermoplastics and thermosets.

Between elastomers, polyimethylsiloxane (PDMS) is the most employed for the realization of devices for life science applications (Ding et al., 2020). It is flexible, optical transparent, gas permeable and biocompatible (Ning et al., 2016). Its mechanical properties and its hydrophobicity are tunable respectively changing the ratio of PDMS base to curing agent and making surface plasma treatments (Guttenplan et al., 2021). It has a low autofluorescence and a good deformability that allows easy microfluidic connections (Piruska et al., 2005; Amani Wan Salim et al., 2013). For its ease of use and its low cost, it is very useful in prototyping new devices (Hassan et al., 2020). PDMS elasticity is also exploited to mimic biological processes involving a mechanical deformation, such as breathing (Huh et al., 2010b; Huh, 2015) and gut peristalsis (Kim et al., 2012) or to measure mechanical properties of monolayer cells (Sorba et al., 2019). Other uses of PDMS are (i) in the form of membrane for cell culture at the interface between two compartments (Huh et al., 2010b) and (ii) to produce microwell arrays to confine and induce 3D cell aggregation into spheroid, embryoid body or organoids (Lee et al., 2018b). Various fabrication methods are available for the fabrication of PDMS devices, from conventional soft lithography and micromolding techniques to new strategies such as hybrid stamp approach (Kung et al., 2015), sacrificial template methods (Cheng et al., 2016), razor-printing (Cosson et al., 2015) and 3D printing (using a PDMS resin) (Bhattacharjee et al., 2018). PDMS has some limits of applications due to its incompatibility with organic solvents (not particularly relevant for OOC applications) and its tendency to adsorb protein and small analytes (Toepke and Beebe, 2006). Some treatment with plasma, UV or coatings are performed to improve the PDMS surface (Ning et al., 2016; Khetani et al., 2020). Moreover, it can leach un-crosslinked oligomers that can cause toxicity in cells and affect their behavior, altering for example the predictions of pharmacokinetics/pharmacodynamics studies (Carter et al., 2020).

Thermoplastics are a class of polymers that can be melted and

reshaped many times through heating usually by means of thermomolding (Becker and Gärtner, 2008). These materials are mostly optically transparent, more rigid than elastomers and resistant to the diffusion of small molecules (Hassan et al., 2020), moderately resistant to alcool but dissoluble in most organic solvents (Ren et al., 2013). Unfortunately, being lowly gas-permeable, thermoplastic sealed microchannel and microchamber are not suitable for long-term cell studies (Ren et al., 2013). Moreover, their stiffness does not allow to realized diaphragm valves (Ren et al., 2013). Depending on their application thermoplastics surface can be functionalized by means of surface grafting techniques or dynamic coating (Ren et al., 2013). Thermoplastic polymers such as polystyrene (PS), polycarbonate (PC), polyurethane (PU), polymethylmethacrylate (PMMA) and polyethylene glycol diacrylate (PEGDA) are generally used in microfluidic systems (Ning et al., 2016; van Midwoud et al., 2012). PS is highly biocompatible and used for cell growth and adhesion (Lee et al., 2019). PC membranes are usually integrated among microchannels in OOC structures for modeling tissue-tissue interfaces (Pocock et al., 2017; Shah et al., 2016). PU is a high mechanical strength material, resilient and resistant to abrasion, used in the fabrication of biomedical devices such as heart valves, pacemakers, haemodialysis membrane and artificial heart (Piccin et al., 2007) but also as membrane in thermoplastic microfluidic devices (Pourmand et al., 2018). PMMA has been employed as substrate for OOC due to its stiffness, good optical transparency and low auto-fluorescence background (Chen et al., 2016b; Miller and Shuler, 2016b). PEGDA thermoplastic is used to realize different type of microfluidic valve and pump (Rogers et al., 2011, 2014). Thermoplastics are suitable for commercial production since fabrication techniques as thermomoulding can ensure high production-rate and low cost but they are not economic for prototyping (Ren et al., 2013). For fast prototyping, photocurable soft lithography compatible liquid PS prepolymer and a fast curing PMMA prepolymer have been exploited as negative photoresists and shaped by means UV or visible light exposure (Nargang et al., 2014; Kotz et al., 2018).

Differently from thermoplastics, in thermoset plastics the polymer chains cross-link into a rigid network structure that make difficult the reshaping of material. Thermosets, generally used as negative photoresists (e. g. SU-8) for microchannels fabrication, are optically transparent, resistant to heat degradation and to chemical attack of most solvents. Their mechanical strength permits the realization of high-aspect ratio and free-standing microstructures. However, their rigidity and high cost can limit their applications in biochips (Ren et al., 2013).

Paper is another material explored in microfluidics for its low cost, lightweight and ease to use. The porous structure of cellulose matrix is exploited for cell growth in 3D layout. In addition, sensor films can be integrated in paper-based devices for the monitoring of physiological microenvironment (Boyce et al., 2016; Mosadegh et al., 2015). 3D tumor cells have been growth in a paper roll device for the analysis of cellular environment and response (Young et al., 2018; Rodenhizer et al., 2016). Although the manufacturing of paper-based microfluidic device is simple, few applications have been demonstrated on paper chips (Ren et al., 2013). In these devices, the detection methods are relatively limited and it is difficult to integrate microcomponents such as valves.

Hydrogel is a hydrophilic macromolecular polymer gel constructed of a network of crosslinked polymer chains. The type and degree of crosslinking (depending on gelation and fabrication methods) affects the network properties, like swelling, elastic modulus porosity, permeability and degradability (Maitra and Shukla, 2014). Physically or chemically cross linking can provide hydrogels a three dimensional network structure and make them insoluble, allowing immobilization and release of biomolecules. The ability of hydrogels to embed a large amount of water (more than 30% w/v) make them similar to natural soft tissues, while their properties to swell under specific biological conditions allow applications in biomedical fields, such as drug delivery and tissue engineering (Maitra and Shukla, 2014). Hydrogels are also among the most used materials for mimicking the mechanics and biochemistry of native extracellular membrane (Ding et al., 2020). These polymer networks, permeable to gas, water and solute, allow cell adhesion and migration, growth, differentiation and maturation of organoids (Guttenplan et al., 2021). ECM models in hydrogel are employed to study processes such as angiogenesis (Natividad-Diaz et al., 2019), cancer metastasis (Lugo-Cintrón et al., 2020), and osteoblast migration (Movilla et al., 2018). Combining crosslinked strategies with lithography technique hydrogel scaffold are realized for 3D cell culture. Hydrogels have been likewise used to fabricate entire microfluidic devices for the study of blood vessel and to produce engineered tissue with functional vasculature (Cabodi et al., 2005). Hydrogels can be formed from natural polymers such as for example collagen, gelatin, matrigel, fibrin and alginate, or synthetic ones such as polyethylene glycol and its derivatives (PEG-DA), polycaprolactone (PCL) or synthetic/natural hybrids (Hassan et al., 2020; Liu et al., 2015). Remarkably, hydrogels are compatible with a variety of fabrication techniques, including soft lithography, 3D printing, micropatterning, electrospinning, UV curing, that enable the design of different structures (Guttenplan et al., 2021).

Collagens are the most common components of the native ECM and of connective tissues (Hassan et al., 2020). These natural hydrogels have several cell-binding sites for cell adhesion, growth and differentiation, that make them suitable for integration in platform model of heart, liver, skeletal muscle, neuronal network and tumor spheroids (Tasoglu and Demirci, 2013; Elomaa and Yang, 2017; Fedorovich et al., 2012; Roseti et al., 2017). Moreover, collagen has been employed as structural component in microfluidic devices for the development of artificial microvessels (Liu et al., 2015). Although Gelatin is similar to collagen in composition, it has a lower cost and is less antigenic. It is combined with other materials for supporting cell cultures in OOC platforms. Matrigel, a protein mixture extracted from mouse tumor cells, is used not only to model ECM in many tissue type, but also for cell adhesion, proliferation and for the formation of functional organoids (Hoang and Ma, 2021).

Within the category of natural compounds, Fibrin is an elastic protein involved in clotting, manly proposed for vascular network engineering but also used as scaffold for cell encapsulation and as artificial component of ECM. Alginate, a polysaccharide extracted from brown algae, is widely employed for several applications for its low-cost, low toxicity, easy functionalization and immediate gelation at mild condition. For example, Choi et al. (2007) realized microfluidic channels in calcium alginate for mass transfer sensing and for detection of chemical environment control surrounding encapsulated cells.

Natural hydrogels possess interesting properties for OOC applications such as high biocompatibility and biodegradability, but they have some limitations related to their relatively weak mechanical properties, limited long term stability and batch-to-batch variability. Synthetic hydrogel (and also hybrid) has been developed to provide materials with reproducible chemical and physical properties and tunable mechanical properties and degradation rate. Hydrogels based on PEG and its derivative (e.g. PEG-DA) are the most investigated synthetic hydrogel for tissue engineering. PCL found application in drug delivery and bone tissue scaffold. These synthetic biomaterials have some drawbacks related to the absence of cell adhesion ligands on the surface. To combine the advantages from both natural and synthetic biomaterials, hybrid hydrogels have been prepared. For example, as soft hydrogel is not suitable to mimic the hard and mineralized ECM of bone, fibrin incorporating hydroxyapatite (Jusoh et al., 2015) and mineralized collagen (Hao et al., 2018) are employed to study cancer metastatic into bone, bone angiogenesis and to investigate mechanical stimulation efficacy on bone formation. Finally, it is worth mentioning that “smart” responsive hydrogels able to respond to external stimuli are presently in the development phase.

4.4. Cell lines and technologies

For OOC implementation, various kinds of cells and cultures have been employed depending on the organ and the target application. In

general, simple monocultures are limited under several aspects and the use of co-cultures is crucial to reproduce organotypic microenvironments encompassing homotypic and heterotypic cell-cell interactions. Critical parameters for co-cultures include the type of cells, culture media, order in which cells are cultured, and numbers/ratio of cell types (Hodgkinson et al., 2022).

In terms of cells (Table 2), human primary cells have limited number of population doublings. Thus, immortalized cell lines are often employed to avoid senescence and improve availability, life span and reproducibility. However, while differentiating, they both show different characteristics after each passage and it is difficult to keep them in culture for long periods without changes (Geraili et al., 2018). In contrast, stem cells can differentiate into different cell types and exhibit the capacity for self-renewal. Among them induced pluripotent stem cells can be considered as the next-generation toolkit (Huang et al., 2021), in particular human-induced pluripotent stem cells (hiPSCs) which have been hailed as an effective replacement for human embryonic stem cells (hESCs). hiPSCs are represented by somatic cells, usually fibroblasts, that undergo a reprogramming process that converts already differentiated somatic cells into hiPSCs. Remarkably, the use of induced human stem cells is contributing to the development of patient-specific drugs and regenerative medicine (Geraili et al., 2018; Zakrzewski et al., 2019). Beyond cell lines, spheroids and organoids have been integrated in microfluidic platform, e.g. for tumor models with perfusable channels. Biomaterial based scaffolds and 3D cell bioprinting are also contributing in providing additional capacity for the fabrication of more advanced OOC models (Park et al., 2018).

In designing an OOC, both the cell-to-liquid ratio and the surface-to-volume ratio have to be considered since they can affect the response. In this respect, it is worth noting as OOC platforms differ from the in vivo case having large media volumes if compared to the limited amount of tissues and this results in a continuous dilution of the metabolites. Furthermore, OOC also present a different surface-to-volume ratio which influences cell autocrine and paracrine signaling (Barros et al., 2021). In various MOC studies, attention has been dedicated in building the devices maintaining ratios among the different organ masses as close as possible to the in vivo case. Vascularization, barrier functions, mechanical clues (e.g. associated to flow, breath or peristalsis), inflammatory processes, gas gradients and in particular oxygen concentrations are other important aspects to be carefully taken into account.

Table 2
Cell lines for OOC platforms. [adapted from https://promocell.com/in-the-lab/human-primary-cells-and-immortal-cell-lines/]

	Human primary cells	Cell lines	HiPSC (human induced pluripotent stem cell) and ESC (embryonic stem cells)
Senescence	Can replicate over a limited period of time	Can replicate over a long period of time	Have self-renewal
Culture	more demanding: Require more skills, special media and additives (growth factors) and adjustment for each cell type	Standard culture conditions easy to work with and keep alive	Sensitive, must be handled with care, require appropriate culture media with growth factors and extracellular matrix proteins.
Identity	Maintain the characteristics of the original tissue	Questionable, misidentification possible	ESC differentiate into different cell type,
Morphology	Show healthy cell morphology	Loss of polarity, lack of key morphological features	HiPSC derive from an adult somatic cell and is induced to
Phenotype	Maintain original phenotype for a limited number of passages depending on cell type and conditions	Change in phenotypes (need to be validated), functional alteration	convert into a stem cell that will give rise to a specifically differentiated cell
Genome	Genetically stable	Altered genomic content	Stable
Relevance in vivo	high	low	High
Reproducibility of results	Lower, donor-to-donor variations need to be considered	Higher, uniform cell type	___
Cell availability	Limited	Unlimited	Unlimited (HiPSC) Limited (ESC)
Costs	High	Low	High
Ethics	Regulations for use of human tissues	Non relevant	Ethical issues relating to ESCs surmountable by HIPS

5. Conclusions

Current drug development methodologies present severe limitations in their ability to appropriately take into account the complex in vivo physiopathology of human tissues. Both conventional 2D culture and (costly) animal models fail to provide accurate predictions on human clinical outcomes with striking discrepancies in efficacy and side effects when compared to human trials (Dhiman et al., 2019; Ren et al., 2020; Nam et al., 2015). This results in high costs and low success rate in translation to the clinic, which are responsible for the declining number of approved drugs, the increasing duration of the drug development process and a higher risk for drug withdrawal from the market at front of huge investments (Radhakrishnan et al., 2020).

To overcome these deficiencies, new platforms with enhanced predictive potential are under development. Exploiting advances in microfluidics and cell culture technologies, organs-on-chips can recapitulate pathophysiology, in vivo biophysical conditions, cell-cell/cell-matrix interactions, organ-organ crosstalk and the underlying biochemical pathways of different diseases providing accurate and versatile in vitro models. Advantages with respect to traditional methodologies have been discussed in Fig. 3, while Table 3 provides a summary of the state of the art for the OOC and MOC platforms which were discussed in detail in the previous sections.

Remarkably, recent advances have enabled to build relevant models of several human organs and diseases. Apart from drug efficacy and toxicity, enhanced in vitro models for micro-tissues vascularization and biological barriers have been optimized for investigating drug transport and barriers' permeability with increased accuracy and contribute to developing novel drugs delivery systems across relevant in-vivo barriers (e.g. exploiting nanodelivery). A recent trend consists in coupling multiple organ modules linked by vascular perfusion in order to recapitulate organ-level structures, simulate multi-organ interactions and assess drug metabolism/clearance/toxicity in a comprehensive 'body-on-a-chip' platform (Wang et al., 2018). Microfluidic technologies facilitate combinatorial approaches to assay relevant libraries of drug candidates and evaluate toxicity against multiple tissues in a more adequate and predictive way than previously possible. In addition, the integration of miniaturized sensors opens the way to further automation and number up of the assays.

These huge progresses have been facilitated by cutting-edge techniques, spanning from microfabrication processes inherited from microelectronics to soft lithographies, micromachining, rapid prototyping techniques, laser-assisted stereolithography, 3D printing and bioprinting. A further relevant building block was the emergence of protocols for the efficient directed differentiation of human induced pluripotent stem cells at high quantity and quality (Zhang et al., 2018b),

Table 3
Summary of discussed OOC and MOC platforms and their major characteristics.

ORGAN–ON–CHIP	CULTURED CELLS IN DEVICE	Main scope/aim	Key features	Diseases	Drug	Barrier
1.1 Intestine	➢ Human colorectal adenocarcinoma cells (Caco2) (Caplin et al., 2015b) ➢ Co-colture of enterobacteria and Caco2 (Caplin et al., 2015b) ➢ HiPSC derived-human intestinal-like tubules (Naumovska et al., 2020)	➢ Drug absorption and bioavailability ➢ nutrient/biomolecules exchange ➢ environmental factors ➢ gut/host-microbiota interplay and alterations of gut microbiota composition and function (dysbiosis) ➢ gut inflammation, imbalance between pro-inflammatory and anti-inflammatory signals	➢ peristaltic movements ➢ villi microstructures, ➢ gut/host-microbiota interplay ➢ gut inflammation influence	➢ intestinal dysfunction, ➢ intestinal inflammation ➢ gut severe, chronic and cancerous diseases	➢ Drug absorption and bioavailability ➢ Efficacy ➢ toxicity and side effects	➢ intestinal epithelial barrier ➢ permeability, tightness of cell junctions
1.2 Lung	➢ Human small airway epithelial cells (SAEC) (Huh et al., 2007) ➢ Human pulmonary alveolar epithelial cells (HPAEpiC) and human pulmonary microvascular endothelial cells (HPMEC) (Huh et al., 2010b) ➢ HiPSCs -derived lung cells (Zakrzewski et al., 2019) ➢ Human dermal microvascular endothelial cells (HDMEC) ➢ Human lung fibroblasts (HLF)	➢ Targeted instead than systemic administration ➢ influence of shear stress on paracellular and transcellular transport	➢ pulmonary microenvironment ➢ branching/breathing movements → cyclic strain and mechanical forces	➢ respiratory and pulmonary diseases ➢ viral and bacterial lung infections, ➢ chronic obstructive pulmonary disease (COPD) pulmonary edemas, tuberculosis and lung cancer, SARS-CoV and other respiratory virus infection injury ➢ airway repair after an injury ➢ Wound healing	➢ Drug absorption and bioavailability ➢ Efficacy drug-induced toxicity and side effects	➢ lung-blood barrier for inhaled agents ➢ alveolar-capillary barrier ➢ air-liquid interface (ALI)
1.3 Skin	➢ Human immortalized keratinocytes (HaCaT) (Ren et al., 2021) ➢ HiPSC-derived fibroblasts and keratinocytes (Geraili et al., 2018) ➢ Melanocytes, Immune cells, Neurons ➢ + integration of biopsy and off chip models	➢ Risk assessment for external agents and cosmetic products ➢ Transdermal drug delivery/ administration ➢ Drug penetration in bloodstream	➢ considerable differences vs animal skin in terms of structural and biochemical properties, lipid profile, hair density and stratum corneum thickness	➢ Dermatological studies ➢ Wound healing	➢ Transdermal drug delivery/ administration ➢ Drug penetration in bloodstream	➢ skin barrier
1.4 Vasculature	➢ Human umbilical vein endothelial cells (HUVEC) (Caplin et al., 2015b) ➢ Porcine aortic endothelial cells (PAEC) (Caplin et al., 2015b) ➢ Human embryonic stem cell (hESC)-derived pericytes (Geraili et al., 2018) ➢	➢ Intravenous administration and drug transport, ➢ recirculation at physiologically relevant perfusion rates and application of shear stress at in vivo levels ➢ vasculogenesis, sprouting angiogenesis and anastomosis ➢ blood organ barriers	➢ network of perfused microvessels ➢ Drug and nutrient transport (→increased lifespan for OOC) ➢ hemodynamic forces and vascular paarenchymal mechanotransduction vasculogenesis and angiogenesis	➢ diseases of the vascular system (i.e. atherosclerosis and deep vein thrombotic) ➢ vascularized micro organs (VMO) and micro tumors (VMT) ➢ tumor proliferation invasion, intravasation, extravasion	➢ Drug Transport, efficacy, ➢ anti-cancer and anti-angiogenic drugs	➢ blood organ barriers

(*continued on next page*)

Table 3 (*continued*)

ORGAN–ON–CHIP	CULTURED CELLS IN DEVICE	Main scope/aim	Key features	Diseases	Drug	Barrier
2.1 Blood-Brain Barrier	➢ Human brain endothelial cells (hCMEC/D3) (Caplin et al., 2015b) ➢ Primary human-derived microvascular endothelial cells (HBMVEC) (Geraili et al., 2018) ➢ HiPSC-derived neurons (Geraili et al., 2018) ➢ HiPSC-derived brain microvascular endothelial cells (BMECs) ➢ Co-colture of neurons, glial cells, endothelial cells and skeletal muscle cells	➢ mimicking in vivo physiological brain microenvironment/ barrier and relevant conditions/functions	➢ High-fidelity in mimicking in vivo physiological microenvironment	➢ neurodegenerative and brain diseases ➢	➢ Drug delivery through BBB junctions ➢ vascular network permeability	➢ functionality and disruption ➢ inflammatory disruption of BBB ➢ metabolic consequences and repair mechanisms
2.2 Tumor	➢ Patient-derived cells ➢ Tumor spheroids ➢ Variety of tumor cell lines	➢ vascularized tumor model ➢ use of (standard and liquid) biopsy & patient-derived samples, patient-specific tumor cell functions, ex vivo analysis of tumor cell dynamics and heterogeneity, ➢ microtumors arrays for testing combinatorial treatments with high throughput.	➢ 3D solid tumor tissues (tumor spheroids/ organoids/tumoroids) ➢ tumour microenvironment, extracellular matrix, cell–cell interactions, blood vasculature, and presence of nutrients, metabolites and oxygen gradients ➢ tumor angiogenesis and tumor and vasculature interactions ➢ metastatic cascade	➢ Cancer and metastatic cascade: proliferation invasion, intravasation, extravasion	➢ Drug development and screening ➢ Personalized therapies	➢ blood organ barriers
2.3.1 Heart	➢ Cardiomyocyte cells (Caplin et al., 2015b) ➢ Embryonic cardiomyoblast cell line(H9C2) (Giridharan et al., 2010) ➢ HiPSC-derived cardiomyocyte (Geraili et al., 2018)	➢ influence of mechanical cues ➢ microtissue-generated contractile forces ➢ studying cardiotoxicity and cardioprotective efficacy of cardiovascular drugs ➢ amyotrophic lateral sclerosis and neuromuscular development	➢ influence of mechanical cues ➢ microtissue-generated contractile forces ➢ cardiac/myocardial mechanics and heart muscle contractility ➢ force/strain sensors integration	➢ Cardiovascular diseases	➢ cardiovascular drugs ➢ toxicity and side effects ➢ cardiotoxicity and cardioprotective efficacy	
2.3.2 Bone	➢ Human foetal osteoblast cell line (hFOB) ➢ Co-colture osteocyte and osteoclast ➢ Osteoblast-like cell line (MG63) ➢ Chondrocytes	➢ Recreating biomechanical structures of the bone with scaffold materials and co-coltures models ➢ mechanobiology and mechanotransduction	➢ Use of scaffold materials ➢ influence of mechanical cues ➢ osteocyte-osteoclast signaling ➢ proliferation and osteogenic differentiation of foetal osteoblast cell line ➢ vascularized bone-on-chip models	➢ Bone diseases	➢ Efficacy ➢ toxicity and side effects	
2.4.1 Liver	➢ Human liver carcinoma cesll (HEpG2) and Umbilical endothelial cells (HUVEC) (Caplin et al., 2015b) ➢ HiPSC -derived hepatic progenitor cells	➢ Hepatotoxicity test of drugs and compounds ➢ Investigating drug-induced liver injury ➢Studying hepatic drug metabolism changes in humans overcoming species-specific differences in	➢ drug metabolism ➢ multi-organ interactions	➢ liver pathologies ➢ drug-induced liver injury (DILI)	➢ drug metabolism ➢ drug-induced liver toxicity	

(*continued on next page*)

Table 3 (*continued*)

ORGAN–ON–CHIP	CULTURED CELLS IN DEVICE	Main scope/aim	Key features	Diseases	Drug	Barrier
	(HPC) and mesenchimal stem cells (MCSs) and enteroendocrine cells (ECs) (Giobbe et al., 2015) ➢ HiPSC- derived hepatocytes (iHep)	➢hepatic drug metabolism				
2.4.2 Kidney	➢ Madin darby canine kidney (MDCK) (Caplin et al., 2015b) ➢ Human primary renal proximal tubule epithelial cell line (RPTEC) (Frohlich et al., 2012) ➢ Human renal epithelial cells (HREC) (Ferrell et al., 2010) ➢ hiPSC-derived human podocytes (Musah et al., 2017b) ➢ Human immortalized proximal tubular epithelial cell with organic anion transporter 1 (CiPTEC-OAT1)	➢ Nephrotoxicity test of drugs and compounds ➢ Detecting drug-induced kidney injury	➢ drug clearance ➢ multi-organ interactions	➢ kidney pathologies ➢ drug-induced kidney injury (DIKI)	➢ drug-induced nephrotoxicity studies	
2.5 Multi-organ	➢ Hepatocellular carcinoma (HepG2/C3A) and Madin-Darby canine kidney (MDCK) (Shintu et al., 2012b) ➢ Hepatic cell line (HepaRG) and human epatic stellate cells (HHStec) (Wagner et al., 2013b)	➢ miniature 'body-on-a-chip' microphysiological systems ➢ organ-organ interaction/crosstalk, ➢ physiological relations, methabolic pathways, ➢ significant biological barriers ➢ whole-body drug response with in vivo-like sequential organ-to-organ transfer of media	➢ Drug development, toxicity tests and metabolism of xenobiotics ➢Recapitulating metabolic pathways with ➢intestine models accounting for absorption and metabolism of drugs, liver for their metabolism and kidney for clearance/excretion	➢ systemic studies on orally-administered or inhaled substances or transdermal administration and subsequent drug metabolism ➢ multi-organ platforms for predicting antitumor drug response and metastasis	➢ evaluation of systemic effectiveness, accuracy and safety of drugs	➢ By integrating relevant barrier models

in order to make available the pertinent and supporting cells necessary for accurate disease and barrier models.

In conclusion, drug research is rapidly advancing with novel technologies at the disposal of researchers and companies. Today, more predictive approaches based on accurate in vitro replicas of human tissues, specific diseases and multi-organ models can respond to the pressing need for effective drug development protocols improving throughput and resource-efficiency beyond the possibilities of conventional 2D culture systems and animal testing. Furthermore, modern organ-on-chip systems offer tremendous promise for elucidating the mechanisms responsible for currently-incurable diseases. Several milestones were already achieved in this direction. Future challenges are expected to regard compromises between standardization, reproducibility and reliability in recapitulating disease microenvironment and drug response (Brancato et al., 2020) as well as to proceed toward patient-derived testing platforms for a personalized precision medicine.

Declaration of competing interest

The authors declare that they have no known competing financial interests or personal relationships that could have appeared to influence the work reported in this paper.

Data availability

No data was used for the research described in the article.

Funding

This work was funded by Italian National PON-AIM1800370-activity 2 (topic Health), by the Apulia region program "RESEARCH FOR INNOVATION" (REFIN n° 6277F79D-UNISAL036) and by FSC/PON FSE—FESR 2014–2020, project DOT1712250 code 2, XXXVI cycle, CUP F85F20000270006.

References

Abaci, H.E., Gledhill, K., Guo, Z., Christiano, A.M., Shuler, M.L., 2015. Lab Chip 15 (3), 882–888. https://doi.org/10.1039/C4LC00999A.

Abaci, H.E., Guo, Z., Coffman, A., Gillette, B., Lee, W.-h., Sia, S.K., Christiano, A.M., 2016. Adv. Healthc. Mater. 5 (14), 1800–1807. https://doi.org/10.1002/adhm.201500936.

Abudupataer, M., Zhu, S.C., Yan, S.Q., Xu, K.H., Zhang, J.J., Luo, S.M., Ma, W.R., Alam, M.F., Tang, Y.Y., Huang, H., Chen, N., Wang, L., Yan, G.Q., Li, J., Lai, H., Wang, C.S., Zhu, K., Zhang, W.J., 2021. Elife 10, 26. https://doi.org/10.7554/eLife.69310.sa2.

Agarwal, A., Goss, J.A., Cho, A., McCain, M.L., Parker, K.K., 2013. Lab Chip 13 (18), 3599–3608. https://doi.org/10.1039/c3lc50350j.

Ai, X.N., Wu, Y., Lu, W.B., Zhang, X.R., Zhao, L., Tu, P.F., Wang, K.W., Jiang, Y., 2020a. Adv. Sci. 7 (11) https://doi.org/10.1002/advs.202000111.

Ai, X.N., Zhao, L., Lu, Y.Y., Hou, Y., Lv, T., Jiang, Y., Tu, P.F., Guo, X.Y., 2020b. Anal. Chem. 92 (17), 11696–11704. https://doi.org/10.1021/acs.analchem.0c01590.

Ainslie, G.R., Davis, M., Ewart, L., Lieberman, L.A., Rowlands, D.J., Thorley, A.J., Yoder, G., Ryan, A.M., 2019. Lab Chip 19 (19), 3152–3161. https://doi.org/10.1039/c9lc00492k.

Alberti, M., Dancik, Y., Sriram, G., Wu, B., Teo, Y.L., Feng, Z., Bigliardi-Qi, M., Wu, R.G., Wang, Z.P., Bigliardi, P.L., 2017. Lab Chip 17 (9), 1625–1634. https://doi.org/10.1039/C6LC01574C.

Amani Wan Salim, W.W., H Park, J., Ul Haque, A., Marshall Porterfield, D., 2013. Recent Pat. Space Technol. 3 (1), 24–39.

Appl. In Vitro Toxicol. 1 (2), 2015, 165–171. https://doi.org/10.1089/aivt.2015.0002.

Arik, Y.B., van der Helm, M.W., Odijk, M., Segerink, L.I., Passier, R., van den Berg, A., van der Meer, A.D., 2018. Biomicrofluidics 12 (4). https://doi.org/10.1063/1.5023041.

Arjmand, B., Hamidpour, S.K., Rabbani, Z., Tayanloo-Beik, A., Rahim, F., Aghayan, H.R., Larijani, B., 2022. Front. Neurol. 12, 17. https://doi.org/10.3389/fneur.2021.788462.

Arndt, S., Seebach, J., Psathaki, K., Galla, H.J., Wegener, J., 2004. Biosens. Bioelectron. 19 (6), 583–594. https://doi.org/10.1016/s0956-5663(03)00269-0.

Asbill, C., Kim, N., El-Kattan, A., Creek, K., Wertz, P., Michniak, B., 2000. Pharm. Res. (N. Y.) 17 (9), 1092–1097. https://doi.org/10.1023/A:1026405712870.

Ashammakhi, N., Wesseling-Perry, K., Hasan, A., Elkhammas, E., Zhang, Y.S., 2018. Kidney Int. 94 (6), 1073–1086. https://doi.org/10.1016/j.kint.2018.06.034.

Ashammakhi, N., Darabi, M.A., Celebi-Saltik, B., Tutar, R., Hartel, M.C., Lee, J., Hussein, S.M., Goudie, M.J., Cornelius, M.B., Dokmeci, M.R., Khademhosseini, A., 2020a. Small Methods 4 (1). https://doi.org/10.1002/smtd.201900589.

Ashammakhi, N., Nasiri, R., Barros, N.R., Tebon, P., Thakor, J., Goudie, M., Shamloo, A., Martin, M.G., Khademhosseini, A., 2020b. Biomaterials 255, 120196. https://doi.org/10.1016/j.biomaterials.2020.120196.

Atac, B., Wagner, I., Horland, R., Lauster, R., Marx, U., Tonevitsky, A.G., Azar, R.P., Lindner, G., 2013. Lab Chip 13 (18), 3555–3561. https://doi.org/10.1039/c3lc50227a.

Atkuri, K.R., Herzenberg, L.A., Niemi, A.-K., Cowan, T., Herzenberg, L.A., 2007. Proc. Natl. Acad. Sci. USA 104 (11), 4547–4552. https://doi.org/10.1073/pnas.0611732104.

Au - Risueño, I., Au - Valencia, L., Au - Holgado, M., Au - Jorcano, J.L., Au - Velasco, D., 2021. JoVE (171), e62353. https://doi.org/10.3791/62353.

Ayuso, J.M., Truttschel, R., Gong, M.M., Humayun, M., Virumbrales-Munoz, M., Vitek, R., Felder, M., Gillies, S.D., Sondel, P., Wisinski, K.B., Patankar, M., Beebe, D. J., Skala, M.C., 2018. OncoImmunology 8 (3). https://doi.org/10.1080/2162402X.2018.1553477, 1553477-1553477.

Bagnaninchi, P.O., Drummond, N., 2011. Proc. Natl. Acad. Sci. U.S.A. 108 (16), 6462–6467. https://doi.org/10.1073/pnas.1018260108.

Bale, S.S., Vernetti, L., Senutovitch, N., Jindal, R., Hegde, M., Gough, A., McCarty, W.J., Bakan, A., Bhushan, A., Shun, T.Y., Golberg, I., DeBiasio, R., Usta, O.B., Taylor, D.L., Yarmush, M.L., 2014. Exp. Biol. Med. 239 (9), 1180–1191. https://doi.org/10.1177/1535370214531872.

Bang, S., Lee, S.-R., Ko, J., Son, K., Tahk, D., Ahn, J., Im, C., Jeon, N.L., 2017. Sci. Rep. 7 (1), 8083. https://doi.org/10.1038/s41598-017-07416-0.

Barkal, L.J., Procknow, C.L., Álvarez-García, Y.R., Niu, M., Jiménez-Torres, J.A., Brockman-Schneider, R.A., Gern, J.E., Denlinger, L.C., Theberge, A.B., Keller, N.P., Berthier, E., Beebe, D.J., 2017. Nat. Commun. 8 (1), 1770. https://doi.org/10.1038/s41467-017-01985-4.

Barros, A.S., Costa, A., Sarmento, B., 2021. Adv. Drug Deliv. Rev. 170, 386–395. https://doi.org/10.1016/j.addr.2020.09.008.

Baselt, D.R., Lee, G.U., Natesan, M., Metzger, S.W., Sheehan, P.E., Colton, R.J., 1998. Biosens. Bioelectron. 13 (7–8), 731–739.

Bavli, D., Prill, S., Ezra, E., Levy, G., Cohen, M., Vinken, M., Vanfleteren, J., Jaeger, M., Nahmias, Y., 2016. Proc. Natl. Acad. Sci. U.S.A. 113 (16), E2231–E2240. https://doi.org/10.1073/pnas.1522556113.

Beaurivage, C., Naumovska, E., Chang, Y.X., Elstak, E.D., Nicolas, A., Wouters, H., van Moolenbroek, G., Lanz, H.L., Trietsch, S.J., Joore, J., Vulto, P., Janssen, R.A.J., Erdmann, K.S., Stallen, J., Kurek, D., 2019. Int. J. Mol. Sci. 20 (22), 5661.

Becker, H., Gärtner, C., 2008. Anal. Bioanal. Chem. 390 (1), 89–111. https://doi.org/10.1007/s00216-007-1692-2.

Bein, A., Shin, W., Jalili-Firoozinezhad, S., Park, M.H., Sontheimer-Phelps, A., Tovaglieri, A., Chalkiadaki, A., Kim, H.J., Ingber, D.E., 2018. Cell. Mol. Gastroenterol. Hepatol. 5 (4), 659–668. https://doi.org/10.1016/j.jcmgh.2017.12.010.

Benam, K.H., Dauth, S., Hassell, B., Herland, A., Jain, A., Jang, K.J., Karalis, K., Kim, H. J., MacQueen, L., Mahmoodian, R., Musah, S., Torisawa, Y.S., van der Meer, A.D., Villenave, R., Yadid, M., Parker, K.K., Ingber, D.E., 2015. Engineered in vitro disease models. Vol 10. In: Abbas, A.K., Galli, S.J., Howley, P.M. (Eds.), Annual Review of Pathology: Mechanisms of Disease, vol. 10, pp. 195–262. Annual Reviews: Palo Alto.

Benam, K.H., Villenave, R., Lucchesi, C., Varone, A., Hubeau, C., Lee, H.H., Alves, S.E., Salmon, M., Ferrante, T.C., Weaver, J.C., Bahinski, A., Hamilton, G.A., Ingber, D.E., 2016. Nat. Methods 13 (2), 151. https://doi.org/10.1038/nmeth.3697.

Bennet, T.J., Randhawa, A., Hua, J., Cheung, K.C., 2021. Cells 10 (7), 51. https://doi.org/10.3390/cells10071602.

Bhatia, S.N., Ingber, D.E., 2014. Nat. Biotechnol. 32 (8), 760–772. https://doi.org/10.1038/nbt.2989.

Bhattacharjee, N., Parra-Cabrera, C., Kim, Y.T., Kuo, A.P., Folch, A., 2018. Adv. Mater. 30 (22), 1800001 https://doi.org/10.1002/adma.201800001.

Biglari, S., Le, T.Y.L., Tan, R.P., Wise, S.G., Zambon, A., Codolo, G., De Bernard, M., Warkiani, M., Schindeler, A., Naficy, S., Valtchev, P., Khademhosseini, A., Dehghani, F., 2019. Adv. Healthc. Mater. 8 (1), 12. https://doi.org/10.1002/adhm.201801307.

Bircsak, K.M., DeBiasio, R., Miedel, M., Alsebahi, A., Reddinger, R., Saleh, A., Shun, T., Vernetti, L.A., Gough, A., 2021. Toxicology 450, 152667. https://doi.org/10.1016/j.tox.2020.152667.

Borghardt, J.M., Kloft, C., Sharma, A., 2018. Can. Respir. J. J. Can. Thorac. Soc. 2018, 2732017 https://doi.org/10.1155/2018/2732017.

Bovard, D., Sandoz, A., Luettich, K., Frentzel, S., Iskandar, A., Marescotti, D., Trivedi, K., Guedj, E., Dutertre, Q., Peitsch, M.C., Hoeng, J., 2018. Lab Chip 18 (24), 3814–3829. https://doi.org/10.1039/c8lc01029c.

Boyce, M.W., Kenney, R.M., Truong, A.S., Lockett, M.R., 2016. Anal. Bioanal. Chem. 408 (11), 2985–2992. https://doi.org/10.1007/s00216-015-9189-x.

Brancato, V., Oliveira, J.M., Correlo, V.M., Reis, R.L., Kundu, S.C., 2020. Biomaterials 232. https://doi.org/10.1016/j.biomaterials.2019.119744.

Brown, J.A., Codreanu, S.G., Shi, M., Sherrod, S.D., Markov, D.A., Neely, M.D., Britt, C. M., Hoilett, O.S., Reiserer, R.S., Samson, P.C., McCawley, L.J., Webb, D.J., Bowman, A.B., McLean, J.A., Wikswo, J.P., 2016. J. Neuroinflammation 13. https://doi.org/10.1186/s12974-016-0760-y.

Buja, I., Sabella, E., Monteduro, A.G., Rizzato, S., Bellis, L.D., Elicio, V., Formica, L., Luvisi, A., Maruccio, G., 2022. Biosensors 12 (3), 147.

Cabodi, M., Choi, N.W., Gleghorn, J.P., Lee, C.S.D., Bonassar, L.J., Stroock, A.D., 2005. J. Am. Chem. Soc. 127 (40), 13788–13789. https://doi.org/10.1021/ja054820t.

Campillo, N., Oliveira, V.R., da Palma, R.K., 2021. Chemosensors 9 (9), 17. https://doi.org/10.3390/chemosensors9090248.

Caplin, J.D., Granados, N.G., James, M.R., Montazami, R., Hashemi, N., 2015a. Adv. Healthc. Mater. 4 (10), 1426–1450. https://doi.org/10.1002/adhm.201500040.

Caplin, J.D., Granados, N.G., James, M.R., Montazami, R., Hashemi, N., 2015b. Adv Healthc Mater 4 (10), 1426–1450. https://doi.org/10.1002/adhm.201500040.

Carter, S.-S.D., Atif, A.-R., Kadekar, S., Lanekoff, I., Engqvist, H., Varghese, O.P., Tenje, M., Mestres, G., 2020. Organs-on-a-Chip 2, 100004. https://doi.org/10.1016/j.ooc.2020.100004.

Chen, Y., Li, P., Huang, P.-H., Xie, Y., Mai, J.D., Wang, L., Nam-Trung, N., Huang, T.J., 2014. Lab Chip 14 (4), 626–645. https://doi.org/10.1039/c3lc90136j.

Chen, M.B., Lamar, J.M., Li, R., Hynes, R.O., Kamm, R.D., 2016a. Cancer Res. 76 (9), 2513–2524. https://doi.org/10.1158/0008-5472.can-15-1325.

Chen, X., Shen, J., Zhou, M., 2016b. J. Micromech. Microeng. 26 (10), 107001 https://doi.org/10.1088/0960-1317/26/10/107001.

Chen, M.B., Whisler, J.A., Fröse, J., Yu, C., Shin, Y., Kamm, R.D., 2017. Nat. Protoc. 12 (5), 865–880. https://doi.org/10.1038/nprot.2017.018.

Chen, Z.K., Kheiri, S., Gevorkian, A., Young, E.W.K., Andre, V., Deisenroth, T., Kumacheva, E., 2021. Lab Chip 21 (20), 3952–3962. https://doi.org/10.1039/d1lc00619c.

Cheng, S.-B., Xie, M., Xu, J.-Q., Wang, J., Lv, S.-W., Guo, S., Shu, Y., Wang, M., Dong, W.-G., Huang, W.-H., 2016. Anal. Chem. 88 (13), 6773–6780. https://doi.org/10.1021/acs.analchem.6b01130.

Chiriacò, M.S., Primiceri, E., Monteduro, A.G., Bove, A., Leporatti, S., Capello, M., Ferri-Borgogno, S., Rinaldi, R., Novelli, F., Maruccio, G., 2013. Lab Chip 13 (4), 730–734. https://doi.org/10.1039/c2lc41127j.

Chiriacò, M.S., de Feo, F., Primiceri, E., Monteduro, A.G., de Benedetto, G.E., Pennetta, A., Rinaldi, R., Maruccio, G., 2015. Talanta 142, 57–63. https://doi.org/10.1016/j.talanta.2015.04.040.

Chiriacò, M.S., Primiceri, E., De Feo, F., Montanaro, A., Monteduro, A.G., Tinelli, A., Megha, M., Carati, D., Maruccio, G., 2016. Biosens. Bioelectron. 79, 9–14. https://doi.org/10.1016/j.bios.2015.11.100.

Chiriacò, M.S., Rizzato, S., Primiceri, E., Spagnolo, S., Monteduro, A.G., Ferrara, F., Maruccio, G., 2018. Microelectron. Eng. 202, 31–36. https://doi.org/10.1016/j.mee.2018.10.008.

Choi, N.W., Cabodi, M., Held, B., Gleghorn, J.P., Bonassar, L.J., Stroock, A.D., 2007. Nat. Mater. 6 (11), 908–915. https://doi.org/10.1038/nmat2022.

Christoffersson, J., Aronsson, C., Jury, M., Selegard, R., Aili, D., Mandenius, C.F., 2019. Biofabrication 11 (1), 13. https://doi.org/10.1088/1758-5090/aaf657.

Chung, K., Zhan, M., Srinivasan, J., Sternberg, P.W., Gong, E., Schroeder, F.C., Lu, H., 2011. Lab Chip 11 (21), 3689–3697. https://doi.org/10.1039/c1lc20400a.

Chung, M., Ahn, J., Son, K., Kim, S., Jeon, N.L., 2017. Adv. Healthc. Mater. 6 (15) https://doi.org/10.1002/adhm.201700196.

Cidem, A., Bradbury, P., Traini, D., Ong, H.X., 2020. Front. Bioeng. Biotechnol. 8 https://doi.org/10.3389/fbioe.2020.581995.

Cohen, A., Ioannidis, K., Ehrlich, A., Regenbaum, S., Cohen, M., Ayyash, M., Tikva, S.S., Nahmias, Y., 2021. Sci. Transl. Med. (582), 13. https://doi.org/10.1126/scitranslmed.abd6299.

Colombelli, A., Primiceri, E., Rizzato, S., Monteduro, A.G., Maruccio, G., Rella, R., Manera, M.G., 2021. Chemosensors 9 (1), 10.

Contreras-Naranjo, J.C., Wu, H.J., Ugaz, V.M., 2017. Lab Chip 17 (21), 3558–3577. https://doi.org/10.1039/c7lc00592j.

Cosson, S., Aeberli, L.G., Brandenberg, N., Lutolf, M.P., 2015. Lab Chip 15 (1), 72–76. https://doi.org/10.1039/C4LC00848K.

Cui, M.Y., Wiraja, C., Zheng, M.J., Singh, G., Yong, K.T., Xu, C.J., 2022. Adv. Ther. 5 (1), 13. https://doi.org/10.1002/adtp.202100138.

De Gregorio, V., Telesco, M., Corrado, B., Rosiello, V., Urciuolo, F., Netti, P.A., Imparato, G., 2020. Front. Bioeng. Biotechnol. 8, 19. https://doi.org/10.3389/fbioe.2020.00163.

de Haan, P., Santbergen, M.J.C., van der Zande, M., Bouwmeester, H., Nielen, M.W.F., Verpoorte, E., 2021. Sci. Rep. 11 (1), 4920. https://doi.org/10.1038/s41598-021-84187-9.

Debreczeni, M.L., Szekacs, I., Kovacs, B., Saftics, A., Kurunczi, S., Gál, P., Dobó, J., Cervenak, L., Horvath, R., 2020. Sci. Rep. 10 (1), 3303. https://doi.org/10.1038/s41598-020-60158-4.

Decsi, B., Krammer, R., Hegedus, K., Ender, F., Gyarmati, B., Szilagyi, A., Totos, R., Katona, G., Paizs, C., Balogh, G.T., Poppe, L., Balogh-Weiser, D., 2019. Micromachines 10 (10), 13. https://doi.org/10.3390/mi10100668.

Del Piccolo, N., Shirure, V.S., Bi, Y., Goedegebuure, S.P., Gholami, S., Hughes, C.C.W., Fields, R.C., George, S.C., 2021. Adv. Drug Deliv. Rev. 175, 113798 https://doi.org/10.1016/j.addr.2021.05.008.

Dellaquila, A., Le Bao, C., Letourneur, D., Simon-Yarza, T., 2021. Adv. Sci. 8 (19), 2100798 https://doi.org/10.1002/advs.202100798.

Deng, J., Wei, W.B., Chen, Z.Z., Lin, B.C., Zhao, W.J., Luo, Y., Zhang, X.L., 2019. Micromachines 10 (10), 26. https://doi.org/10.3390/mi10100676.

Dhiman, N., Kingshott, P., Sumer, H., Sharma, C.S., Rath, S.N., 2019. Biosens. Bioelectron. 137, 236–254. https://doi.org/10.1016/j.bios.2019.02.070.

Di Natale, C., Macagnano, A., Martinelli, E., Paolesse, R., D'Arcangelo, G., Roscioni, C., Finazzi-Agro, A., D'Amico, A., 2003. Biosens. Bioelectron. 18 (10), 1209–1218. https://doi.org/10.1016/s0956-5663(03)00086-1.

Ding, C., Chen, X., Kang, Q., Yan, X., 2020. Front. Bioeng. Biotechnol. 8 https://doi.org/10.3389/fbioe.2020.00823, 823-823.

Douville, N.J., Tung, Y.C., Li, R., Wang, J.D., El-Sayed, M.E.H., Takayama, S., 2010. Anal. Chem. 82 (6), 2505–2511. https://doi.org/10.1021/ac9029345.

Du, Y., Li, N., Yang, H., Luo, C., Gong, Y., Tong, C., Gao, Y., Lü, S., Long, M., 2017. Lab Chip 17 (5), 782–794. https://doi.org/10.1039/C6LC01374K.

Du, Z., Mi, S., Yi, X., Xu, Y., Sun, W., 2018. Biofabrication 10 (3), 034102. https://doi.org/10.1088/1758-5090/aac70c.

Dummer, J., Storer, M., Swanney, M., McEwan, M., Scott-Thomas, A., Bhandari, S., Chambers, S., Dweik, R., Epton, M., 2011. TrAC, Trends Anal. Chem. 30 (7), 960–967. https://doi.org/10.1016/j.trac.2011.03.011.

Duval, C., Chagnoleau, C., Pouradier, F., Sextius, P., Condom, E., Bernerd, F., 2012. Tissue Eng. C Methods. 18 (12), 947–957. https://doi.org/10.1089/ten.tec.2011.0676.

Einoch Amor, R., Nakhleh, M.K., Barash, O., Haick, H., 2019. Eur. Respir. Rev. 28 (152), 190002 https://doi.org/10.1183/16000617.0002-2019.

Elomaa, L., Yang, Y.P., 2017. Tissue Eng. B Rev. 23 (5), 436–450. https://doi.org/10.1089/ten.TEB.2016.0348.

Esch, M.B., Mahler, G.J., Stokor, T., Shuler, M.L., 2014. Lab Chip 14 (16), 3081–3092. https://doi.org/10.1039/c4lc00371c.

Fabre, K., Berridge, B., Proctor, W.R., Ralston, S., Will, Y., Baran, S.W., Yoder, G., Van Vleet, T.R., 2020. Lab Chip 20 (6), 1049–1057. https://doi.org/10.1039/c9lc01168d.

Fan, Y.T., Nguyen, D.T., Akay, Y., Xu, F., Akay, M., 2016. Sci. Rep. 6 https://doi.org/10.1038/srep25062.

Farooqi, H.M.U., Kang, B., Khalid, M.A.U., Salih, A.R.C., Hyun, K., Park, S.H., Huh, D., Choi, K.H., 2021. Nano Converg. 8 (1) https://doi.org/10.1186/s40580-021-00253-y, 3-3.

Fedorovich, N.E., Schuurman, W., Wijnberg, H.M., Prins, H.-J., Van Weeren, P.R., Malda, J., Alblas, J., Dhert, W.J., 2012. Tissue Eng. C Methods 18 (1), 33–44.

Felder, M., Trueeb, B., Stucki, A.O., Borcard, S., Stucki, J.D., Schnyder, B., Geiser, T., Guenat, O.T., 2019. Front. Bioeng. Biotechnol. 7, 5. https://doi.org/10.3389/fbioe.2019.00003.

Feng, J., Zheng, Y., Bhusari, S., Villiou, M., Pearson, S., del Campo, A., 2020. Adv. Funct. Mater. 30 (45), 2004327 https://doi.org/10.1002/adfm.202004327.

Ferrari, E.; Palma, C., 2020, 10 (9). DOI 10.3390/bios10090110..

Ferrell, N., Desai, R.R., Fleischman, A.J., Roy, S., Humes, H.D., Fissell, W.H., 2010. Biotechnol. Bioeng. 107 (4), 707–716. https://doi.org/10.1002/bit.22835.

Fois, C.A.M., Le, T.Y.L., Schindeler, A., Naficy, S., McClure, D.D., Read, M.N., Valtchev, P., Khademhosseini, A., Dehghani, F., 2019. Adv. Healthc. Mater. 8 (21), 1900968 https://doi.org/10.1002/adhm.201900968.

Foster, A.J., Chouhan, B., Regan, S.L., Rollison, H., Amberntsson, S., Andersson, L.C., Srivastava, A., Darnell, M., Cairns, J., Lazic, S.E., Jang, K.J., Petropolis, D.B., Kodella, K., Rubins, J.E., Williams, D., Hamilton, G.A., Ewart, L., Morgan, P., 2019. Arch. Toxicol. 93 (4), 1021–1037. https://doi.org/10.1007/s00204-019-02427-4.

Fralish, Z., Lotz, E.M., Chavez, T., Khodabukus, A., Bursac, N., 2021. Front. Cell Dev. Biol. 9, 35. https://doi.org/10.3389/fcell.2021.764732.

Frohlich, E.M., Zhang, X., Charest, J.L., 2012. Integrative biology : Quantitative Biosciences From Nano To Macro, 4, pp. 75–83. https://doi.org/10.1039/c1ib00096a, 1.

Frost, T.S., Jiang, L.A., Lynch, R.M., Zohar, Y., 2019. Micromachines 10 (8), 18. https://doi.org/10.3390/mi10080533.

Galvan-Chacon, V. P.; Zampouka, A.; Hesse, B.; Bohner, M.; Habibovic, P.; Barata, D., Adv. Eng. Mater., 13. DOI 10.1002/adem.202101467..

Geraili, A., Jafari, P., Hassani, M.S., Araghi, B.H., Mohammadi, M.H., Ghafari, A.M., Tamrin, S.H., Modarres, H.P., Kolahchi, A.R., Ahadian, S., Sanati-Nezhad, A., 2018. Adv Healthc Mater 7 (2). https://doi.org/10.1002/adhm.201700426.

Giaever, I., Keese, C.R., 1993. Nature 366 (6455), 591–592. https://doi.org/10.1038/366591a0.

Gibbs, S., Corsini, E., Spiekstra, S.W., Galbiati, V., Fuchs, H.W., DeGeorge, G., Troese, M., Hayden, P., Deng, W., Roggen, E., 2013. Toxicol. Appl. Pharmacol. 272 (2), 529–541. https://doi.org/10.1016/j.taap.2013.07.003.

Giobbe, G.G., Michielin, F., Luni, C., Giulitti, S., Martewicz, S., Dupont, S., Floreani, A., Elvassore, N., 2015. Nat. Methods 12 (7), 637–640. https://doi.org/10.1038/nmeth.3411.

Giridharan, G.A., Nguyen, M.D., Estrada, R., Parichehreh, V., Hamid, T., Ismahil, M.A., Prabhu, S.D., Sethu, P., 2010. Anal. Chem. 82 (18), 7581–7587. https://doi.org/10.1021/ac1012893.

Gough, A., Soto-Gutierrez, A., Vernetti, L., Ebrahimkhani, M.R., Stern, A.M., Taylor, D.L., 2021. Nat. Rev. Gastroenterol. Hepatol. 18 (4), 252–268. https://doi.org/10.1038/s41575-020-00386-1.

Guttenplan, A.P.M., Tahmasebi Birgani, Z., Giselbrecht, S., Truckenmüller, R.K., Habibović, P., 2021. Adv. Healthc. Mater. 10 (14), 2100371 https://doi.org/10.1002/adhm.202100371.

Haase, K., Offeddu, G.S., Gillrie, M.R., Kamm, R.D., 2020. Adv. Funct. Mater. 30 (48), 2002444 https://doi.org/10.1002/adfm.202002444.

Haes, A.J., Hall, W.P., Chang, L., Klein, W.L., Van Duyne, R.P., 2004. Nano Lett. 4 (6), 1029–1034. https://doi.org/10.1021/nl049670j.

Han, A., Yang, L., Frazier, A.B., 2007. Clin. Cancer Res. 13 (1), 139–143. https://doi.org/10.1158/1078-0432.ccr-06-1346.

Hao, S.; Ha, L.; Cheng, G.; Wan, Y.; Xia, Y.; Sosnoski, D. M.; Mastro, A. M.; Zheng, S. Y., 2018, 14 (12), e1702787. DOI 10.1002/smll.201702787..

Hassan, S., Heinrich, M., Cecen, B., Prakash, J., Zhang, Y.S., 2020. 26 - biomaterials for on-chip organ systems. In: Vrana, N.E., Knopf-Marques, H., Barthes, J. (Eds.), Biomaterials For Organ And Tissue Regeneration. Woodhead Publishing, pp. 669–707.

Henry, O.Y.F., Villenave, R., Cronce, M.J., Leineweber, W.D., Benz, M.A., Ingber, D.E., 2017. Lab Chip 17 (13), 2264–2271. https://doi.org/10.1039/c7lc00155j.

Hewes, S.A., Wilson, R.L., Estes, M.K., Shroyer, N.F., Blutt, S.E., Grande-Allen, K.J., 2020. Tissue Eng. B Rev. 26 (4), 313–326. https://doi.org/10.1089/ten.teb.2019.0334.

Hoang, P., Ma, Z., 2021. Acta Biomater. 132, 23–36. https://doi.org/10.1016/j.actbio.2021.01.026.

Hodgkinson, T., Amado, I.N., O'Brien, F.J., Kennedy, O.D., 2022. Apl. Bioeng. 6 (1), 17. https://doi.org/10.1063/5.0068277.

Huang, D., Liu, T.T., Liao, J.L., Maharjan, S., Xie, X., Perez, M., Anaya, I., Wang, S.W., Mayer, A.T., Kang, Z.X., Kong, W.J., Mainardi, V.L., Garciamendez-Mijares, C.E., Martinez, G.G., Moretti, M., Zhang, W.J., Gu, Z.Z., Ghaemmaghami, A.M., Zhang, Y. S., 2021. Proc. Natl. Acad. Sci. U.S.A. 118 (19), 10. https://doi.org/10.1073/pnas.2016146118.

Huh, D.D., 2015. Ann. Am. Thorac. Soc. 12 (Suppl. 1), S42–S44. https://doi.org/10.1513/AnnalsATS.201410-442MG. Suppl 1.

Huh, D., Fujioka, H., Tung, Y.C., Futai, N., Paine 3rd, R., Grotberg, J.B., Takayama, S., 2007. Proc. Natl. Acad. Sci. U.S.A. 104 (48), 18886–18891. https://doi.org/10.1073/pnas.0610868104.

Huh, D., Matthews, B.D., Mammoto, A., Montoya-Zavala, M., Hsin, H.Y., Ingber, D.E., 2010a. Science 328 (5986), 1662–1668. https://doi.org/10.1126/science.1188302.

Huh, D., Matthews, B.D., Mammoto, A., Montoya-Zavala, M., Hsin, H.Y., Ingber, D.E., 2010b. Science 328 (5986), 1662–1668. https://doi.org/10.1126/science.1188302.

Huh, D., Hamilton, G.A., Ingber, D.E., 2011. Trends Cell Biol. 21 (12), 745–754. https://doi.org/10.1016/j.tcb.2011.09.005.

Huh, D., Leslie, D.C., Matthews, B.D., Fraser, J.P., Jurek, S., Hamilton, G.A., Thorneloe, K.S., McAlexander, M.A., Ingber, D.E., 2012. Sci. Transl. Med. 4 (159) https://doi.org/10.1126/scitranslmed.3004249.

Humayun, M., Chow, C.W., Young, E.W.K., 2018. Lab Chip 18 (9), 1298–1309. https://doi.org/10.1039/c7lc01357d.

Imparato, G., Urciuolo, F., Netti, P.A., 2022. Bioengineering 9 (1), 28.

Ishahak, M., Hill, J., Amin, Q., Wubker, L., Hernandez, A., Mitrofanova, A., Sloan, A., Fornoni, A., Agarwal, A., 2020. Front. Bioeng. Biotechnol. 8 (1311) https://doi.org/10.3389/fbioe.2020.581163.

Jain, P., Sonti, S., Garruto, J., Mehta, R., Banga, A.K., 2012. J. Cosmet. Dermatol. 11 (2), 101–110. https://doi.org/10.1111/j.1473-2165.2012.00610.x.

Jain, A., Barrile, R., van der Meer, A., Mammoto, A., Mammoto, T., De Ceunynck, K., Aisiku, O., Otieno, M., Louden, C., Hamilton, G., Flaumenhaft, R., Ingber, D., 2018a. Clin. Pharmacol. Ther. 103 (2), 332–340. https://doi.org/10.1002/cpt.742.

Jain, A., Barrile, R., van der Meer, A.D., Mammoto, A., Mammoto, T., De Ceunynck, K., Aisiku, O., Otieno, M.A., Louden, C.S., Hamilton, G.A., Flaumenhaft, R., Ingber, D., 2018b. Clin. Pharmacol. Ther. 103 (2), 332–340. https://doi.org/10.1002/cpt.742.

Jang, K.J., Mehr, A.P., Hamilton, G.A., McPartlin, L.A., Chung, S.Y., Suh, K.Y., Ingber, D. E., 2013. Integr. Biol. 5 (9), 1119–1129. https://doi.org/10.1039/c3ib40049b.

Jang, M., Koh, I., Lee, S.J., Cheong, J.H., Kim, P., 2017. Sci. Rep. 7 https://doi.org/10.1038/srep41541.

Jang, K.J., Otieno, M.A., Ronxhi, J., Lim, H.K., Ewart, L., Kodella, K.R., Petropolis, D.B., Kulkarni, G., Rubins, J.E., Conegliano, D., Nawroth, J., Simic, D., Lam, W., Singer, M., Barale, E., Singh, B., Sonee, M., Streeter, A.J., Manthey, C., Jones, B., Srivastava, A., Andersson, L.C., Williams, D., Park, H., Barrile, R., Sliz, J., Herland, A., Haney, S., Karalis, K., Ingber, D.E., Hamilton, G.A., 2019. Sci. Transl. Med. 11 (517) https://doi.org/10.1126/scitranslmed.aax5516.

Jeon, H.M., Kim, K., Choi, K.C., Sung, G.Y., 2020. J. Ind. Eng. Chem. 82, 71–80. https://doi.org/10.1016/j.jiec.2019.09.044.

Jeong, S., Kim, S., Buonocore, J., Park, J., Welsh, C.J., Li, J.R., Han, A., 2018. IEEE Trans. Biomed. Eng. 65 (2), 431–439. https://doi.org/10.1109/tbme.2017.2773463.
Jusoh, N., Oh, S., Kim, S., Kim, J., Jeon, N.L., 2015. Lab Chip 15 (20), 3984–3988. https://doi.org/10.1039/C5LC00698H.
Karamikamkar, S., Behzadfar, E., Cheung, K.C., 2018. Biomed. Microdevices 20 (2). https://doi.org/10.1007/s10544-018-0260-1.
Katz, E., Willner, I., 2003. Electroanalysis 15 (11), 913–947.
Kavand, H.; Nasiri, R.; Herland, A., Adv. Mater. (n/a), 2107876. DOI https://doi.org/10.1002/adma.202107876.
Keese, C.R., Bhawe, K., Wegener, J., Giaever, I., 2002. Biotechniques 33 (4), 842–850. https://doi.org/10.2144/02334rr01.
Khalid, M.A.U., Kim, Y.S., Ali, M., Lee, B.G., Cho, Y.-J., Choi, K.H., 2020. Biochem. Eng. J. 155, 107469 https://doi.org/10.1016/j.bej.2019.107469.
Khedoe, P., Marges, E., Hiemstra, P., Ninaber, M., Geelhoed, M., 2020. Front. Immunol. 11 https://doi.org/10.3389/fimmu.2020.01990.
Khetani, S., Yong, K.W., Guan, K., Singh, A., Phani, A., Kollath, V.O., Kim, S., Karan, K., Sen, A., Sanati-Nezhad, A., 2020. Appl. Mater. Today 20, 100721. https://doi.org/10.1016/j.apmt.2020.100721.
Khot, M.I., Levenstein, M.A., de Boer, G.N., Armstrong, G., Maisey, T., Svavarsdottir, H. S., Andrew, H., Perry, S.L., Kapur, N., Jayne, D.G., 2020. Sci. Rep. 10 (1) https://doi.org/10.1038/s41598-020-72952-1.
Kim, H.J., Huh, D., Hamilton, G., Ingber, D.E., 2012. Lab Chip 12 (12), 2165–2174. https://doi.org/10.1039/C2LC40074J.
Kim, S., Lee, H., Chung, M., Jeon, N.L., 2013. Lab Chip 13 (8), 1489–1500. https://doi.org/10.1039/c3lc41320a.
Kim, S., LesherPerez, S.C., Kim, B.c.C., Yamanishi, C., Labuz, J.M., Leung, B., Takayama, S., 2016. Biofabrication 8 (1), 015021. https://doi.org/10.1088/1758-5090/8/1/015021.
Kim, H.J., Li, H., Collins, J.J., Ingber, D.E., 2016. Proc. Natl. Acad. Sci. U.S.A. 113 (1), E7–E15. https://doi.org/10.1073/pnas.1522193112.
Kim, J.J., Ellett, F., Thomas, C.N., Jalali, F., Anderson, R.R., Irimia, D., Raff, A.B., 2019a. Lab Chip 19 (18), 3094–3103. https://doi.org/10.1039/C9LC00399A.
Kim, B.S., Gao, G., Kim, J.Y., Cho, D.-W., 2019b. Adv. Healthc. Mater. 8 (7), 1801019 https://doi.org/10.1002/adhm.201801019.
Kim, J., Kim, K., Sung, G.Y., 2020. Int. J. Mol. Sci. 21 (22), 8475.
Kimura, H., Yamamoto, T., Sakai, H., Sakai, Y., Fujii, T., 2008. Lab Chip 8 (5), 741–746. https://doi.org/10.1039/B717091B.
Kotz, F., Arnold, K., Wagner, S., Bauer, W., Keller, N., Nargang, T.M., Helmer, D., Rapp, B.E., 2018. Adv. Eng. Mater. 20 (2), 1700699 https://doi.org/10.1002/adem.201700699.
Kulthong, K., Duivenvoorde, L., Sun, H., Confederat, S., Wu, J., Spenkelink, B., de Haan, L., Marin, V., van der Zande, M., Bouwmeester, H., 2020. Toxicology in vitro : an international journal published in association with BIBRA, 65, 104815. https://doi.org/10.1016/j.tiv.2020.104815.
Kung, Y.-C., Huang, K.-W., Fan, Y.-J., Chiou, P.-Y., 2015. Lab Chip 15 (8), 1861–1868. https://doi.org/10.1039/C4LC01211A.
Kustermann, S., Boess, F., Buness, A., Schmitz, M., Watzele, M., Weiser, T., Singer, T., Suter, L., Roth, A., 2013. Toxicol. Vitro 27 (5), 1589–1595. https://doi.org/10.1016/j.tiv.2012.08.019.
Kwak, B., Lee, Y., Lee, J., Lee, S., Lim, J., 2018. J. Contr. Release 275, 201–207. https://doi.org/10.1016/j.jconrel.2018.02.029.
Kwapiszewska, K., Michalczuk, A., Rybka, M., Kwapiszewski, R., Brzózka, Z., 2014. Lab Chip 14 (12), 2096–2104. https://doi.org/10.1039/C4LC00291A.
Lee, S.Y., Sung, J.H., 2018. Biotechnol. Bioeng. 115 (11), 2817–2827. https://doi.org/10.1002/bit.26793.
Lee, S., Jin, S.P., Kim, Y.K., Sung, G.Y., Chung, J.H., Sung, J.H., 2017. Biomed. Microdevices 19 (2), 14. https://doi.org/10.1007/s10544-017-0156-5.
Lee, S.W., Kwak, H.S., Kang, M.-H., Park, Y.-Y., Jeong, G.S., 2018a. Sci. Rep. 8 (1), 2365. https://doi.org/10.1038/s41598-018-20886-0.
Lee, J. M.; Park, D. Y.; Yang, L., 2018, 8 (1), 17145. DOI 10.1038/s41598-018-35216-7..
Lee, S., Lim, J., Yu, J., Ahn, J., Lee, Y., Jeon, N.L., 2019. Lab Chip 19 (12), 2071–2080. https://doi.org/10.1039/C9LC00148D.
Lee, J.M., Choi, J.W., Ahrberg, C.D., Choi, H.W., Ha, J.H., Mun, S.G., Mo, S.J., Chung, B. G., 2020. Microsyst. Nanoeng. 6 (1) https://doi.org/10.1038/s41378-020-0167-x.
Legant, W.R., Pathak, A., Yang, M.T., Deshpande, V.S., McMeeking, R.M., Chen, C.S., 2009. Proc. Natl. Acad. Sci. USA 106 (25), 10097–10102. https://doi.org/10.1073/pnas.0900174106.
Li, X., Tian, T., 2018a. Front. Pharmacol. 9, 1067. https://doi.org/10.3389/fphar.2018.01067.
Li, X., Tian, T., 2018b. Anal. Methods 10 (26), 3122–3130. https://doi.org/10.1039/c8ay00970h.
Li, Y., Wang, S., Huang, R., Huang, Z., Hu, B., Zheng, W., Yang, G., Jiang, X., 2015. Biomacromolecules 16 (3), 780–789. https://doi.org/10.1021/bm501680s.
Li, Z., Su, W., Zhu, Y., Tao, T., Li, D., Peng, X., Qin, J., 2017. Biomicrofluidics 11 (3), 034114. https://doi.org/10.1063/1.4984768.
Li, X., Soler, M., Belushkin, A., Yesilköy, F., Altug, H., 2018. Optofluidic nanoplasmonic biosensor for label-free live cell analysis in real time. SPIE 10509.
Li, Z., Li, D., Guo, Y., Wang, Y., Su, W., 2021. Biotechnol. Lett. 43 (2), 383–392. https://doi.org/10.1007/s10529-020-03043-4.
Lim, J.; Ching, H.; Yoon, J.-K.; Jeon, N. L.; Kim, Y., Nano Convergence 2021, 8 (1), 12. DOI 10.1186/s40580-021-00261-y.
Lin, D.S.Y., Guo, F., Zhang, B.Y., 2019. Nanotechnology 30 (2). https://doi.org/10.1088/1361-6528/aae7de.
Lin, Z., Luo, G., Du, W., Kong, T., Liu, C., Liu, Z., 2020. Small 16 (9), 1903899. https://doi.org/10.1002/smll.201903899.
Lin, K.C., Yen, C.Z., Yang, J.W., Chung, J.H.Y., Chen, G.Y., 2022. Mater. Today Adv. 14, 10. https://doi.org/10.1016/j.mtadv.2022.100216.
Lind, J.U., Busbee, T.A., Valentine, A.D., Pasqualini, F.S., Yuan, H.Y., Yadid, M., Park, S. J., Kotikian, A., Nesmith, A.P., Campbell, P.H., Vlassak, J.J., Lewis, J.A., Parker, K. K., 2017a. Nat. Mater. 16 (3), 303. https://doi.org/10.1038/nmat4782.
Lind, J.U., Yadid, M., Perkins, I., O'Connor, B.B., Eweje, F., Chantre, C.O., Hemphill, M. A., Yuan, H.Y., Campbell, P.H., Vlassak, J.J., Parker, K.K., 2017b. Lab Chip 17 (21), 3692–3703. https://doi.org/10.1039/c7lc00740j.
Liu, J., Zheng, H., Poh, P.S., Machens, H.G., Schilling, A.F., 2015. Int. J. Mol. Sci. 16 (7), 15997–16016. https://doi.org/10.3390/ijms160715997.
Liu, J., Li, S., Bhethanabotla, V.R., 2018. ACS Sens. 3 (1), 222–229. https://doi.org/10.1021/acssensors.7b00876.
Liu, W.W., Song, J., Du, X.H., Zhou, Y., Li, Y., Li, R., Lyu, L., He, Y.T., Hao, J.X., Ben, J., Wang, W., Shi, H.B., Wang, Q., 2019a. Acta Biomater. 91, 195–208. https://doi.org/10.1016/j.actbio.2019.04.053.
Liu, W.M., Sun, M.L., Han, K., Wang, J.Y., 2019b. Anal. Chem. 91 (21), 13601–13610. https://doi.org/10.1021/acs.analchem.9b02768.
Low, L.A., Mummery, C., Berridge, B.R., Austin, C.P., Tagle, D.A., 2021. Nat. Rev. Drug Discov. 20 (5), 345–361. https://doi.org/10.1038/s41573-020-0079-3.
Lugo-Cintrón, K.M., Ayuso, J.M., White, B.R., Harari, P.M., Ponik, S.M., Beebe, D.J., Gong, M.M., Virumbrales-Muñoz, M., 2020. Lab Chip 20 (9), 1586–1600. https://doi.org/10.1039/D0LC00099J.
Maitra, J., Shukla, V.K., 2014. Am. J. Polym. Sci. 4 (2), 25–31.
Maoz, B.M., Herland, A., Henry, O.Y.F., Leineweber, W.D., Yadid, M., Doyle, J., Mannix, R., Kujala, V.J., FitzGerald, E.A., Parker, K.K., Ingber, D.E., 2017. Lab Chip 17 (13), 2294–2302. https://doi.org/10.1039/c7lc00412e.
Marrero, D., Pujol-Vila, F., Vera, D., Gabriel, G., Illa, X., Elizalde-Torrent, A., Alvarez, M., Villa, R., 2021a. Biosens. Bioelectron. 181, 113156 https://doi.org/10.1016/j.bios.2021.113156.
Marrero, D., Pujol-Vila, F., Vera, D., Gabriel, G., Illa, X., Elizalde-Torrent, A., Alvarez, M., Villa, R., 2021b. Biosens. Bioelectron. 181, 15. https://doi.org/10.1016/j.bios.2021.113156.
Marturano-Kruik, A., Nava, M.M., Yeager, K., Chramiec, A., Hao, L., Robinson, S., Guo, E., Raimondi, M.T., Vunjak-Novakovic, G., 2018. Proc. Natl. Acad. Sci. USA 115 (6), 1256–1261. https://doi.org/10.1073/pnas.1714282115.
Maruccio, C., Scigliuzzo, M., Rizzato, S., Scarlino, P., Quaranta, G., Chiriaco, M.S., Monteduro, A.G., Maruccio, G., 2018. J. Intell. Mater. Syst. Struct. https://doi.org/10.1177/1045389X18803461, 1045389X18803461.
Maschmeyer, I., Lorenz, A.K., Schimek, K., Hasenberg, T., Ramme, A.P., Hubner, J., Lindner, M., Drewell, C., Bauer, S., Thomas, A., Sambo, N.S., Sonntag, F., Lauster, R., Marx, U., 2015a. Lab Chip 15 (12), 2688–2699. https://doi.org/10.1039/c5lc00392j.
Maschmeyer, I., Hasenberg, T., Jaenicke, A., Lindner, M., Lorenz, A.K., Zech, J., Garbe, L. A., Sonntag, F., Hayden, P., Ayehunie, S., Lauster, R., Marx, U., Materne, E.M., 2015b. Eur. J. Pharm. Biopharm. 95, 77–87. https://doi.org/10.1016/j.ejpb.2015.03.002.
Mathes, S.H., Ruffner, H., Graf-Hausner, U., 2014. Adv. Drug Deliv. Rev. 69, 81–102. https://doi.org/10.1016/j.addr.2013.12.006.
Maurer, M., Gresnigt, M.S., Last, A., Wollny, T., Berlinghof, F., Pospich, R., Cseresnyes, Z., Medyukhina, A., Graf, K., Gröger, M., Raasch, M., Siwczak, F., Nietzsche, S., Jacobsen, I.D., Figge, M.T., Hube, B., Huber, O., Mosig, A.S., 2019. Biomaterials 220, 119396. https://doi.org/10.1016/j.biomaterials.2019.119396.
Mazzocchi, A.R., Rajan, S.A.P., Votanopoulos, K.I., Hall, A.R., Skardal, A., 2018. Sci. Rep. 8 https://doi.org/10.1038/s41598-018-21200-8.
Mejias, J.C., Nelson, M.R., Liseth, O., Roy, K., 2020. Lab Chip 20 (19), 3601–3611. https://doi.org/10.1039/d0lc00644k.
Mermoud, Y., Felder, M., Stucki, J.D., Stucki, A.O., Guenat, O.T., 2018. Sensor. Actuator. B Chem. 255, 3647–3653. https://doi.org/10.1016/j.snb.2017.09.192.
Meyer, T., Tiburcy, M., Zimmermann, W.H., 2019. Adv. Drug Deliv. Rev. 140, 93–100. https://doi.org/10.1016/j.addr.2019.03.002.
Michel, M., L'Heureux, N., Pouliot, R., Xu, W., Auger, F.A., Germain, L., 1999. In Vitro Cell. Dev. Biol. Anim. 35 (6), 318. https://doi.org/10.1007/s11626-999-0081-x.
Middleton, K., Al-Dujaili, S., Mei, X., Günther, A., You, L., 2017. J. Biomech. 59, 35–42. https://doi.org/10.1016/j.jbiomech.2017.05.012.
Miller, P.G., Shuler, M.L., 2016a. Biotechnol. Bioeng. 113 (10), 2213–2227. https://doi.org/10.1002/bit.25989.
Miller, P.G., Shuler, M.L., 2016b. Biotechnol. Bioeng. 113 (10), 2213–2227. https://doi.org/10.1002/bit.25989.
Miller, J.S., Stevens, K.R., Yang, M.T., Baker, B.M., Nguyen, D.-H.T., Cohen, D.M., Toro, E., Chen, A.A., Galie, P.A., Yu, X., Chaturvedi, R., Bhatia, S.N., Chen, C.S., 2012. Nat. Mater. 11 (9), 768–774. https://doi.org/10.1038/nmat3357.
Miller, P.G., Chen, C.Y., Wang, Y.I., Gao, E., Shuler, M.L., 2020. Biotechnol. Bioeng. 117 (2), 486–497. https://doi.org/10.1002/bit.27188.
Milone, A., Monteduro, A.G., Rizzato, S., Leo, A., Di Natale, C., Kim, S.S., Maruccio, G., 2023. Adv. Sustain. Syst. 7 (2), 2200083. https://doi.org/10.1002/adsu.202200083.
Misun, P.M., Rothe, J., Schmid, Y.R.F., Hierlemann, A., Frey, O., 2016. Microsyst. Nanoeng. 2 (1), 16022 https://doi.org/10.1038/micronano.2016.22.
Mohammadi, M.H., Heidary Araghi, B., Beydaghi, V., Geraili, A., Moradi, F., Jafari, P., Janmaleki, M., Valente, K.P., Akbari, M., Sanati-Nezhad, A., 2016. Adv Healthc Mater 5 (19), 2459–2480. https://doi.org/10.1002/adhm.201600439.
Mollica, H., Palomba, R., Primavera, R., Decuzzi, P., 2019. ACS Biomater. Sci. Eng. 5 (9), 4834–4843. https://doi.org/10.1021/acsbiomaterials.9b00697.
Mondal, S., Hegarty, E., Martin, C., Gokce, S.K., Ghorashian, N., Ben-Yakar, A., 2016. Nat. Commun. 7 https://doi.org/10.1038/ncomms13023.
Mori, N., Morimoto, Y., Takeuchi, S., 2017. Biomaterials 116, 48–56. https://doi.org/10.1016/j.biomaterials.2016.11.031.

Mosadegh, B., Lockett, M.R., Minn, K.T., Simon, K.A., Gilbert, K., Hillier, S., Newsome, D., Li, H., Hall, A.B., Boucher, D.M., Eustace, B.K., Whitesides, G.M., 2015. Biomaterials 52, 262–271. https://doi.org/10.1016/j.biomaterials.2015.02.012.

Mougang, Y.K., Di Zazzo, L., Minieri, M., Capuano, R., Catini, A., Legramante, J.M., Paolesse, R., Bernardini, S., Di Natale, C., 2021. iScience 24 (8), 102851. https://doi.org/10.1016/j.isci.2021.102851.

Movilla, N., Borau, C., Valero, C., García-Aznar, J.M., 2018. Bone 107, 10–17. https://doi.org/10.1016/j.bone.2017.10.025.

Moya, A., Ortega-Ribera, M., Guimerà, X., Sowade, E., Zea, M., Illa, X., Ramon, E., Villa, R., Gracia-Sancho, J., Gabriel, G., 2018. Lab Chip 18 (14), 2023–2035. https://doi.org/10.1039/C8LC00456K.

Murdocca, M., Torino, F., Pucci, S., Costantini, M., Capuano, R., Greggi, C., Polidoro, C., Somma, G., Pasqualetti, V., Ketchanji Mougang, Y., Catini, A., Simone, G., Paolesse, R., Orlandi, A., Mauriello, A., Roselli, M., Magrini, A., Novelli, G., Di Natale, C., Sangiuolo, F.C., 2021. Cancers 13 (16), 4213.

Musah, S., Mammoto, A., Ferrante, T.C., Jeanty, S.S.F., Hirano-Kobayashi, M., Mammoto, T., Roberts, K., Chung, S., Novak, R., Ingram, M., Fatanat-Didar, T., Koshy, S., Weaver, J.C., Church, G.M., Ingber, D.E., 2017a. Nat. Biomed. Eng 1 (5), 12. https://doi.org/10.1038/s41551-017-0069.

Musah, S., Mammoto, A., Ferrante, T.C., Jeanty, S.S.F., Hirano-Kobayashi, M., Mammoto, T., Roberts, K., Chung, S., Novak, R., Ingram, M., Fatanat-Didar, T., Koshy, S., Weaver, J.C., Church, G.M., Ingber, D.E., 2017b. Nat. Biomed. Eng. 1 https://doi.org/10.1038/s41551-017-0069.

Musah, S., Dimitrakak, N., Camacho, D.M., Church, G.M., Ingber, D.E., 2018. Nat. Protoc. 13 (7), 1662–1685. https://doi.org/10.1038/s41596-018-0007-8.

Nagrath, S., Sequist, L.V., Maheswaran, S., Bell, D.W., Irimia, D., Ulkus, L., Smith, M.R., Kwak, E.L., Digumarthy, S., Muzikansky, A., Ryan, P., Balis, U.J., Tompkins, R.G., Haber, D.A., Toner, M., 2007. Nature 450 (7173), 1235–1239. http://www.nature.com/nature/journal/v450/n7173/suppinfo/nature06385_S1.html.

Nam, K.H., Smith, A.S.T., Lone, S., Kwon, S., Kim, D.H., 2015. Jala 20 (3), 201–215. https://doi.org/10.1177/2211068214557813.

Nargang, T.M., Brockmann, L., Nikolov, P.M., Schild, D., Helmer, D., Keller, N., Sachsenheimer, K., Wilhelm, E., Pires, L., Dirschka, M., Kolew, A., Schneider, M., Worgull, M., Giselbrecht, S., Neumann, C., Rapp, B.E., 2014. Lab Chip 14 (15), 2698–2708. https://doi.org/10.1039/C4LC00045E.

Nashimoto, Y., Hayashi, T., Kunita, I., Nakamasu, A., Torisawa, Y.-s., Nakayama, M., Takigawa-Imamura, H., Kotera, H., Nishiyama, K., Miura, T., Yokokawa, R., 2017. Integr. Biol. 9 (6), 506–518. https://doi.org/10.1039/c7ib00024c.

Nashimoto, Y., Okada, R., Hanada, S., Arima, Y., Nishiyama, K., Miura, T., Yokokawa, R., 2020. Biomaterials 229, 119547. https://doi.org/10.1016/j.biomaterials.2019.119547.

Natividad-Diaz, S.L., Browne, S., Jha, A.K., Ma, Z., Hossainy, S., Kurokawa, Y.K., George, S.C., Healy, K.E., 2019. Biomaterials 194, 73–83. https://doi.org/10.1016/j.biomaterials.2018.11.032.

Naumovska, E., Aalderink, G., Wong Valencia, C., Kosim, K., Nicolas, A., Brown, S., Vulto, P., Erdmann, K.S., Kurek, D., 2020. Int. J. Mol. Sci. 21 (14) https://doi.org/10.3390/ijms21144964.

Nawroth, J.C., Lucchesi, C., Cheng, D., Shukla, A., Ngyuen, J., Shroff, T., Varone, A., Karalis, K., Lee, H.H., Alves, S., Hamilton, G.A., Salmon, M., Villenave, R., 2020. Am. J. Respir. Cell Mol. Biol. 63 (5), 591–600. https://doi.org/10.1165/rcmb.2020-0010MA.

Neto, E.; Monteiro, A. C.; Leite Pereira, C.; Simões, M.; Conde, J. P.; Chu, V.; Sarmento, B.; Lamghari, M., Adv. Healthc. Mater. (n/a), 2102305. DOI https://doi.org/10.1002/adhm.202102305.

Neurath, M.F., 2014. Nat. Rev. Immunol. 14 (5), 329–342. https://doi.org/10.1038/nri3661.

Nguyen, H.H., Park, J., Kang, S., Kim, M., 2015. Sensors 15 (5), 10481–10510. https://doi.org/10.3390/s150510481.

Ning, R., Wang, F., Lin, L., 2016. TrAC, Trends Anal. Chem. 80, 255–265. https://doi.org/10.1016/j.trac.2015.08.017.

Nissan, X., Larribere, L., Saidani, M., Hurbain, I., Delevoye, C., Feteira, J., Lemaitre, G., Peschanski, M., Baldeschi, C., 2011. Proc. Natl. Acad. Sci. USA 108 (36), 14861–14866. https://doi.org/10.1073/pnas.1019070108.

Nitsche, K.S., Muller, I., Malcomber, S., Carmichael, P.L., Bouwmeester, H., 2022. Arch. Toxicol. 96 (3), 711–741. https://doi.org/10.1007/s00204-022-03234-0.

No, D.Y., Lee, K.H., Lee, J., Lee, S.H., 2015. Lab Chip 15 (19), 3822–3837. https://doi.org/10.1039/c5lc00611b.

Ong, L.J.Y., Ching, T., Chong, L.H., Arora, S., Li, H., Hashimoto, M., DasGupta, R., Yuen, P.K., Toh, Y.C., 2019. Lab Chip 19 (13), 2178–2191. https://doi.org/10.1039/c9lc00160c.

Ortega, M.A., Fernández-Garibay, X., Castaño, A.G., De Chiara, F., Hernández-Albors, A., Balaguer-Trias, J., Ramón-Azcón, J., 2019. Lab Chip 19 (15), 2568–2580. https://doi.org/10.1039/C9LC00285E.

Osaki, T., Sivathanu, V., Kamm, R.D., 2018a. Curr. Opin. Biotechnol. 52, 116–123. https://doi.org/10.1016/j.copbio.2018.03.011.

Osaki, T., Shin, Y., Sivathanu, V., Campisi, M., Kamm, R.D., 2018b. Adv. Healthc. Mater. 7 (2), 29. https://doi.org/10.1002/adhm.201700489.

Osaki, T., Uzel, S.G.M., Kamm, R.D., 2018c. Sci. Adv. 4 (10), 15. https://doi.org/10.1126/sciadv.aat5847.

Ouwehand, K., Spiekstra, S.W., Waaijman, T., Scheper, R.J., de Gruijl, T.D Gibbs, S., 2011. J. Leukoc. Biol. 90 (5), 1027–1033. https://doi.org/10.1189/jlb.0610374.

Park, J.Y., Ryu, H., Lee, B., Ha, D.-H., Ahn, M., Kim, S., Kim, J.Y., Jeon, N.L., Cho, D.-W., 2018. Biofabrication 11 (1), 015002. https://doi.org/10.1088/1758-5090/aae545.

Park, T.E., Mustafaoglu, N., Herland, A., Hasselkus, R., Mannix, R., FitzGerald, E.A., Prantil-Baun, R., Watters, A., Henry, O., Benz, M., Sanchez, H., McCrea, H.J., Goumnerova, L.C., Song, H.W., Palecek, S.P., Shusta, E., Ingber, D.E., 2019. Nat. Commun. 10, 12. https://doi.org/10.1038/s41467-019-10588-0.

Peel, S., Corrigan, A.M., Ehrhardt, B., Jang, K.J., Caetano-Pinto, P., Boeckeler, M., Rubins, J.E., Kodella, K., Petropolis, D.B., Ronxhi, J., Kulkarni, G., Foster, A.J., Williams, D., Hamilton, G.A., Ewart, L., 2019. Lab Chip 19 (3), 410–421. https://doi.org/10.1039/c8lc00829a.

Perazella, M.A., 2009. Clin. J. Am. Soc. Nephrol. : CJASN 4 (7), 1275–1283. https://doi.org/10.2215/CJN.02050309.

Phan, D.T.T., Wang, X.L., Craver, B.M., Sobrino, A., Zhao, D., Chen, J.C., Lee, L.Y.N., George, S.C., Lee, A.P., Hughes, C.C.W., 2017. Lab Chip 17 (3), 511–520. https://doi.org/10.1039/c6lc01422d.

Phillips, M., Basa-Dalay, V., Blais, J., Bothamley, G., Chaturvedi, A., Modi, K.D., Pandya, M., Natividad, M.P., Patel, U., Ramraje, N.N., Schmitt, P., Udwadia, Z.F., 2012. Tuberculosis 92 (4), 314–320. https://doi.org/10.1016/j.tube.2012.04.002.

Phillips, J.A., Grandhi, T.S.P., Davis, M., Gautier, J.C., Hariparsad, N., Keller, D., Sura, R., Van Vleet, T.R., 2020. Lab Chip 20 (3), 468–476. https://doi.org/10.1039/c9lc00925f.

Piccin, E., Coltro, W.K.T., Fracassi da Silva, J.A., Neto, S.C., Mazo, L.H., Carrilho, E., 2007. J. Chromatogr. A 1173 (1), 151–158. https://doi.org/10.1016/j.chroma.2007.09.081.

Piccinno, E., Monteduro, A.G., Dituri, F., Rizzato, S., Giannelli, G., Maruccio, G., 2021. Int. J. Mol. Sci. 22 (23), 13090 https://doi.org/10.3390/ijms222313090.

Piruska, A., Nikcevic, I., Lee, S.H., Ahn, C., Heineman, W.R., Limbach, P.A., Seliskar, C.J., 2005. Lab Chip 5 (12), 1348–1354.

Pocock, K., Delon, L., Bala, V., Rao, S., Priest, C., Prestidge, C., Thierry, B., 2017. ACS Biomater. Sci. Eng. 3 (6), 951–959. https://doi.org/10.1021/acsbiomaterials.7b00023.

Popova, A.A., Marcato, D., Peravali, R., Wehl, I., Schepers, U., Levkin, P.A., 2018. Adv. Funct. Mater. 28 (3) https://doi.org/10.1002/adfm.201703486.

Pourmand, A., Shaegh, S.A.M., Ghavifekr, H.B., Najafi Aghdam, E., Dokmeci, M.R., Khademhosseini, A., Zhang, Y.S., 2018. Sensor. Actuator. B Chem. 262, 625–636. https://doi.org/10.1016/j.snb.2017.12.132.

Pradhan, S., Banda, O.A., Farino, C.J., Sperduto, J.L., Keller, K.A., Taitano, R., Slater, J. H., 2020. Adv. Healthc. Mater. 9 (8) https://doi.org/10.1002/adhm.201901255.

Primiceri, E., Chiriacò, M.S., D'Amone, E., Urso, E., Ionescu, R.E., Rizzello, A., Maffia, M., Cingolani, R., Rinaldi, R., Maruccio, G., 2010. Biosens. Bioelectron. 25 (12), 2711–2716. https://doi.org/10.1016/j.bios.2010.04.032.

Primiceri, E., Chiriacò, M.S., Dioguardi, F., Monteduro, A.G., D'Amone, E., Rinaldi, R., Giannelli, G., Maruccio, G., 2011. Lab Chip 11 (23), 4081–4086. https://doi.org/10.1039/c1lc20540d.

Radhakrishnan, J., Varadaraj, S., Dash, S.K., Sharma, A., Verma, R.S., 2020. Drug Discov. Today 25 (5), 879–890. https://doi.org/10.1016/j.drudis.2020.03.002.

Raimondi, M.T., Albani, D., Giordano, C., 2019. Trends Mol. Med. 25 (9), 737–740. https://doi.org/10.1016/j.molmed.2019.07.006.

Raimondi, I., Izzo, L., Tunesi, M., Comar, M., Albania, D., Giordano, C., 2020. Front. Bioeng. Biotechnol. 7 https://doi.org/10.3389/fbioe.2019.00435.

Ramadan, Q., Ting, F.C.W., 2016. Lab Chip 16 (10), 1899–1908. https://doi.org/10.1039/C6LC00229C.

Ramis, G., Martinez-Alarcon, L., Quereda, J.J., Mendonca, L., Majado, M.J., Gomez-Coelho, K., Mrowiec, A., Herrero-Medrano, J.M., Abellaneda, J.M., Pallares, F.J., Rios, A., Ramirez, P., Munoz, A., 2013. Biomed. Microdevices 15 (6), 985–995. https://doi.org/10.1007/s10544-013-9790-8.

Ren, K., Zhou, J., Wu, H., 2013. Accounts Chem. Res. 46 (11), 2396–2406. https://doi.org/10.1021/ar300314s.

Ren, L., Zhou, X.W., Nasiri, R., Fang, J., Jiang, X., Wang, C.R., Qu, M.Y., Ling, H.N., Chen, Y.H., Xue, Y.M., Hartel, M.C., Tebon, P., Zhang, S.M., Kim, H.J., Yuan, X.C., Shamloo, A., Dokmeci, M.R., Li, S., Khademhosseini, A., Ahadian, S., Sun, W.J., 2020. Small Methods 4 (10). https://doi.org/10.1002/smtd.202000438.

Ren, X., Getschman, A.E., Hwang, S., Volkman, B.F., Klonisch, T., Levin, D., Zhao, M., Santos, S., Liu, S., Cheng, J., Lin, F., 2021. Lab Chip 21 (8), 1527–1539. https://doi.org/10.1039/d0lc01194k.

Risau, W., 1997. Nature 386 (6626), 671–674. https://doi.org/10.1038/386671a0.

Risueno, I., Valencia, L., Jorcano, J.L., Velasco, D., 2021. Apl. Bioeng. 5 (3), 12. https://doi.org/10.1063/5.0046376.

Rizzato, S., Scigliuzzo, M., Chiriacò, M.S., Scarlino, P., Monteduro, A.G., Maruccio, C., Tasco, V., Maruccio, G., 2017. J. Micromech. Microeng. 27 (12), 125002 https://doi.org/10.1088/1361-6439/aa8186.

Rizzato, S., Monteduro, A.G., Buja, I., Maruccio, C., Sabella, E., De Bellis, L., Luvisi, A., Maruccio, G., 2023. Biosensors 13 (2), 197. https://doi.org/10.3390/bios13020197.

Rizzato, S., Primiceri, E., Monteduro, A.G., Colombelli, A., Leo, A., Manera, M.G., Rella, R., Maruccio, G., 2018. Beilstein J. Nanotechnol. 9, 1582–1593. https://doi.org/10.3762/bjnano.9.150.

Rizzato, S., Leo, A., Monteduro, A.G., Chiriacò, M.S., Primiceri, E., Sirsi, F., Milone, A., Maruccio, G., 2020. Micromachines 11 (5), 491. https://doi.org/10.3390/mi11050491.

Rodenhizer, D., Gaude, E., Cojocari, D., Mahadevan, R., Frezza, C., Wouters, B.G., McGuigan, A.P., 2016. Nat. Mater. 15 (2), 227–234. https://doi.org/10.1038/nmat4482.

Rodriguez, L.G., Wu, X., Guan, J.-L., 2005. Wound-healing assay. In: Cell Migration. Springer, pp. 23–29.

Rogers, C.I., Pagaduan, J.V., Nordin, G.P., Woolley, A.T., 2011. Anal. Chem. 83 (16), 6418–6425. https://doi.org/10.1021/ac201539h.

Rogers, C.I., Oxborrow, J.B., Anderson, R.R., Tsai, L.-F., Nordin, G.P., Woolley, A.T., 2014. Sensor. Actuator. B Chem. 191, 438–444. https://doi.org/10.1016/j.snb.2013.10.008.

Roseti, L., Parisi, V., Petretta, M., Cavallo, C., Desando, G., Bartolotti, I., Grigolo, B., 2017. Mater. Sci. Eng. C 78, 1246–1262. https://doi.org/10.1016/j.msec.2017.05.017.
Sabhachandani, P., Motwani, V., Cohen, N., Sarkar, S., Torchilin, V., Konry, T., 2016. Lab Chip 16 (3), 497–505. https://doi.org/10.1039/c5lc01139f.
Savoji, H., Mohammadi, M.H., Rafatian, N., Toroghi, M.K., Wang, E.Y., Zhao, Y.M., Korolj, A., Ahadian, S., Radisic, M., 2019. Biomaterials 198, 3–26. https://doi.org/10.1016/j.biomaterials.2018.09.036.
Schmid, Y.R.F., Bürgel, S.C., Misun, P.M., Hierlemann, A., Frey, O., 2016. ACS Sens. 1 (8), 1028–1035. https://doi.org/10.1021/acssensors.6b00272.
Scialla, S., Palazzo, B., Barca, A., Carbone, L., Fiore, A., Monteduro, A.G., Maruccio, G., Sannino, A., Gervaso, F., 2017. Mater. Sci. Eng. C-Mater. Biol. Appl. 76, 1166–1174. https://doi.org/10.1016/j.msec.2017.03.060.
Sekine, H., Shimizu, T., Sakaguchi, K., Dobashi, I., Wada, M., Yamato, M., Kobayashi, E., Umezu, M., Okano, T., 2013. Nat. Commun. 4 (1), 1399. https://doi.org/10.1038/ncomms2406.
Sellgren, K.L., Butala, E.J., Gilmour, B.P., Randell, S.H., Grego, S., 2014. Lab Chip 14 (17), 3349–3358. https://doi.org/10.1039/C4LC00552J.
Serasanambati, M., Broza, Y.Y., Marmur, A., Haick, H., 2019. iScience 11, 178–188. https://doi.org/10.1016/j.isci.2018.12.008.
Shaegh, S.A.M., Ferrari, F.D., Zhang, Y.S., Nabavinia, M., Mohammad, N.B., Ryan, J., Pourmand, A., Laukaitis, E., Sadeghian, R.B., Nadhman, A., Shin, S.R., Nezhad, A.S., Khademhosseini, A., Dokmeci, M.R., 2016. Biomicrofluidics 10 (4), 044111. https://doi.org/10.1063/1.4955155.
Shah, R.K., Shum, H.C., Rowat, A.C., Lee, D., Agresti, J.J., Utada, A.S., Chu, L.Y., Kim, J. W., Fernandez-Nieves, A., Martinez, C.J., Weitz, D.A., 2008. Mater. Today 11 (4), 18–27. https://doi.org/10.1016/s1369-7021(08)70053-1.
Shah, P., Fritz, J.V., Glaab, E., Desai, M.S., Greenhalgh, K., Frachet, A., Niegowska, M., Estes, M., Jäger, C., Seguin-Devaux, C., Zenhausern, F., Wilmes, P., 2016. Nat. Commun. 7 (1), 11535 https://doi.org/10.1038/ncomms11535.
Shang, Y.X., Chen, Z.Y., Zhang, Z.H., Yang, Y.Z., Zhao, Y.J., 2020. Bio-Des. Manuf. 3 (3), 266–280. https://doi.org/10.1007/s42242-020-00073-9.
Shintu, L., Baudoin, R., Navratil, V., Prot, J.M., Pontoizeau, C., Defernez, M., Blaise, B.J., Domange, C., Pery, A.R., Toulhoat, P., Legallais, C., Brochot, C., Leclerc, E., Dumas, M.E., 2012a. Anal. Chem. 84 (4), 1840–1848. https://doi.org/10.1021/ac2011075.
Shintu, L., Baudoin, R., Navratil, V., Prot, J.M., Pontoizeau, C., Defernez, M., Blaise, B.J., Domange, C., Pery, A.R., Toulhoat, P., Legallais, C., Brochot, C., Leclerc, E., Dumas, M.E., 2012b. Anal. Chem. 84 (4), 1840–1848. https://doi.org/10.1021/ac2011075.
Shum, H.C., Lee, D., Yoon, I., Kodger, T., Weitz, D.A., 2008. Langmuir 24 (15), 7651–7653. https://doi.org/10.1021/la801833a.
Si, L.L., Bai, H.Q., Oh, C.Y., Jin, L., Prantil-Baun, R., Ingber, D.E., 2021. Microbiol. Spectr. 9 (2), 10. https://doi.org/10.1128/Spectrum.00257-21.
Sidorov, V.Y., Samson, P.C., Sidorova, T.N., Davidson, J.M., Lim, C.C., Wikswo, J.P., 2017. Acta Biomater. 48, 68–78. https://doi.org/10.1016/j.actbio.2016.11.009.
Skardal, A., Shupe, T., Atala, A., 2016. Drug Discov. Today 21 (9), 1399–1411. https://doi.org/10.1016/j.drudis.2016.07.003.
Sobrino, A., Phan, D.T.T., Datta, R., Wang, X.L., Hachey, S.J., Romero-Lopez, M., Gratton, E., Lee, A.P., George, S.C., Hughes, C.C.W., 2016a. Sci. Rep. 6, 11. https://doi.org/10.1038/srep31589.
Sobrino, A., Phan, D.T.T., Datta, R., Wang, X., Hachey, S.J., Romero-López, M., Gratton, E., Lee, A.P., George, S.C., Hughes, C.C.W., 2016b. Sci. Rep. 6 (1), 31589 https://doi.org/10.1038/srep31589.
Song, H.J., Lim, H.Y., Chun, W., Choi, K.C., Sung, J.H., Sung, G.Y., 2017. J. Ind. Eng. Chem. 56, 375–381. https://doi.org/10.1016/j.jiec.2017.07.034.
Song, H.J., Lim, H.Y., Chun, W., Choi, K.C., Lee, T.-y., Sung, J.H., Sung, G.Y., 2018a. J. Ind. Eng. Chem. 60, 355–359. https://doi.org/10.1016/j.jiec.2017.11.022.
Song, J., Miermont, A., Lim, C.T., Kamm, R.D., 2018b. Sci. Rep. 8 (1), 17949 https://doi.org/10.1038/s41598-018-36381-5.
Sorba, F., Poulin, A., Ischer, R., Shea, H., Martin-Olmos, C., 2019. Lab Chip 19 (12), 2138–2146. https://doi.org/10.1039/c9lc00075e.
Soucy, J.R., Bindas, A.J., Koppes, A.N., Koppes, R.A., 2019. iScience 21, 521–548. https://doi.org/10.1016/j.isci.2019.10.052.
Srinivasan, B., Kolli, A.R., Esch, M.B., Abaci, H.E., Shuler, M.L., Hickman, J.J., 2015. Jala 20 (2), 107–126. https://doi.org/10.1177/2211068214561025.
Sriram, G., Alberti, M., Dancik, Y., Wu, B., Wu, R.G., Feng, Z.X., Ramasamy, S., Bigliardi, P.L., Bigliardi-Qi, M., Wang, Z.P., 2018. Mater. Today 21 (4), 326–340. https://doi.org/10.1016/j.mattod.2017.11.002.
Stucki, A.O., Stucki, J.D., Hall, S.R.R., Felder, M., Mermoud, Y., Schmid, R.A., Geiser, T., Guenat, O.T., 2015. Lab Chip 15 (5), 1302–1310. https://doi.org/10.1039/c4lc01252f.
Stucki, J.D., Hobi, N., Galimov, A., Stucki, A.O., Schneider-Daum, N., Lehr, C.M., Huwer, H., Frick, M., Funke-Chambour, M., Geiser, T., Guenat, O.T., 2018. Sci. Rep. 8, 13. https://doi.org/10.1038/s41598-018-32523-x.
Sun, Q., Tan, S.H., Chen, Q.S., Ran, R., Hui, Y., Chen, D., Zhao, C.X., 2018. ACS Biomater. Sci. Eng. 4 (12), 4425–4433. https://doi.org/10.1021/acsbiomaterials.8b00904.
Sun, W.J., Luo, Z.M., Lee, J., Kim, H.J., Lee, K., Tebon, P., Feng, Y.D., Dokmeci, M.R., Sengupta, S., Khademhosseini, A., 2019. Adv. Healthc. Mater. 8 (4), 12. https://doi.org/10.1002/adhm.201801363.
Swami, P., Sharma, A., Anand, S., Gupta, S., 2021. Biosens. Bioelectron. 182, 113190 https://doi.org/10.1016/j.bios.2021.113190.
Tan, K., Keegan, P., Rogers, M., Lu, M.J., Gosset, J.R., Charest, J., Bale, S.S., 2019. Lab Chip 19 (9), 1556–1566. https://doi.org/10.1039/c8lc01262h.
Tang, Q.Q., Li, X.Y., Lai, C., Li, L., Wu, H.K., Wang, Y.J., Shi, X.T., 2021. Bioact. Mater. 6 (1), 169–178. https://doi.org/10.1016/j.bioactmat.2020.07.016.
Tasoglu, S., Demirci, U., 2013. Trends Biotechnol. 31 (1), 10–19. https://doi.org/10.1016/j.tibtech.2012.10.005.
Thacker, V.V., Sharma, K., Dhar, N., Mancini, G.F., Sordet-Dessimoz, J., McKinney, J.D., 2021. EMBO Rep. 22 (6), 19. https://doi.org/10.15252/embr.202152744.
Theobald, J., Ghanem, A., Wallisch, P., Banaeiyan, A.A., Andrade-Navarro, M.A., Taskova, K., Haltmeier, M., Kurtz, A., Becker, H., Reuter, S., Mrowka, R., Cheng, X. L., Wolfl, S., 2018. ACS Biomater. Sci. Eng. 4 (1), 78–89. https://doi.org/10.1021/acsbiomaterials.7b00417.
Theobald, J., Maaty, M.A.A., Kusterer, N., Wetterauer, B., Wink, M., Cheng, X.L., Wolfl, S., 2019. Sci. Rep. 9, 11. https://doi.org/10.1038/s41598-019-40851-9.
Toepke, M.W., Beebe, D.J., 2006. Lab Chip 6 (12), 1484–1486. https://doi.org/10.1039/B612140C.
Tsamandouras, N., Kostrzewski, T., Stokes, C.L., Griffith, L.G., Hughes, D.J., Cirit, M., 2017. J. Pharmacol. Exp. Therapeut. 360 (1), 95–105. https://doi.org/10.1124/jpet.116.237495.
Vailhé, B., Vittet, D., Feige, J.-J., 2001. Lab. Invest. 81 (4), 439–452. https://doi.org/10.1038/labinvest.3780252.
Valencia, L., Canalejas-Tejero, V., Clemente, M., Fernaud, I., Holgado, M., Jorcano, J.L., Velasco, D., 2021. Sci. Rep. 11 (1), 14. https://doi.org/10.1038/s41598-021-91875-z.
van den Berge, M., Ten Hacken, N.H.T., Cohen, J., Douma, W.R., Postma, D.S., 2011. Chest 139 (2), 412–423. https://doi.org/10.1378/chest.10-1210.
van den Broek, L.J., Bergers, L., Reijnders, C.M.A., Gibbs, S., 2017. Stem Cell Rev. Rep. 13 (3), 418–429. https://doi.org/10.1007/s12015-017-9737-1.
van der Helm, M.W., van der Meer, A.D., Eijkel, J.C.T., van den Berg, A., Segerink, L.I., 2016. Tissue Barriers 4 (1). https://doi.org/10.1080/21688370.2016.1142493.
van Dijk, C.G.M., Brandt, M.M., Poulis, N., Anten, J., van der Moolen, M., Kramer, L., Homburg, E., Louzao-Martinez, L., Pei, J.Y., Krebber, M.M., van Balkom, B.W.M., de Graaf, P., Duncker, D.J., Verhaar, M.C., Luttge, R., Cheng, C., 2020. Lab Chip 20 (10), 1827–1844. https://doi.org/10.1039/d0lc00059k.
van Midwoud, P.M., Janse, A., Merema, M.T., Groothuis, G.M., Verpoorte, E., 2012. Anal. Chem. 84 (9), 3938–3944. https://doi.org/10.1021/ac300771z.
Varone, A., Nguyen, J.K., Leng, L., Barrile, R., Sliz, J., Lucchesi, C., Wen, N.R., Gravanis, A., Hamilton, G.A., Karalis, K., Hinojosa, C.D., 2021. Biomaterials 275, 12. https://doi.org/10.1016/j.biomaterials.2021.120957.
Vernetti, L., Gough, A., Baetz, N., Blutt, S., Broughman, J.R., Brown, J.A., Foulke-Abel, J., Hasan, N., J Kelly, E., Kovbasnjuk, O., Repper, J., Senutovitch, N., Stabb, J., Yeung, C., Zachos, N.C., Donowitz, M., Estes, M., Himmelfarb, J., Truskey, G., Wikswo, J.P., Taylor, D.L., 2017. Sci. Rep. 7 https://doi.org/10.1038/srep42296.
Vormann, M.K., Vriend, J., Lanz, H.L., Gijzen, L., van den Heuvel, A., Hutter, S., Joore, J., Trietsch, S.J., Stuut, C., Nieskens, T.T.G., Peters, J.G.P., Ramp, D., Caj, M., Russel, F. G.M., Jacobsen, B., Roth, A., Lu, S., Polli, J.W., Naidoo, A.A., Vulto, P., Masereeuw, R., Wilmer, M.J., Suter-Dick, L., 2021. J. Pharmaceut. Sci. 110 (4), 1601–1614. https://doi.org/10.1016/j.xphs.2021.01.028.
Wagner, I., Materne, E.M., Brincker, S., Sussbier, U., Fradrich, C., Busek, M., Sonntag, F., Sakharov, D.A., Trushkin, E.V., Tonevitsky, A.G., Lauster, R., Marx, U., 2013a. Lab Chip 13 (18), 3538–3547. https://doi.org/10.1039/c3lc50234a.
Wagner, I., Materne, E.M., Brincker, S., Sussbier, U., Fradrich, C., Busek, M., Sonntag, F., Sakharov, D.A., Trushkin, E.V., Tonevitsky, A.G., Lauster, R., Marx, U., 2013b. Lab Chip 13 (18), 3538–3547. https://doi.org/10.1039/c3lc50234a.
Wang, T., Green, R., Nair, R.R., Howell, M., Mohapatra, S., Guldiken, R., Mohapatra, S.S., 2015. Sensors (Basel, Switzerland 15 (12), 32045–32055. https://doi.org/10.3390/s151229909.
Wang, X., Phan, D.T.T., Sobrino, A., George, S.C., Hughes, C.C.W., Lee, A.P., 2016. Lab Chip 16 (2), 282–290. https://doi.org/10.1039/C5LC01050K.
Wang, Y.I., Abaci, H.E., Shuler, M.L., 2017. Biotechnol. Bioeng. 114 (1), 184–194. https://doi.org/10.1002/bit.26045.
Wang, Y.I., Carmona, C., Hickman, J.J., Shuler, M.L., 2018. Adv. Healthc. Mater. 7 (2) https://doi.org/10.1002/adhm.201701000.
Wang, T., Green, R., Howell, M., Martinez, T., Dutta, R., Mohapatra, S., Mohapatra, S.S., 2020. Nanomed. Nanotechnol. Biol. Med. 30, 102294 https://doi.org/10.1016/j.nano.2020.102294.
Wang, L., Wu, J., Chen, J., Dou, W., Zhao, Q., Han, J., Liu, J., Su, W., Li, A., Liu, P., An, Z., Xu, C., Sun, Y., 2021. Talanta 226, 122097. https://doi.org/10.1016/j.talanta.2021.122097.
Ware, B.R., Khetani, S.R., 2017. Trends Biotechnol. 35 (2), 172–183. https://doi.org/10.1016/j.tibtech.2016.08.001.
Wegener, J., Keese, C.R., Giaever, I., 2000. Exp. Cell Res. 259 (1), 158–166.
Whelan, I.T., Moeendarbary, E., Hoey, D.A., Kelly, D.J., 2021. Biofabrication 13 (3), 22. https://doi.org/10.1088/1758-5090/ac04f7.
Wilmer, M.J., Ng, C.P., Lanz, H.L., Vulto, P., Suter-Dick, L., Masereeuw, R., 2016. Trends Biotechnol. 34 (2), 156–170. https://doi.org/10.1016/j.tibtech.2015.11.001.
Wong, J.F., Simmons, C.A., 2019. Lab Chip 19 (6), 1060–1070. https://doi.org/10.1039/c8lc01321g.
World Health Organisation [WHO]. The Top 10 Causes of Death. Geneva: World Health Organization..
Wu, M.X., Ouyang, Y.S., Wang, Z.Y., Zhang, R., Huang, P.H., Chen, C.Y., Li, H., Li, P., Quinn, D., Dao, M., Suresh, S., Sadovsky, Y., Huang, T.J., 2017. Proc. Natl. Acad. Sci. U.S.A. 114 (40), 10584–10589. https://doi.org/10.1073/pnas.1709210114.
Wu, Q., Wei, X., Pan, Y., Zou, Y., Hu, N., Wang, P., 2018. Biomed. Microdevices 20 (4), 82. https://doi.org/10.1007/s10544-018-0329-x.
Wu, Z.H., Gong, Z.Y., Ao, Z., Xu, J.H., Cai, H.W., Muhsen, M., Heaps, S., Bondesson, M., Guo, S.S., Guo, F., 2020. ACS Appl. Bio Mater. 3 (9), 6273–6283. https://doi.org/10.1021/acsabm.0c00768.
Wufuer, M., Lee, G., Hur, W., Jeon, B., Kim, B.J., Choi, T.H., Lee, S., 2016. Sci. Rep. 6 (1), 37471 https://doi.org/10.1038/srep37471.

Xiao, C., Luong, J.H., 2003. Biotechnol. Prog. 19 (3), 1000–1005.
Xiao, Y., Kim, D., Dura, B., Zhang, K., Yan, R., Li, H., Han, E., Ip, J., Zou, P., Liu, J., Chen, A.T., Vortmeyer, A.O., Zhou, J., Fan, R., 2019. Adv. Sci. 6 (8), 1801531 https://doi.org/10.1002/advs.201801531.
Xu, H., Li, Z., Yu, Y., Sizdahkhani, S., Ho, W.S., Yin, F., Wang, L., Zhu, G., Zhang, M., Jiang, L., Zhuang, Z., Qin, J., 2016. Sci. Rep. 6 (1), 36670 https://doi.org/10.1038/srep36670.
Yang, X.Y., Li, K.Y., Zhang, X., Liu, C., Guo, B.K., Wen, W.J., Gao, X.H., 2018. Lab Chip 18 (3), 486–495. https://doi.org/10.1039/c7lc01224a.
Yang, W.G., Cai, S.X., Yuan, Z., Lai, Y.B., Yu, H.B., Wang, Y.C., Liu, L.Q., 2019. Mater. Des. 183. https://doi.org/10.1016/j.matdes.2019.108182.
Yin, L., Du, G., Zhang, B., Zhang, H., Yin, R., Zhang, W., Yang, S.M., 2020. Sci. Rep. 10 (1), 6568. https://doi.org/10.1038/s41598-020-63096-3.
Yin, F.C., Zhang, X., Wang, L., Wang, Y.Q., Zhu, Y.J., Li, Z.Y., Tao, T.T., Chen, W.W., Yu, H., Qin, J.H., 2021. Lab Chip 21 (3), 571–581. https://doi.org/10.1039/d0lc00921k.
Young, M., Rodenhizer, D., Dean, T., D'Arcangelo, E., Xu, B., Ailles, L., McGuigan, A.P., 2018. Biomaterials 164, 54–69. https://doi.org/10.1016/j.biomaterials.2018.01.038.
Young, A.T., Rivera, K.R., Erb, P.D., Daniele, M.A., 2019. ACS Sens. 4 (6), 1454–1464. https://doi.org/10.1021/acssensors.8b01549.
Zakrzewski, W., Dobrzynski, M., Szymonowicz, M., Rybak, Z., 2019. Stem Cell Res. Ther. 10 (1), 68. https://doi.org/10.1186/s13287-019-1165-5.
Zamprogno, P., Wuthrich, S., Achenbach, S., Thoma, G., Stucki, J.D., Hobi, N., Schneider-Daum, N., Lehr, C.M., Huwer, H., Geiser, T., Schmid, R.A., Guenat, O.T., 2021. Commun. Biol. 4 (1), 10. https://doi.org/10.1038/s42003-021-01695-0.
Zeitouni, N.E., Chotikatum, S., von Köckritz-Blickwede, M Naim, H.Y., 2016. Mol. Cell. Pediatr. 3 (1), 14. https://doi.org/10.1186/s40348-016-0041-y.
Zhang, C., Zhao, Z.Q., Rahim, N.A.A., van Noort, D., Yu, H., 2009. Lab Chip 9 (22), 3185–3192. https://doi.org/10.1039/b915147h.
Zhang, Y.S., Arneri, A., Bersini, S., Shin, S.R., Zhu, K., Goli-Malekabadi, Z., Aleman, J., Colosi, C., Busignani, F., Dell'Erba, V., Bishop, C., Shupe, T., Demarchi, D., Moretti, M., Rasponi, M., Dokmeci, M.R., Atala, A., Khademhosseini, A., 2016. Biomaterials 110, 45–59. https://doi.org/10.1016/j.biomaterials.2016.09.003.
Zhang, Y. S.; Aleman, J.; Shin, S. R.; Kilic, T., 2017, 114 (12), E2293-e2302. DOI 10.1073/pnas.1612906114..
Zhang, M., Xu, C., Jiang, L., Qin, J.H., 2018a. Toxicol. Res. 7 (6), 13. https://doi.org/10.1039/c8tx00156a.
Zhang, B.Y., Korolj, A., Lai, B.F.L., Radisic, M., 2018b. Nat. Rev. Mater. 3 (8), 257–278. https://doi.org/10.1038/s41578-018-0034-7.
Zhang, J., Chen, Z.Z., Zhang, Y.Y., Wang, X.C., Ouyang, J., Zhu, J.F., Yan, Y.C., Sun, X. W., Wang, F., Li, X.R., Ye, H., Sun, S.Q., Yu, Q.D., Sun, J.W., Ge, J.J., Li, Q.W., Han, Q.Q., Pu, Y.P., Gu, Z.Z., 2021. Lab Chip 21 (19), 3804–3818. https://doi.org/10.1039/d1lc00099c.
Zhang, X.; Karim, M.; Hasan, M. M., 2022, 14 (3). DOI 10.3390/cancers14030648..
Zhu, Y. J.; Sun, L. Y.; Wang, Y.; Cai, L. J.; Zhang, Z. H.; Shang, Y. X.; Zhao, Y. J., Adv. Mater., 10. DOI 10.1002/adma.202108972..
Zizzari, A., Bianco, M., Carbone, L., Perrone, E., Amato, F., Maruccio, G., Rendina, F., Arima, V., 2017. Materials 10 (12). https://doi.org/10.3390/ma10121411.
Zoio, P., Oliva, A., 2022. Pharmaceutics 14 (3), 30. https://doi.org/10.3390/pharmaceutics14030682.